
**Astroglial and therapeutic factors affect
demyelination in murine models with toxic
demyelination**

Doctoral Thesis

In partial fulfillment of the requirements for the degree

“Doctor rerum naturalium (Dr. rer. nat.)“

in the Molecular Medicine Study Program

at the Georg-August-University Göttingen

submitted by

Ramona Pförtner

born in Osterode am Harz, Germany

Göttingen, January 2013

Members of the Thesis Committee

Supervisor

Prof. Dr. Wolfgang Brück

Department of Neuropathology

University Medical Center, Georg-August-University Göttingen

Second Member of the Thesis Committee

Prof. Dr. Mikael Simons

Department of Cellular Neuroscience

Max-Planck-Institute for Experimental Medicine Göttingen

Third Member of the Thesis Committee

Prof. Dr. Eberhard Fuchs

Department of Clinical Neurobiology

German Primate Center, Leibniz Institute for Primate Research Göttingen

Date of disputation: March 13th, 2013

***For
my grandfather***

Affidavit

I hereby declare that my doctoral thesis entitled “Astroglial and therapeutic factors affect demyelination in murine models with toxic demyelination” has been written independently with no other sources and aids than quoted.

A handwritten signature in blue ink, consisting of the name 'Ramona Pfortner' written in a cursive style. The signature is positioned above a horizontal line.

Ramona Pfortner

Göttingen, January 2013

Related publications

Original Articles:

- Brück W*, **Pförtner R***, Pham T, Zhang J, Hayardeny L, Piryatinsky V, Hanisch U, Regen T, Rossum D, Brakelmann L, Hagemeyer K, Kuhlmann T, Stadelmann C, John GR, Kramann N and Wegner C (2012) Reduced astrocytic NF-κB activation by laquinimod protects from cuprizone-induced demyelination. *Acta Neuropathol* 124:411-24.
*equal contribution
- Wegner C, Stadelmann C, **Pförtner R**, Raymond E, Feigelson S, Alon R, Timan B, Hayardeny L and Brück W (2010) Laquinimod interferes with migratory capacity of T cells and reduces IL-17 levels, inflammatory demyelination and acute axonal damage in mice with experimental autoimmune encephalomyelitis. *J Neuroimmunol* 227:133-43.

Abstracts:

- **Pförtner R**, Kramann R, Brück W and Wegner C “Preventive laquinimod treatment reduces cuprizone-induced pathology in a dose-dependent manner”, presented as poster at 28th Congress of the European Committee for Treatment and Research in Multiple Sclerosis, October 10-13th 2012, Lyon, France
- **Pförtner R**, Brück W and Wegner C “Laquinimod reduces demyelination and inflammation in cuprizone-treated mice”, presented as poster at 10th European Meeting on Glial Cells in Health and Disease, September 13-17th 2011, in Prague, Czech Republic
- **Pförtner R**, Brück W and Wegner C “Effect of laquinimod on cuprizone-induced demyelination in mice”, presented as poster at the 9th Göttingen Meeting of the German Neuroscience Society, March 23-27th 2011, Göttingen, Germany

Contents

Acknowledgements	I
Abstract	II
List of figures	IV
List of tables	V
Abbreviations	VI

1. Introduction

1.1 Multiple sclerosis.....	1
1.1.1 Clinical course and diagnostics	1
1.1.2 Established treatment.....	3
1.2 Pathogenesis and pathology of MS.....	4
1.2.1 Epidemiology and Etiology.....	4
1.2.2 Pathogenesis of MS.....	6
1.2.3 Pathology of MS	7
1.3 Animal models of MS	9
1.3.1 Experimental autoimmune encephalomyelitis.....	9
1.3.2 Cuprizone-induced demyelination.....	10
1.3.3 Focal lyssolecithin-induced demyelination	11
1.4 Treatment of inflammatory demyelinating diseases with the new drug laquinimod	12
1.4.1 Laquinimod in MS	12
1.4.2 Laquinimod in EAE	14
1.5 Role of astrocytic factors in inflammatory demyelinating diseases.....	15
1.5.1 Astrocytic changes in MS	15
1.5.2 Astrocytic changes in EAE	16
1.6 The astrocytic leukodystrophy Alexander`s disease and its related animal model.....	17
1.6.1 Alexander`s disease	17
1.6.2 Human GFAP overexpressing transgenic mice	18
1.7 Aims	20

2. Materials and methods

2.1	Materials and solutions	22
2.1.1	Chemicals	22
2.1.2	Enzymes/proteins	24
2.1.3	Kits.....	24
2.1.4	Consumables.....	25
2.1.5	Technical devices	25
2.1.6	Solutions.....	26
2.1.7	Software	29
2.2	Animal experiments	29
2.2.1	Mice.....	29
2.2.2	Genotyping of transgenic mice	30
2.2.2.1	DNA extraction	30
2.2.2.2	Genotyping of Tg(hGFAP) mice	30
2.2.3	Cuprizone treatment.....	32
2.2.4	Extraction of mouse sera	33
2.2.5	Laquinimod treatment.....	33
2.2.6	Intracerebral stereotactic injection	33
2.2.6.1	Focal demyelination induced by lysolecithin	34
2.2.6.2	Stereotactical injection of cuprizone or serum.....	34
2.3	Histology	35
2.3.1	Histochemical staining	36
2.3.1.1	Hematoxylin and eosin (HE) staining	36
2.3.1.2	Luxol fast blue-periodic acid Schiff (LFB-PAS) staining	36
2.3.1.3	Bielschowsky silver impregnation	36
2.3.2	Immunohistochemistry and fluorescence staining	37
2.4	Electron microscopy (EM)	39
2.5	Morphometry and data acquisition	40
2.6	Mass spectrometry analysis	40
2.7	Primary cell cultures	41
2.7.1	Isolation of primary astrocytes from newborn mice	41
2.7.2	Cell viability assay (MTT assay)	43

2.7.3	Membrane integrity assay	43
2.7.4	Migration assay	43
2.8	Statistical analysis	44

3. Results

3.1	Evaluating the effect of LAQ on toxic de- and remyelination in mice	45
3.1.1	Reduced cuprizone-induced weight loss and oligodendroglial apoptosis under LAQ in wild type mice.....	45
3.1.2	Dose-dependent inhibition of cuprizone-induced demyelination by LAQ.....	47
3.1.3	Decreased cuprizone-induced microglial activation, axonal damage and astrogliosis by LAQ	49
3.1.4	Similar cerebral cuprizone concentrations in mice treated with LAQ and vehicle	50
3.1.5	Reduced cuprizone-induced pathology under LAQ also in Rag1-deficient mice ..	51
3.1.6	Decreased astrocytic NF- κ B activation under LAQ treatment after cuprizone	53
3.1.7	No LAQ effect on LPC-induced demyelination	54
3.1.8	Similar remyelination under LAQ after cuprizone withdrawal.....	56
3.2	Investigating the impact of human GFAP overexpression on toxic demyelination in mice	57
3.2.1	Increased astrogliosis, but regular myelin and oligodendroglial density in naïve Tg(hGFAP) mice	57
3.2.2	Reduced cuprizone-induced oligodendroglial apoptosis in Tg(hGFAP) mice.....	60
3.2.3	Less cuprizone-induced demyelination in Tg(hGFAP) animals	62
3.2.4	Less microglial activation and axonal damage in Tg(hGFAP) mice after cuprizone challenge	63
3.2.5	Similar cerebral cuprizone concentrations in Tg(hGFAP) and wild type mice	64
3.2.6	Reduced astrocytic NF- κ B activation in Tg(hGFAP) mice after cuprizone.....	65
3.3	Examining the short-term effects of cuprizone <i>in vitro</i> and <i>in vivo</i>	66
3.3.1	No effect of cuprizone on astrocytic viability, but on astrocytic migration <i>in vitro</i>	66
3.3.2	No effect of serum from cuprizone-treated mice on astrocytic viability and migration <i>in vitro</i>	68
3.3.3	No direct cuprizone effect on glial cells after intracerebral injection <i>in vivo</i>	70

3.3.4	No direct effect of serum from cuprizone-treated mice after intracerebral injection <i>in vivo</i>	70
-------	--	----

4. Discussion

4.1	Reduced cuprizone-induced pathology under LAQ by down-regulation of astrocytic NF-κB activation	74
4.1.1	Reduced cuprizone-induced weight loss and oligodendroglial apoptosis under LAQ.....	74
4.1.2	Dose-dependent inhibition of demyelination under LAQ.....	74
4.1.3	Less microglial activation, axonal damage and astrogliosis under LAQ	75
4.1.4	Similar cerebral cuprizone concentrations in LAQ- and vehicle-treated mice.....	76
4.1.5	LAQ-related changes independent of T and B cells.....	76
4.1.6	Reduced astrocytic NF- κ B activation by LAQ.....	77
4.1.7	No impact of LAQ on remyelination after cuprizone withdrawal	78
4.1.8	No effect of LAQ on LPC-induced demyelination	78
4.1.9	Pronounced effects of LAQ on cuprizone-induced pathology compared to other immunomodulatory drugs	79
4.1.10	Further potential factors contributing to central LAQ effects.....	80
4.1.11	Conclusion.....	81
4.2	Less cuprizone-induced demyelination and astrocytic NF-κB activation in transgenic mice overexpressing human GFAP.....	81
4.2.1	Regular cerebral myelin and oligodendrocyte density in naïve Tg(hGFAP) transgenic mice	81
4.2.2	Reduced oligodendroglial apoptosis in Tg(hGFAP) mice.....	82
4.2.3	Less cuprizone-induced demyelination in Tg(hGFAP) mice.....	82
4.2.4	Reduction of cuprizone-induced microglial activation and axonal damage in Tg(hGFAP) mice	83
4.2.5	Similar cerebral cuprizone concentrations in Tg(hGFAP) and wild type mice.....	83
4.2.6	Reduction of astrocytic NF- κ B activation in Tg(hGFAP) mice	84
4.2.7	Evidence for altered astrocytic function in Tg(hGFAP) mice.....	85
4.2.8	Conclusion.....	85
4.3	No marked direct effects of short-term cuprizone challenge on astrocytic survival <i>in vitro</i> and on glial cells <i>in vivo</i>	86

4.3.1	No effect of cuprizone on astrocytic survival, but on astrocytic migration <i>in vitro</i>	86
4.3.2	Presence of oligodendrocytes and astrocytes after focal intracerebral injection of cuprizone	87
4.3.3	Conclusion.....	88
4.4	Concluding remarks on astrocytic involvement in demyelinating diseases	88

5. Summary and Conclusions

Summary and Conclusions	90
References.....	92
Curriculum Vitae.....	107

Acknowledgements

First I would like to thank my supervisor **Dr. Dr. Christiane Theodossiou-Wegner** for her scientific guidance throughout my PhD years and for her excellent support. I acknowledge her for her patience and for sharing her scientific expertise with me. I would like to also express gratitude to **Prof. Dr. Wolfgang Brück** for giving me the opportunity to join his lab. I would also acknowledge him for supervising my project and for his scientific advices and discussion. I am grateful to **Prof. Dr. Christine Stadelmann-Nessler** for her scientific expertise, technical support and her helpful advices.

I want to thank **Prof. Dr. Mikael Simons** for agreeing to act as second examiner and for his supporting comments and ideas on my progress reports. I also want to acknowledge **Prof. Dr. Eberhard Fuchs** for his interest in my project and for his supportive contributions as member of my thesis committee.

I sincerely thank our collaborator **Marta Patfalusi** from the *Department Analytics, Aurigon-Toxicop Research Center in Budapest, Hungary* for mass spectrometry analyses of my samples.

I acknowledge **Dr. Nadine Kramann** for proofreading of this thesis, for her technical advisory in the cell culture experiments and for her support.

I want to thank **Dr. Claudia Wrzos** for training and support in stereotactical injections and the daily work load in the lab.

Many thanks to our laboratory assistants **Brigitte, Katja, Jasmin, Heidi and Angela** for their theoretical and practical support in the experiments as well as for the nice conversations and the enjoyable atmosphere in the lab.

I owe many thanks to **Martina, Claudia, Verena, Anne, Franziska, Nielsen, Nadine, Tobias...** and of course **all other colleagues** for the time we have spent together and for having lots of fun not only in the lab. I enjoyed the time I spent with you very much!

I want to acknowledge the **Molecular Medicine PhD program** as well as our always friendly secretaries **Cynthia and Chris** for administrative support.

Special thanks to my parents **Manfred and Gaby** and my brother **Sandro** for supporting me over all years and in every decision. Thank you for your unlimited love and persistent confidence in me. Finally, I would like to thank **Eduard** for having been there when needed. Without him many achievements would not have been possible.

Abstract

Astrocytes might play an important role in demyelinating diseases such as multiple sclerosis (MS) since serum autoantibodies directed against the astrocytic water channel aquaporin-4 cause inflammatory demyelinating lesions in the MS-related disease neuromyelitis optica. Oral cuprizone challenge leads to demyelination of the corpus callosum and cortex in mice, whereby the blood-brain-barrier remains intact. Astrocytic activation of nuclear factor kappa of activated B cells (NF- κ B) plays a key role for mediating demyelination under cuprizone. Recent clinical trials in MS indicate that laquinimod (LAQ) is an oral substance with more pronounced effects on disability and brain atrophy than on relapses suggesting that LAQ might exert effects not only on peripheral immune cells, but also on central nervous system (CNS)-resident cells.

The aim of the present study was to investigate intrinsic and therapy-induced astrocytic effects on cuprizone-induced pathology in mice. One aim was to assess the effects of LAQ on toxic demyelination. A further aim was to study the impact of increased astrocytic glial fibrillary acidic protein (GFAP) expression on cuprizone-induced changes.

Eight- to ten-weeks-old male C57BL/6 mice were given 0.25% cuprizone for one or six weeks. Histological and immunohistochemical analyses were performed to evaluate therapy-induced and astrocytic effects on cuprizone-induced changes on glia, myelin and axons in the corpus callosum. In addition, astrocytic NF- κ B activation was assessed by nuclear translocation of p65 in GFAP-positive astrocytes.

To examine the effects of LAQ, mice were treated with 0, 5 or 25 mg/kg LAQ per day during cuprizone challenge. After one week of cuprizone, oligodendrocyte apoptosis was reduced by 62% in mice treated with 25 mg/kg LAQ compared to vehicle-treated animals. After six weeks of cuprizone, LAQ reduced demyelination in a dose-dependent manner and attenuated microglial activation, axonal damage and reactive astrogliosis compared to the vehicle group. Similar results were observed in recombination activating gene 1 (Rag1)-deficient mice constitutively lacking T and B cells indicating that the effect of LAQ in the cuprizone model is CNS-intrinsic. Astrocytic NF- κ B activation was significantly decreased by 46% under 25 mg/kg LAQ compared to the vehicle group after six weeks of cuprizone. These data indicate that LAQ might protect from cuprizone-induced pathology through CNS-

intrinsic mechanisms by reducing NF- κ B activation in astrocytes. Recently published data in primary astrocytic cultures support these findings by showing that LAQ directly inhibited the astrocytic NF- κ B activation and thereby down-regulated the astrocytic pro-inflammatory response.

The impact of increased astrogliosis on cuprizone-induced demyelination was evaluated in transgenic mice overexpressing human GFAP. These animals show an increased astrogliosis even without external stimuli. After one week of cuprizone, transgenic mice displayed still higher densities of preserved mature oligodendrocytes and an 80% reduction of oligodendroglial apoptoses compared to the corresponding wild type animals. After six weeks of cuprizone, transgenic mice showed decreased demyelination, microglial activation and axonal damage as well as an 80% reduction of astrocytic NF- κ B activation compared to wild type animals. These data indicate that reduced astrocytic NF- κ B activation might also contribute to reduced cuprizone-induced pathology in mice overexpressing human GFAP.

These data suggest that down-regulating the astrocytic NF- κ B activation might be a potential therapeutic approach for the future treatment of demyelinating diseases such as MS. The CNS-intrinsic effects of LAQ on astrocytic activation might explain the clinical findings of more pronounced effects on disability and brain atrophy than on relapses. The findings from this work could contribute to a better understanding and further development of novel protective therapies limiting tissue damage in demyelinating diseases such as MS.

List of figures

Fig. 1: Structural formula of Roquinimex® and laquinimod	13
Fig. 2: No weight loss under LAQ treatment during 6 weeks cuprizone challenge	45
Fig. 3: Decreased cuprizone-induced oligodendroglial apoptosis under LAQ treatment ...	46
Fig. 4: Callosal demyelination is reduced in a dose-dependent manner under LAQ after 6 weeks of cuprizone	48
Fig. 5: LAQ treatment reduces cuprizone-induced microglial activation, axonal damage and gliosis	49
Fig. 6: Similar cuprizone concentration in brains of LAQ- and vehicle-treated mice after 1 week and 6 weeks of cuprizone	50
Fig. 7: Low cuprizone concentration in plasma of LAQ- and vehicle-treated mice after 1 week of cuprizone	51
Fig. 9: Reduced demyelination, activated microglia, acute axonal damage and astrogliosis in LAQ-treated Rag1 ^{-/-} mice compared to vehicle-treated controls after 6 weeks of cuprizone	52
Fig. 8: No cuprizone-induced weight loss in LAQ-treated Rag1 ^{-/-} mice	52
Fig. 10: LAQ reduces astrocytic NF- κ B activation after 6 weeks of cuprizone challenge	53
Fig. 11: No effect of 25 mg/kg LAQ on LPC-induced demyelination	54
Fig. 12: No effect of 40 mg/kg LAQ on LPC-induced demyelination	55
Fig. 13: No effect of LAQ on remyelination after cuprizone-induced demyelination	56
Fig. 14: Increased astrogliosis in naïve Tg(hGFAP) mice	58
Fig. 15: Regular myelin content, activated microglia and number of mature oligodendrocytes in Tg(hGFAP) mice at the age of 8 weeks	59
Fig. 16: Reduced weight loss in Tg(hGFAP) mice after cuprizone	60
Fig. 17: Decreased oligodendroglial apoptosis in Tg(hGFAP) mice	61
Fig. 18: Less callosal demyelination in Tg(hGFAP) mice	62
Fig. 19: Reduced cuprizone-induced microglial activation and axonal damage in human GFAP transgenic mice	63
Fig. 20: Similar cuprizone concentration in brains of human GFAP transgenic and wild type mice	64
Fig. 21: Low cuprizone concentration in plasma of human GFAP transgenic and wild type mice	65

Fig. 22: Reduction of astrocytic NF- κ B activation in Tg(hGFAP) mice	65
Fig. 23: No effect of cuprizone on primary astrocytes from wild type mice	66
Fig. 24: Mildly reduced astrocytic migration under high cuprizone doses	67
Fig. 25: No effect of serum from cuprizone-treated mice on mitochondrial respiration in primary astrocytes from wild type animals	68
Fig. 26: No effect of serum from cuprizone-treated mice on migration of primary mouse astrocytes	69
Fig. 27: No effect of cuprizone after focal injection in wild type mice	71
Fig. 28: No effect of serum from cuprizone-treated mice after focal injection in wild type animals	72

Parts of figures 2-6 and 8-10 have been published previously (Brück *et al.* 2012, *Acta Neuropathol* 124:411-24).

List of tables

Tab. 1: Primary antibodies for immunohistochemistry and fluorescence staining	38
Tab. 2: Secondary antibodies for immunohistochemistry and fluorescence staining	39

Abbreviations

A	:	Adenosine
Act1	:	NF-κB activator 1
AgNO ₃	:	Silver nitrate
APP	:	Amyloid precursor protein
AQP4	:	Aquaporin-4
ARE	:	Antioxidant response element
Arg	:	Arginine
ATP	:	Adenosine-5-triphosphate
AxD	:	Alexander`s disease
BBB	:	Blood-brain-barrier
BDNF	:	Brain-derived neurotrophic factor
bp	:	Base pairs
C	:	Cytosine
cAMP	:	Cyclic adenosine monophosphate
CCL2	:	Chemokine ligand 2
CCR2	:	Chemokine receptor 2
CIS	:	Clinically isolated syndrome
Cl	:	Chlorine
cm	:	Centimeter
CNPase	:	2',3'-cyclic nucleotide 3'-phosphodiesterase
CNS	:	Central nervous system
CO ₂	:	Carbon dioxide
CREB	:	cAMP response element-binding protein
CSF	:	Cerebrospinal fluid
CuSO ₄	:	Copper(II) sulfate
Cy	:	Cyanine
Cys	:	Cysteine
DAB	:	3,3'-diaminobenzidine
DAPI	:	4',6-diamidino-2-phenylindole
DDSA	:	Dodeceny succinic anhydride

DMEM	:	Dulbecco's Modified Eagle Medium
DMP	:	2,4,6 tri(dimethylaminomethyl)phenol
DNA	:	Desoxyribonucleic acid
dNTP	:	Desoxynucleoside triphosphate
EAE	:	Experimental autoimmune encephalomyelitis
EBNA-1	:	Epstein-Barr virus nuclear antigen 1
EBV	:	Epstein-Barr virus
<i>E. coli</i>	:	<i>Escherichia coli</i>
EDTA	:	Ethylenediamine tetraacetic acid disodiumsalt dihydrate
EEC	:	European Economic Community
EM	:	Electron microscopy
<i>et al</i>	:	And others
FCS	:	Fetal calf serum
Fig	:	Figure
G	:	Guanosine
g	:	Gram
GFAP	:	Glial fibrillary acidic protein
H	:	Hydrogen
h	:	Hour
HBSS	:	Hank's Buffered Salt Solution
HCl	:	Hydrochloric acid
HE	:	Hematoxylin Eosin
HLA	:	Histocompatibility leukocyte antigen
H ₂ O ₂	:	Hydrogen peroxide
HPLC	:	High performance liquid chromatography
IFN	:	Interferon
IgG	:	Immunoglobulin G
IL	:	Interleukin
i. m.	:	Intramuscular
IkB	:	Inhibitor of kappa B
i. p.	:	Intraperitoneal
i. v.	:	Intravenous
kg	:	Kilogram
KIR	:	Inwardly rectifying potassium channel

l	:	Liter
LAQ	:	Laquinimod
LFB-PAS	:	Luxol fast blue-periodic acid Schiff
LPC	:	L- α -lysophosphatidyl choline (lysolecithin)
LPS	:	Lipopolysaccharide
M	:	Molar
MBP	:	Myelin basic protein
mg	:	Milligram
min	:	Minutes
ml	:	Milliliter
mm	:	Millimeter
MOG	:	Myelin oligodendrocyte glycoprotein
MR	:	Magnetic resonance imaging
MRM	:	Multiple reaction monitoring
MS	:	Multiple sclerosis
m/z	:	Mass-to-charge ratio
N	:	Nitrogen
n	:	Number of experiments
NaCl	:	Sodium chloride
NaOH	:	Sodium hydroxide
NAWM	:	Normal-appearing white matter
NF- κ B	:	Nuclear factor kappa of activated B cells
ng	:	Nanogram
nm	:	Nanometer
NMO	:	Neuromyelitis optica
Nrf2	:	Nuclear factor (erythroid-derived 2)-like 2
OPC	:	Oligodendrocyte precursor cells
PBMC	:	Peripheral blood mononuclear cells
PBS	:	Phosphate-buffered saline
PCR	:	Polymerase chain reaction
PFA	:	Paraformaldehyde
Pen/strep	:	Penicillin/streptomycin
PLL	:	Poly-L-lysine
PLP	:	Proteolipid protein

PP	:	Primary progressive
ppn	:	Peripheral parenteral nutrition
R	:	Arginine
Rag1	:	Recombination activation gene 1
RFU	:	Relative fluorescence unit
rpm	:	Rounds per minute
RR	:	Relapsing-remitting
s	:	Seconds
s. c.	:	Subcutaneous
SDS	:	Sodium dodecyl sulfate
SEM	:	Standard error of the mean
SP	:	Secondary progressive
STAT	:	Signal transducer and activator of transcription
T	:	Thymidine
Tab	:	Table
TBE	:	Tris/borate/EDTA
Tg(hGFAP)	:	Mice with moderate overexpression of human GFAP, line 73.7
TGF β	:	Transforming growth factor beta
Th	:	T helper cell
TNF α	:	Tumor necrosis factor alpha
UV	:	Ultraviolet
v	:	Volume
V	:	Volt
vs	:	Versus

1 Introduction

1.1 Multiple sclerosis

Multiple sclerosis (MS), also known as encephalomyelitis disseminata, is the most common chronic neurological disease leading to disability in early to middle adulthood. MS was first described by Jean Martin Charcot in 1868 and is currently believed to be an autoimmune disorder causing inflammatory demyelination in the central nervous system (CNS) including the brain and spinal cord. Traditionally, demyelinated areas were thought to be predominantly located in the white matter and lesions in the white matter were regarded as most important pathological feature in MS. However, recent studies have demonstrated extensive grey matter demyelination as well as wide-spread changes in the normal-appearing white matter (NAWM). Diffuse pathological changes in the NAWM as well as white and grey matter atrophy indicate that changes in MS are not restricted to focal lesions, but affect the whole CNS. These diffuse changes are not well understood, but axonal and glial changes are likely to play a role.

1.1.1 Clinical course and diagnostics

The disease course of MS differs from patient to patient and is not exactly predictable. Symptoms occur either as discrete attacks (relapsing forms) or slowly accumulating over time (progressive forms). At disease onset two main courses of the disease exist: The first and most common form is the relapsing-remitting form of MS (RR-MS) which affects about 80% to 85% of patients. Early symptoms usually include visual as well as sensory disturbances, limb weakness, clumsiness and gait ataxia. RR-MS patients typically develop suddenly occurring symptoms evolving over several days and improving within weeks. After a relapse, remaining signs of CNS dysfunction may persist.

Later on during the disease course, most of the cases (about 80% of RR-MS patients in 20 years) show a continuous disease progression which is not related to relapses

(secondary progressive (SP)-MS) (Lublin and Reingold, 1996; Kremenchutzky *et al.*, 2006). Patients with SP-MS accumulate progressive disability over time.

About 15% to 20% of patients suffer from the second form of MS showing a gradually progressive clinical course from onset with no acute attacks known as primary progressive (PP)-MS. Typical symptoms include leg weakness, as well as bowel and bladder symptoms. Up to now, the factors which are responsible for the different courses of the disease are not known.

As initial stage of the clinical disease, the clinically isolated syndrome (CIS) is described as first neurologic episode that lasts at least 24 hours and is caused by inflammatory demyelination of the CNS. An episode may be monofocal in which symptoms are caused by a single lesion in the CNS or multifocal in which multiple sites exhibit symptoms. Not all patients who experience a CIS go on to develop MS. However, if CIS patients show oligoclonal bands within the cerebrospinal fluid (CSF) and disseminated brain lesions on magnetic resonance imaging (MRI), then these patients have a high risk of developing MS with further relapses (Morrissey *et al.*, 1993).

MS is typically diagnosed based on the clinical presentation as well as evidence of oligoclonal immunoglobulin G (IgG) bands in CSF and disseminated lesions on MRI (Miller *et al.*, 1989). The so-called “McDonald criteria” are diagnostic criteria for MS focusing on clinical and radiologic data of the dissemination of MS lesions in time and space. Using the McDonald criteria the outcome of a diagnostic evaluation is “MS”, “possible MS” or “not MS” (McDonald *et al.*, 2001). A recently revision of the McDonald criteria allows a more rapid diagnosis of MS by a single MRI scan (Polman *et al.*, 2011). Thus, a rapid diagnosis can be made by a single brain MRI study presenting lesion dissemination in time and space and both active lesions uptaking gadolinium as well as non-enhancing lesions. Lesion dissemination in space is presented by more than one T2 lesion in at least two of four areas of the CNS: Periventricular, juxtacortical, infratentorial and spinal cord. Lesion dissemination in time is presented either by an asymptomatic gadolinium-enhancing lesion on the first scan or by at least one new T2 and/or gadolinium-enhancing lesion on follow-up MRI.

1.1.2 Established treatment

During the acute phases of MS, the standard treatment consists of high-dose methylprednisolone, a synthetic glucocorticoid, given intravenously (i. v.) for three to five days. If the treatment with methylprednisolone fails to improve symptoms within two weeks, plasmapheresis will be considered in patients with severe symptoms. Different immunomodulatory drugs are available for long-term treatment of RR-MS: Glatiramer acetate (Copaxone®), Interferon beta (IFN β) 1a (Avonex®), IFN β 1a (Rebif®) and IFN β 1b (Betaferon®). Copaxone® is administered subcutaneously (s. c.) and is supposed to attenuate pro-inflammatory T cell responses showing T helper cell 2 (Th2) activation (Vieira *et al.*, 2003). IFN β proteins have antiviral as well as immunomodulatory properties. Two forms of recombinant IFN β proteins are available for MS therapy - IFN β 1a and 1b. IFN β 1a is produced by mammalian cells whereas IFN β 1b is produced in genetically modified *E. coli*. Avonex® is administered intramuscular (i. m.), Rebif® and Betaferon® by s. c. application.

If patients continue to have relapses under the standard immunomodulatory treatments, then an escalation therapy should be considered. The first choice treatments are natalizumab (Tysabri®) applied i. v. and fingolimod (Gilenya®) given orally. Both drugs are more potent and have immunomodulatory properties. Tysabri® is a recombinant monoclonal antibody produced in murine myeloma cells. Natalizumab appears to diminish the transmission of immune cells into the CNS by binding to $\alpha 4\beta 1$ -integrin receptor molecules on the surfaces of lymphocytes expressing $\alpha 4$ -integrin expressed by T lymphocytes. Tysabri® blocks immune cell adhesion to blood vessel walls and hence blocks migration of T cells into the CNS (Miller *et al.*, 2003; Rice *et al.*, 2005). Fingolimod is a sphingosine 1-phosphate receptor modulator that inhibits migration of lymphocytes out of lymph nodes into the circulation. Hence, Gilenya® prevents lymphocytes to reach the CNS and as a consequence reduces relapses and progression of the disease (Chiba *et al.*, 1998). The second choice for intensified treatment of RR-MS is mitoxantrone.

All these drugs mainly target the peripheral immune system. Medications with myelin- or axon-protecting effects could prevent the increase in disability through the course of MS by limiting the tissue damage, especially neurodegeneration. Hence, there is a need for medications entering the CNS and directly inhibit myelin and axonal damage. Since most

of the established drugs need parenteral application, the development of oral medications was necessary and facilitates the daily life for patients with fear or weariness of injections.

1.2 Pathogenesis and pathology of MS

1.2.1 Epidemiology and Etiology

The prevalence of MS is approximately 2500,000 patients worldwide and varies around the world. A north to south gradient in disease prevalence shows high prevalence rates on the northern hemisphere compared to low rates on the southern (Kurtzke *et al.*, 1979). The prevalence is highest in northern Europe, southern Australia and the middle part of North America. In Germany about 127 people are affected per 100,000 persons (Hein and Hopfenmüller, 2000). Approximately 120,000 cases were reported in 2001 in Germany, whereby 2,500 patients are newly diagnosed every year. Migration studies show that migration from an area of high prevalence of MS to an area of low prevalence before the age of 15 to 16 leads to an acquisition of the low risk, whereas migration after an age of 15 to 16 does not change the risk (Kurtzke *et al.*, 1970; Kurtzke, 2000).

Females are affected more often than males suggesting that sex hormones are one factor influencing MS. MS has a female predominance which has developed from 2:1 to 3:1. Recent studies indicate that an increase in the number of female RR-MS patients leads to a renewed increase in sex ratio of MS (Ramagopalan *et al.*, 2010). The relevance of sex hormones is supported by lower relapse rates during pregnancy and disease rebound after pregnancy (Runmarker *et al.*, 1995). Further evidence comes from studies reporting a worsening of MS during menstruation and the ameliorating therapeutic effects of the pregnancy hormone estriol in RR-MS (Sicotte *et al.*, 2002).

Genetic and environmental factors influence the development of MS. Family and twin studies indicate that the prevalence is substantially increased in family members of MS patients. First-degree relatives of a MS patient (such as children, siblings or non-identical twins) have a 2.5% to 5% risk of developing the disease. The risk of MS for second-degree relatives (such as cousins, uncles/aunts, nephew/nieces) is around 1%. For an identical twin of a MS patient who shares all the same genes is the risk of MS increased to 25% to 30%

(Ebers *et al.*, 1986; Sadovnick *et al.*, 1993). After searching for individual susceptibility genes, the most striking gene or genes are found on chromosome 6p21 in the area of the major histocompatibility complex (histocompatibility leukocyte antigen (HLA) in humans). The risk for MS is increased with the presence of one or more HLA-DRB1*15 alleles (Banwell *et al.*, 2011). This allele is considered to play a role in 17% to 60% of the hereditary MS cases (Haines *et al.*, 1998). Recent genetic studies investigating over 7,000 MS patients identified over 50 genetic factors involving mainly immunologically relevant genes, but also environmental factors such as vitamin D (Sawcer *et al.*, 2011). However, a contribution of non-genetic factors to MS etiology is also clear since identical twins show a concordance rate of only 25% to 30% (Ebers *et al.*, 1986; Sadovnick *et al.*, 1993).

Discussed environmental factors are sunlight exposure, vitamin D, hygiene, smoking and geographical microbiological factors. One possible factor could be the decrease in sunlight exposure depending on the latitude leading to a decrease in UV radiation and decreased biosynthesis of vitamin D (Acheson *et al.*, 1960). A further factor for MS represents the hygiene status since it comes to a delayed or overall reduction in childhood infections in developed countries leading to an increase in autoimmune reactions/diseases (Th1-mediated) and allergies (Th2-mediated) (Strachan, 1989; Folkerts *et al.*, 2000). Hence, the hygiene hypothesis suggests that there is a shift from Th1 to Th2 responses as a result of the cleaner environment (Strachan, 1989; Folkerts *et al.*, 2000).

As additional environmental factor, infectious agents have been postulated to be potential triggers of MS. Many viruses have been discussed, but especially Epstein-Barr virus (EBV) seems to be related to MS. An association between EBV and pediatric MS is found since serological evidence for remote EBV is present in ca. 80% of pediatric MS patients (Alotaibi *et al.*, 2004), but only in 42% of healthy control cases. It is thought that EBV shows similarities to myelin basic protein (MBP) and hence molecular mimicry involving HLA molecules has been debated (Lang *et al.*, 2002). Furthermore, the interaction of EBV and HLA-DRB1*15 is discussed since HLA alleles recognize EBV nuclear antigen 1 (EBNA-1) epitopes.

Exposure to cigarette smoke is also discussed as further environmental risk factor for MS. Smokers have an approximately 1.5 higher risk for developing MS than non-smokers and they show more rapid disease advancement (Riise *et al.*, 2003).

1.2.2 Pathogenesis of MS

Based on data from animal experiments, MS is generally considered as a predominantly T cell-mediated autoimmune disease. Findings from animals with experimental autoimmune encephalomyelitis (EAE) suggest that MS develops after activation of autoreactive T lymphocytes (CD4⁺ and CD8⁺) leading to inflammatory demyelination of the CNS (Schluesener and Wekerle, 1985; Sedgwick and Mason, 1986; Huseby *et al.*, 2001). Activated T cells are thought to cross the blood-brain-barrier (BBB) and enter the CNS (Hickey *et al.*, 1991). Once in the CNS, these T cells further compromise the integrity of the BBB and are thought to target one or more myelin antigens within the CNS (Westland *et al.*, 1999). B cells are also thought to play a role in the pathogenesis of MS. T cells from MS patients do not differ quantitatively, but qualitatively in comparison to healthy subjects. Myelin-reactive T and B cells from MS patients show a memory or activated phenotype and can activate CD4⁺ T cells, whereas healthy persons typically display a naive phenotype (Lovett-Racke *et al.*, 1998; Scholz *et al.*, 1998).

Autoreactive T cells cause inflammation within the CNS by secretion of proinflammatory cytokines: Activation of CD4⁺ autoreactive T cells results in secretion of the proinflammatory cytokines interleukin (IL)-2, IFN γ and tumor necrosis factor alpha (TNF α) and hence leading to an injurious cytokine phenotype (CD4⁺ Th1). In contrast, myelin-reactive T cells from healthy persons produce more cytokines leading to an anti-inflammatory cytokine phenotype (CD4⁺ Th2) (Hermans *et al.*, 1997). Human T cells can differentiate into Th1 lymphocytes after activation of the transcription factor signal transducer and activator of transcription (Stat)-4 in these lymphocytes by cytokines (such as IL-12) or type 1 interferons (such as IFN γ) (Bacon *et al.*, 1995). IL-4 and IL-10 are involved in the differentiation of CD4⁺ T lymphocytes favoring Th2 outcomes in EAE (Betelli *et al.*, 1998; Falcone *et al.*, 1998). Besides Th1 and Th2 cells, the role of Th17 proinflammatory T cells in MS is also discussed since Th17 cells have a central role in disease development which is indicated by a high density of IL-17 in active MS lesions (Tzartos *et al.*, 2008).

1.2.3 Pathology of MS

MS is characterized by multifocal plaques. MS lesions can occur anywhere in the CNS, but most lesions arise in the optic nerve, periventricular areas, brain stem and spinal cord. As the most important pathological feature, MS lesions in the white matter have been considered. Macroscopically, lesions are brownish-grey with harder consistency because of gliotic processes (Charcot, 1868; 1873). Microscopically, MS has four pathological hallmarks: Inflammation, demyelination, axonal damage and astrogliosis. Acute lesions display pronounced inflammation dominated by T cells and macrophages, followed by B cells and plasma cells (Lucchinetti *et al.*, 2000; Frischer *et al.*, 2009).

Demyelination is associated with axonal damage and reactive astrogliosis in the CNS. Axonal injury starts early in the disease course (Ferguson *et al.*, 1997; Trapp *et al.*, 1998; Kuhlmann *et al.*, 2002). This acute axonal damage seems to play an important role because it leads to irreversible axonal loss that is thought to be responsible for chronic disability (Bjartmar and Trapp, 2001). As response to tissue damage, astrocytes underlying cellular and functional changes known as reactive astrogliosis including elevation of glial fibrillary acidic protein (GFAP) (Roessmann and Gambetti, 1986).

MS lesions are distinguished according to their stage of demyelinating activity and the presence of immune cells (Brück *et al.*, 1995). Active demyelinating lesions are characterized by macrophages engulfing myelin debris and are distributed throughout the lesion or at the lesion edge. In contrast, macrophages engulfing myelin debris are only located at the rim of the lesion in smouldering lesions (Prineas *et al.*, 2001). In chronic inactive lesions only single T cells are present in perivascular regions without evidence for ongoing demyelination.

Early, actively MS lesions are considered as heterogeneous (Lucchinetti *et al.*, 2000). The concept of heterogeneity is based on four different patterns of demyelination categorised according to their myelin protein loss, geography and extension of plaques, pattern of oligodendrocyte destruction and the immunopathological evidence of complement activation. Pattern I and II are similar to T-cell-mediated or T-cell plus antibody-mediated autoimmune encephalomyelitis. However, the other two patterns, pattern III and IV, are based on oligodendrocyte dystrophy which is similar to either toxin- or virus-induced demyelination rather than autoimmunity.

In MS patients, grey matter is known to undergo extensive changes especially in chronic MS patients. More than 90% of patients with chronic MS show cortical lesions (Wegner *et al.*, 2006). Grey matter lesions are present in areas of cortical, deep and spinal grey matter (Wegner and Stadelmann, 2009). Three types of cortical lesions have been described in MS: Leukocortical lesions (type I), intracortical (type II) and subpial lesions (type III). Type I lesions involve grey and immediately adjacent white matter. Type II lesions lie purely within the neocortex and type III lesions extend from the pial surface into the cortex. Subpial lesions (type III) are the most extensive and can cover up to 70% of the cortical area in MS patients (Bø *et al.*, 2003).

Diffuse pathological changes in NAWM and cortical demyelination are mainly found in progressive MS, but even patients with early MS show cortical demyelination (Lucchinetti *et al.*, 2011). The NAWM outside of plaques shows inflammatory processes and a generalized activation of microglia (Kutzelnigg *et al.*, 2005). Furthermore, demyelination and axonal damage in focal lesions of MS patients extend into NAWM and lead to reduced original lesion site (Evangelou *et al.*, 2000a). Axonal damage in plaques followed by secondary Wallerian degeneration has been discussed to result from diffuse changes of the NAWM (Evangelou *et al.*, 2000b; Lovas *et al.*, 2000). Additionally, an increased BBB permeability is observed in NAWM (Kirk *et al.*, 2003).

After pathological loss of myelin, remyelination may occur. During this process new myelin sheaths are generated around axons. Initially, oligodendrocyte precursor cells (OPC) are recruited to the lesion and then differentiate into myelinating oligodendrocytes which enwrap the demyelinated axons with new myelin sheaths (Levine and Reynolds, 1999). However, in the majority of MS patients, remyelination is impaired even if OPC are present (Chang *et al.*, 2002). MRI studies from autopsies of MS patients demonstrate that only 40% of lesions show remyelinated areas (Barkhof *et al.*, 2003). Recent studies show that remyelination is more frequent in early MS lesions (ca. 80% remyelinated) compared to chronic MS lesions (ca. 60% remyelinated) (Goldschmidt *et al.*, 2009). One explanation for the limited remyelination in the majority of chronic MS lesions might be an impaired differentiation of OPC into myelinating oligodendrocytes (Kuhlmann *et al.*, 2008).

Experimental data indicate that the remyelination capacity decreases with age in mice after cuprizone-induced demyelination, whereby a restricted oligodendrocyte differentiation is thought to play a role (Shen *et al.*, 2008). Other possible explanations for an

impaired remyelination come from experiments in mice with lysolecithin-induced demyelination. In this animal model, the depletion of macrophages leads to a delayed OPC recruitment and hence impaired remyelination (Kotter *et al.*, 2005). Further studies in recombination activation gene (Rag) 1-deficient mice lacking constitutively T and B cells demonstrate an inhibition of remyelination processes after lysolecithin-induced demyelination (Bieber *et al.*, 2003).

1.3 Animal models of MS

1.3.1 Experimental autoimmune encephalomyelitis

Experimental autoimmune encephalomyelitis (EAE) represents the most common animal model of MS. This autoimmune disease causes inflammatory demyelinating lesions within the CNS and is most frequently used in rats and mice. Depending on species, EAE pathology differs. In mice, white matter of the spinal cord is mainly affected.

EAE can be induced by active immunization with myelin antigens such as MBP, myelin oligodendrocyte glycoprotein (MOG), proteolipid protein (PLP) or myelin-associated oligodendrocytic basic protein and 2',3'-cyclic nucleotide 3'-phosphodiesterase (CNP). EAE is commonly induced by active immunization of mice with a small peptide carrying the sequence of MOG from amino acid position 35 to 55 (MOG₃₅₋₅₅) which is emulsified in complete Freund's adjuvant. EAE can also be induced by passive adoptive transfer of encephalitogenic T cells from actively immunized animals into naïve mice.

The EAE model is often used to investigate potential new treatments for MS. Previous studies show an inhibition of disease in EAE after treatment with IFN β (Yasuda *et al.*, 1999) and copolymer-1 (Teitelbaum *et al.*, 1996). The oral immunomodulator linomide (Roquinimex®) was also tested in this model and shown to inhibit EAE (Karussis *et al.*, 1993a, b).

1.3.2 Cuprizone-induced demyelination

Cuprizone has already been established as a neurotoxin for different species in the 1960s (Carlton, 1967). Historically, feeding of high cuprizone concentrations was used to cause scrapie-like spongiform encephalopathy in different species such as rats, mice, guinea pigs and hamsters (Carlton, 1967, 1969). These high concentrations such as 0.5% cuprizone are highly toxic when administered early during development and produce giant hepatic mitochondria in mice (Suzuki, 1969; Kesterson and Carlton, 1972; Flatmark *et al.*, 1980). The main pathological features of mice treated with high cuprizone concentrations are brain edema, demyelination, astrogliosis and hydrocephalus (Pattison and Jebbett, 1971a; b).

Feeding the neurotoxicant cuprizone at a dose of 0.2% to 0.25% to eight to ten-week-old C57BL/6 mice leads to consistent demyelination of the corpus callosum and cortex after five to six weeks (Hiremath *et al.*, 1998; Skripuletz *et al.*, 2008). Cuprizone is known to induce oligodendrocyte apoptosis starting already after two days of cuprizone feeding and reaching maximal numbers after 10 and 21 days (Hesse *et al.*, 2010; Buschmann *et al.*, 2012). The loss of oligodendrocytes results in subsequent microglial activation, astrogliosis and demyelination in the following four to five weeks (Hiremath *et al.*, 1998). The BBB is intact in this model and cuprizone-induced demyelination is thought to be mediated by direct CNS effects which take place in the near absence of immune cells since Rag1-deficient mice lacking constitutively T and B cells are indistinguishable from wild type mice after cuprizone feeding (Matsushima and Morell, 2001; Hiremath *et al.*, 2008). The extent of demyelination differs regionally and temporally in species as well as in species strain (Skripuletz *et al.*, 2008; Taylor *et al.*, 2009).

One week after removal of the toxin spontaneous and complete remyelination occurs in young mice (Blakemore, 1973). Therefore, the murine cuprizone-induced de- and remyelination model is a widely used non-invasive model to investigate effects directly related to demyelination and remyelination within the CNS.

The exact mechanism of cuprizone-induced oligodendrocyte death is not well understood, but it is assumed that the copper chelator cuprizone leads to copper deficiency. However, administration of copper at high levels up to 100 ppm does not reduce cuprizone-induced effects suggesting that copper deficiency cannot be the major mechanism of cuprizone action (Carlton, 1967). It has been speculated whether a disturbed energy

metabolism might lead to oligodendrocyte death (Kipp *et al.*, 2009). Mitochondria are responsible for the energy metabolism by producing adenosine-5-triphosphate (ATP) and they are important for calcium homeostasis and apoptosis. Copper-containing mitochondrial enzymes such as monoamine oxidase, cytochrome oxidase and superoxide dismutase might cause a disturbance of energy metabolism due to copper chelating.

Previous studies indicate a crucial role of astrocytic NF- κ B activation for cuprizone-induced oligodendrocyte damage (Raasch *et al.*, 2011). In this study, inhibition of NF- κ B activation in I κ B kinase-deficient mice caused a preservation of cerebral myelin under cuprizone as well as reduced expression of pro-inflammatory mediators and decreased glial response. Only mice deficient in astrocytic, but not oligodendroglial, NF- κ B activation showed myelin preservation under cuprizone. Further support for an astrocytic contribution in this model comes from studies with mice constitutively deficient in the astrocytic adaptor protein Act1 (NF- κ B activator 1). These mice also show reduced cuprizone-induced demyelination (Kang *et al.*, 2012). Cuprizone-induced demyelination is also reduced in mice constitutively deficient in IL-17A and IL-17 receptor (Kang *et al.*, 2012). Neuropathological studies demonstrate that IL-17 is also expressed in astrocytes in MS lesions (Tzartos *et al.*, 2008).

Data on *in vitro* effects of cuprizone are controversial. Previous studies reported an inhibition of oligodendrocyte maturation without diminishing the numbers of precursors (Cammer, 1999). However, other studies indicated no direct effect of cuprizone on oligodendrocytes alone. Only the combination of cuprizone together with TNF α and/or IFN γ increased cell death (Pasquini *et al.*, 2007). A third study reported neither astrocytic nor microglial NF- κ B activation *in vitro* after cuprizone treatment, either alone or in combination with lipopolysaccharide (LPS) or TNF α (Raasch *et al.*, 2011).

1.3.3 Focal lysolecithin-induced demyelination

Lysolecithin (L- α -lysophosphatidyl choline; LPC) is a membrane solubilizing agent and has been used to induce focal areas of demyelination (Hall, 1972) in mice, rats, rabbits and cats. Stereotactic injection of LPC into the spinal white matter of rodents produces ellipsoid-shaped areas of demyelination (Woodruff and Franklin, 1999a; Blakemore and Franklin,

2008). So far, only few studies are published focusing on LPC-induced lesions in the corpus callosum of mice.

Focal injection of LPC leads at least partially to focal BBB leakage followed by infiltration of peripheral inflammatory cells. T cells, neutrophils and monocytes are seen at the injection site after 6-12 hours following LPC injection. At later time points, macrophages and microglia are recruited to the injection site and become activated (Ousman and David, 2000). Spontaneous remyelination starts a few days after LPC injection. In mice, remyelination takes place within three weeks after LPC injection, when most of the demyelinated axons are enwrapped by myelinating cells (Blakemore, 1976; Jeffery and Blakemore, 1995).

LPC is particularly toxic for myelin and partially spares oligodendrocytes (Blakemore and Franklin, 2008). Other studies claim direct toxic effects of LPC on myelin-producing cells (Woodruff and Franklin, 1999b). In addition, axons and astrocytes can also be affected around the injection site.

1.4 Treatment of inflammatory demyelinating diseases with the new drug laquinimod

1.4.1 Laquinimod in MS

Initially, Roquinimex® - the predecessor of laquinimod (LAQ) - demonstrated clinical efficacy in a phase II study showing significantly reduced MRI and clinical activity (Wolinsky *et al.*, 2000). However, phase III studies revealed cardiopulmonary toxicities of Roquinimex® leading to termination of development of the drug (Noseworthy *et al.*, 2000). Finally, LAQ was then produced by structural modifications that optimized efficacy and minimized toxicity (Jönsson *et al.*, 2004). In detail, the 5-H and 12-N-methyl groups on the Roquinimex® molecule were substituted by 5-Cl and 12-N-ethyl groups (Fig. 1).

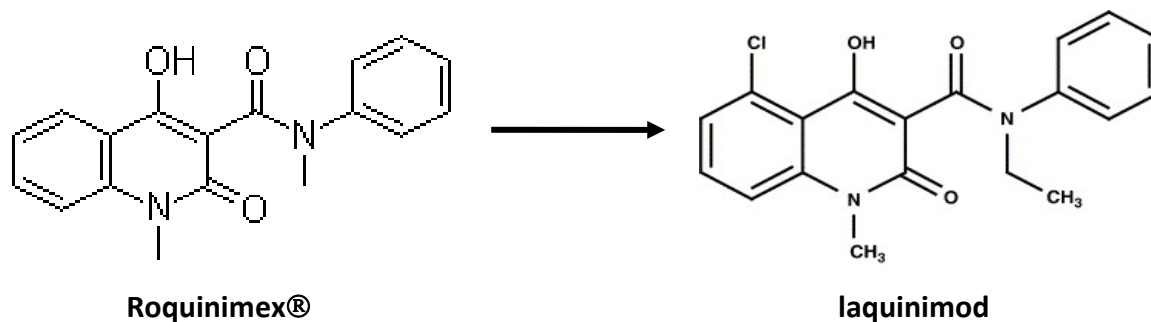


Fig. 1: Structural formula of Roquinimex® and laquinimod. The 5-H and 12-N-methyl groups on the Roquinimex® molecule are substituted by 5-Cl and 12-N-ethyl groups on the laquinimod molecule.

LAQ is an oral immunomodulatory substance that has been shown to be effective, safe and well-tolerated. Initial phase II studies indicated that LAQ reduced the formation of MRI-active lesions in RR-MS (Polman *et al.*, 2005; Comi *et al.*, 2008). Recent findings from the first phase III study “ALLEGRO” show that LAQ has even more pronounced effects on sustained disability progression as well as on brain atrophy compared to its effect on relapses (Comi *et al.*, 2012). In this phase III study, LAQ led to a significant reduction of the risk for sustained disability progression and of the rate of MRI-measured brain volume loss by about one-third. In the second phase III study “BRAVO”, adjusted to baseline expanded disability status scale and disease activity, LAQ reduced the annualised relapse rate by 21%, the risk of disability progression by 30% and brain volume loss by about 28%.

More evidence for a neuroprotective effect of LAQ comes from a recent study in which LAQ-treated MS patients show higher serum levels of brain-derived neurotrophic factor (BDNF) (Thöne *et al.*, 2012). Together with the clinical effects from the phase III studies “ALLEGRO” and “BRAVO”, these data suggest that LAQ might have direct CNS-protective effects in addition to its known peripheral anti-inflammatory properties. Analyses of transcriptional gene-expression profiles induced by LAQ *in vitro* in peripheral blood mononuclear cells (PBMC) derived from healthy subjects and RR-MS patients indicate that LAQ suppresses the NF- κ B pathway (Gurevich *et al.*, 2010).

Up to now, the observed discrepancy between more pronounced effects of LAQ on disability and brain atrophy than on relapses is not completely understood. An attractive hypothesis is that LAQ might exert effects not only on peripheral cells, but also on CNS-resident cells.

1.4.2 Laquinimod in EAE

As principle autoimmune animal model of MS, the EAE has proven useful in the development of new treatments such as LAQ for MS. Previous studies indicate that LAQ inhibits relapses in EAE when given before disease onset in mice (Brunmark *et al.*, 2002) and Lewis rats (Yang *et al.*, 2004) and when given after disease onset in C57BL/6 mice (Runstrom *et al.*, 2006). Previous studies using whole-body autoradiography demonstrate that 7% to 8% of LAQ penetrates through the intact BBB of naive mice and reaches the brain in relation to the blood concentration. In contrast, in EAE mice 13% to 14% of LAQ reaches the brain, since the BBB permeability is increased (Brück and Wegner, 2011). The analyses of cytokine profiles indicate that LAQ redirects the cytokine production in favour of the Th2/Th3 cytokines IL-4, IL-10 and transforming growth factor beta (TGF β) (Yang *et al.*, 2004).

In immunized C57BL/6 mice, clinical signs of EAE are reduced in a dose-dependent manner after preventive LAQ treatment at a dose of 5 mg/kg or 25 mg/kg (Wegner *et al.*, 2010). Therapeutic LAQ treatment at a dose of 25 mg/kg also reduces already present clinical signs of EAE. Furthermore, preventive and therapeutic LAQ treatment regimens lead to a reduction of clinical signs, inflammation and demyelination, which might be mediated by down-regulation of proinflammatory cytokines such as IL-17 by LAQ. Within EAE lesions, less acute axonal damage is observed in LAQ-treated animals compared to vehicle-treated mice (Wegner *et al.*, 2010).

Recent studies indicate that LAQ induces type II myeloid cells and increases regulatory T cells (Schulze-Topphoff *et al.*, 2012). The authors of this study suggest that LAQ modulates adaptive T cell immune responses by affecting cells of the innate immune system and hence may not influence T cells directly. Further studies demonstrate a more severe EAE disease course in BDNF conditional knockout mice lacking BDNF expression in myeloid cells as well as in T cells. These findings indicate that LAQ might act via modulation of BDNF (Thöne *et al.*, 2012). Other studies show that LAQ treatment leads to retention of proinflammatory monocytes in the blood, whereby LAQ reduces their entry into the CNS and prevents EAE (Mishra *et al.*, 2012).

These experimental data mainly confirm that LAQ has peripheral immune effects and also shows potential central effects on BDNF expression, but these data do not fully explain the neuroprotective effects observed in the phase III clinical trials “ALLEGRO” and “BRAVO”.

Up to now, there are no studies in non-inflammatory animal models to test whether LAQ directly affects CNS-resident cells.

1.5 Role of astrocytic factors in inflammatory demyelinating diseases

Astrocytes are thought to play an active and dual role in CNS inflammatory diseases such as MS. On the one hand, astrocytes can enhance the immune response and inhibit myelin repair. On the other hand they can be protective and limit CNS inflammation and support oligodendrocyte and axonal regeneration (Sofroniew, 2009).

As supportive glial cell component in neural tissue, astrocytes express GFAP which is a type III intermediate filament protein. A marked increase of GFAP is a major feature of complex changes occurring in astrocytes after demyelination and most other CNS injuries. GFAP is mainly expressed in astrocytes of the CNS, but also in multipotent radial neural stem cells of the brain and in astrocyte-related cells outside the CNS (Sofroniew and Vinters, 2010).

1.5.1 Astrocytic changes in MS

Astrocytes can prevent widespread tissue damage by formation of a glial scar around demyelinated lesions which serves as a physical barrier. However, hyaluron which is produced by reactive astrocytes accumulates in chronic demyelinated MS lesions and inhibits OPC maturation (Back *et al.*, 2005). Although it is not fully understood which role astrocytes play in MS, some studies strengthen that astrocytes might be important for MS. Previous studies show that reactive astrocytes in active and chronic MS lesions up-regulate the voltage-sensitive sodium channel Nav1.5 (Black *et al.*, 2010). Furthermore, GFAP is increased in CSF in patients with progressive MS (Malmeström *et al.*, 2003) and astrocytic IL-17 expression is found in active areas of MS lesions (Tzartos *et al.*, 2008). Additionally, serum levels of antibodies to the astrocytic inwardly rectifying potassium channel (KIR) 4.1

are elevated in MS patients compared to healthy persons or those with other neurological diseases (Srivastava *et al.*, 2012).

Further evidence for an important role of astrocytes in demyelinating diseases comes from the related disease neuromyelitis optica (NMO). NMO causes inflammatory demyelinating lesions primarily in the spinal cord and optic nerve, but also in the brain. This disease is characterized by serum autoantibodies directed against the astrocytic water channel aquaporin-4 (AQP4) (Lennon *et al.*, 2005). NMO lesions are distinguished by a loss of AQP4, GFAP, as well as subsequent loss of oligodendrocytes leading to demyelination. Infiltration of granulocytes and macrophages as well as perivascular deposits of activated complement is found in the lesions. It is suggested that complement-dependent astrocyte cytotoxicity is involved in NMO leading to leukocyte infiltration, cytokine release and BBB disruption causing oligodendrocyte death as well as myelin loss (Lucchinetti *et al.*, 2002; Misu *et al.*, 2006).

1.5.2 Astrocytic changes in EAE

For a better understanding of MS and other diseases it is of high interest whether astrocytes have a detrimental or beneficial role after CNS injuries or after CNS defects. Therefore, generation of mice with altered GFAP expression provides a useful tool to study astrocytic changes in animal models of MS. Mice constitutively deficient for GFAP demonstrate a more severe disease course in EAE compared to wild type mice (Liedtke *et al.*, 1998). Furthermore, conditional inhibition of reactive astrocytosis by administration of ganciclovir in mice expressing the herpes simplex virus thymidine kinase under the mouse GFAP promoter results in more severe EAE and increased macrophage infiltration (Toft-Hansen *et al.*, 2011). Further studies investigating the role of astrocytes in wild type SJL/J mice with EAE report a down-regulation of connexin 43, the major gap junction protein of astrocytes, in inflamed white matter (Brand-Schieber *et al.*, 2005).

1.6 The astrocytic leukodystrophy Alexander`s disease and its related animal model

1.6.1 Alexander`s disease

Alexander`s disease (AxD) is a rare and typically fatal disorder. Up to now, about 550 cases of AxD have been reported. The disease was first characterized in 1949 by William Stewart Alexander who described a 15-month-old boy with a rapidly progressing neurological illness associated with a hydrocephalus (Alexander, 1949). AxD is classified as leukodystrophy since it mainly affects white matter accompanied by a severe myelin deficit particularly in the frontal lobes.

Histological postmortem studies show extensive astrocytic inclusions known as Rosenthal fibers. These Rosenthal fibers, the pathological hallmark of AxD, are formed by cytoplasmic protein aggregates within astrocytes. These aggregates contain GFAP, vimentin, the cytoskeletal crosslinker plectin, ubiquitin, the small heat shock proteins 25 and α B-crystallin (Iwaki *et al.*, 1993; der Perng *et al.*, 2006; Tian *et al.*, 2006).

The disease is divided in three forms based on the age of onset and the type of symptoms: Infantile, juvenile and adult form. The infantile type of the disease is the most aggressive, fatal and frequent form (80% of all cases) starting between the age of one month and two years. Clinical symptoms include progressive megalencephaly, seizures, progressive spastic paresis, mental regression, epilepsy, ataxia and hydrocephalus (Alexander, 1949; Borrett and Becker, 1985). The juvenile form (14% of all cases) starts between four to ten years of age. Patients typically suffer from dysphasia. Death ensues within several years after onset to the late teens with occasional longer survival. Almost all cases of infantile and juvenile AxD are sporadic. Adult cases are rare (6% of all cases). The adult form starts at the age of 20 to 45 years and symptoms can be similar to MS or the juvenile form (Seil *et al.*, 1968; Howard *et al.*, 1993; Schwankhaus *et al.*, 1995). The most frequent symptoms are related to bulbar dysfunction like dysarthria and dysphasia. It is the mildest type with longer survival times. However, rare familial cases of adult AxD have been reported showing a dominant or recessive mode of inheritance suggesting a genetic origin of the disease (Wohlwill *et al.*, 1959; Honnorat *et al.*, 1993; Howard *et al.*, 1993; Schwankhaus *et al.*, 1995).

AxD was the first human disorder found to be related to an isolated and genetically defined dysfunction of astrocytes. About 95% of AxD patients show mutations in the astrocytic intermediate filament GFAP (Brenner *et al.*, 2001). These mutations are heterozygous and found within the human GFAP gene on chromosome 17q21 (Bongcam-Rudloff *et al.*, 1991). However, in rare cases of AxD no mutations in the GFAP coding region or adjacent introns have been found. More than 40 GFAP mutations have been reported, but over a third of all patients carry mutations in arginine residues in either of two amino acids, R79 (17% of all cases) or R239 (20% of all cases) (Prust *et al.*, 2011). The most frequent mutations are heterozygous point mutations within the coding sequence (R79H, R239Cys, R239H) (Rodriguez *et al.*, 2001; Li *et al.*, 2005). The phenotype of R239 mutations results in more severe clinical disease than the mutation of the R79 site.

The diagnosis of AxD involves MRI examination as well as genetic testing and only in rare cases a brain biopsy. Typical cases display widespread MRI changes involving extensive frontal white matter changes, periventricular changes as well as abnormalities of basal ganglia, thalami and brain stem (van der Knaap *et al.*, 2001). However, in atypical cases of AxD the pathological examination of brain tissue at biopsy is necessary to confirm the diagnosis. However, most cases of AxD can be diagnosed by DNA analysis of PBMCs (Brenner *et al.*, 2001).

1.6.2 Human GFAP overexpressing transgenic mice

Messing and colleagues generated and first described human GFAP overexpressing mice (Messing *et al.* 1998). The constitutively elevated expression of human GFAP in these animals is driven by the human GFAP promoter. The mice are hemizygous for the transgene and are generally viable and fertile. Only animals with very high levels of this transgene die within a few weeks after birth. Furthermore, the degree of overexpression increases with age. The homology between human and mouse GFAP is relatively high (91% identity and 95% similarity at the amino acid level) (Brenner *et al.*, 1990), but it seems likely that this 5% difference in amino acids together with the expression level contribute to the clinical and pathological changes observed in mice overexpressing human GFAP.

Astrocytes of mice overexpressing human GFAP show intracellular eosinophilic protein aggregates that appear histologically identical to Rosenthal fibers of AxD. The finding of Rosenthal fibers in brains of these transgenic animals led to the discovery of dominant GFAP mutations in AxD (Messing *et al.*, 1998). Mice overexpressing human GFAP at levels approximately 3-5 fold over endogenous baseline levels show Rosenthal fibers and are further referred to as line 73.7 or Tg(hGFAP) animals in this thesis (Messing *et al.*, 1998; Cho and Messing, 2009). Astrocytes of this transgenic line are also hypertrophic and up-regulate small heat shock proteins.

Microarray analyses of the transcription profiles in these Tg(hGFAP) mice show marked immune and stress responses leading to an apparent loss of neurons or neuronal dysfunction in animals which are severely affected, but still viable (Hagemann *et al.*, 2005). Differences in the astrocytic-neuronal interactions in distinct regions of these Tg(hGFAP) mice were reported (Meisingset *et al.*, 2010). The authors of this study found an impaired astrocytic and neuronal metabolism in the cerebral cortex of these transgenic animals and a decreased transfer of glutamine from astrocytes to neurons compared to wild type mice. In the cerebellum of these Tg(hGFAP) animals, glutamine appeared increased and evidence for brain edema was found in an increased amount of brain water and the osmoregulators myo-inositol and taurine (Meisingset *et al.*, 2010).

In vitro studies of these Tg(hGFAP) mice indicate that astrocytes of these animals are more vulnerable and compromised than astrocytes of wild type mice. Astrocytes of these transgenic animals show an increased formation of cytoplasmic inclusions similar to Rosenthal fibers in 28% of GFAP-positive cells. Furthermore, these Tg(hGFAP) mice demonstrate a reduced astrocytic growth rate which is partially reflected by a decreased cell proliferation as well as an increased cell death of their cultured astrocytes. The proteasomal activity appears to be reduced by 35% compared to wild types and the cytoskeleton seems to be disrupted in these transgenic animals. Additionally, these Tg(hGFAP) mice show a compromised astrocytic resistance to stress which is indicated by an increased sensitivity to H₂O₂ (Cho and Messing, 2009). In the present thesis, only these Tg(hGFAP) mice (line 73.7 with moderate overexpression of human GFAP) were used for the described experiments.

1.7 Aims

The overall aim of the present study is to examine intrinsic and therapy-induced glial - in particular astrocytic - effects on cuprizone-induced pathology in mice. The first aim of the present work is to study the effects of LAQ on toxic demyelination. The second part intends to evaluate the impact of increased GFAP expression on cuprizone-induced changes. A further minor aim of this study is to assess the effects of cuprizone *in vitro* and *in vivo*.

LAQ is a new oral immunomodulatory drug for MS that has well-documented effects on inflammation in the periphery, but up to now, little is known about its direct activity within the CNS. The aim of the first part of this work is to elucidate the impact of LAQ on CNS-intrinsic inflammation. Therefore, this project will investigate the effects of LAQ on cuprizone-induced de- and remyelination *in vivo*. To assess the effects on oligodendrocytes, apoptosis and oligodendroglial density will be evaluated in LAQ-treated and vehicle-treated wild type animals after one week of cuprizone. Demyelination, inflammation, axonal damage and glial pathology will be examined after six weeks of cuprizone treatment in LAQ-treated and vehicle-treated wild type mice. To test whether LAQ exerts effects independent of T and B cells, Rag1-deficient mice will also be treated with or without LAQ during cuprizone challenge. NF- κ B activation in astrocytes will be investigated in LAQ-treated and vehicle-treated animals. Remyelination will also be evaluated in LAQ-treated as well as vehicle-treated wild type mice. Secondly, the effect of LAQ on demyelination will be also examined in a second model with focal rapid demyelination, the LPC-induced demyelination model.

Mice overexpressing human wild type GFAP [Tg(hGFAP)] show an increased astrogliosis even without external stimuli. The aim of the second part of this work is to examine the impact of an increased astrogliosis on cuprizone-induced demyelination *in vivo*. Apoptosis and numbers of oligodendrocytes will be investigated in Tg(hGFAP) animals after one week of cuprizone. Demyelination, inflammation, axonal damage and glial pathology will be assessed after six weeks of cuprizone treatment in these mice. In addition, NF- κ B activation in astrocytes will also be investigated in these transgenic animals.

The third part of this work investigates direct effects of cuprizone on astrocytes *in vitro* and *in vivo*. First, the effect of cuprizone on astrocytic viability will be assessed *in vitro*.

Secondly, local effects of focal intracerebral cuprizone injection on myelin, oligodendrocytes and astrocytes will be evaluated *in vivo*.

The overall aim of this study is to investigate intrinsic and therapy-induced astrocytic effects on cuprizone-induced pathology in mice. The findings from this project might contribute to a better understanding of the complex disease MS and enable the development of novel protective therapies restricting tissue damage in demyelinating diseases such as MS.

2 Materials and methods

2.1 Materials and solutions

2.1.1 Chemicals

Chemicals	Provider
Acetic acid, 10% solution	Merck Millipore, Germany
Agarose	StarLab GmbH, Germany
AgNO ₃ (silver nitrate)	Carl Roth, Germany
Ammonium chloride (10x)	BD Biosciences, Germany
Ammonia solution, 32%	Merck Millipore, Germany
Azure II, powder	Merck Millipore, Germany
Boric acid	Carl Roth, Germany
Di-sodium tetraborate decahydrate (borax)	Merck Millipore, Germany
Chloral hydrate	Fagron GmbH & Co. KG, Germany
Citric acid	Merck Millipore, Germany
Cuprizone	Sigma-Aldrich, Germany
CuSO ₄ (copper(II) sulfate)	Merck Millipore, Germany
DAB (3,3'-diaminobenzidine)	Sigma-Aldrich, Germany
DAPI (4',6-diamidino-2-phenylindole)	Sigma-Aldrich, Germany
DDSA (dodeceny succinic anhydride)	Serva Electrophoresis, Germany
DePeX mounting medium	VWR International, Germany
DMP-30 (2,4,6 tri(dimethylaminomethyl) phenol)	Serva Electrophoresis, Germany
dNTP (desoxynucleoside triphosphate) mix	Fermentas, Germany
DMEM [Dulbecco's modified eagle medium) (High glucose (4.5 g/l)]	PAA laboratories, Germany
Eosin G	Merck Millipore, Germany
Ethanol, 96%	Merck Millipore, Germany
Ethidium bromide	Sigma-Aldrich, Germany
EDTA (ethylenediamine tetraacetic acid disodiumsalt dihydrate)	Carl Roth, Germany

Chemicals	Provider
FCS (fetal calf serum)	Biochrom AG, Germany
Formalin (37% formaldehyde solution, free from acid)	Merck Millipore, Germany
GeneRuler™, 100 base pairs (bp) DNA ladder Plus	Fermentas, Germany
Glutaraldehyde, 25% aqueous solution	Merck Millipore, Germany
Ground mouse chow (complete feed for rats & mice-maintenance, ground)	Ssniff Spezialdiäten GmbH, Germany
HBSS (Hank's buffered salt solution)	Gibco, Germany
HCl (hydrochloric acid)	Merck Millipore, Germany
Hydrogen peroxide, 30% solution	Merck Millipore, Germany
Isopropyl alcohol	Merck Millipore, Germany
Ketamine, 10%	Inresa Arzneimittel GmbH, Germany
LAQ (laquinimod) (ABR-215062) (RLB#054 M0004)	TEVA Pharmaceutical Industries, LTD, Israel
LFB (luxol fast blue)	BDH Laboratory supplies, VWR Int. Ltd., Poole, UK)
Lithium carbonate	Merck Millipore, Germany
LPS (lipopolysaccharide)	Sigma-Aldrich, Germany
Lysolecithin (L- α -lysophosphatidyl choline)	Sigma-Aldrich, Germany
Mayers Hämalaun	Merck Millipore, Germany
Metapyrin, 500 mg/ml	Serumwerk Bernburg AG, Germany
Methylene blue	Merck Millipore, Germany
Monastral blue	Sigma-Aldrich, Germany
NaCl (sodium chloride), 0.9% solution	B. Braun Melsungen AG, Germany
NaOH (sodium hydroxide solution), 1 M	Merck Millipore, Germany
Nitric acid, 65% solution	Merck Millipore, Germany
Osmium tetroxide, powder	Carl Roth, Germany
Paraffin (paraplast plus)	Tyco Healthcare, Germany
PBS (Dulbecco's phosphate-buffered saline): 10x powder	Biochrom AG, Germany
PBS, sterile	PAA laboratories, Germany
PCR buffer, 5x Green GoTaq® Reaction buffer	Promega, Germany
Pen/strep (penicillin/streptomycin)	Gibco, Germany

Chemicals	Provider
Periodic acid	: Merck Millipore, Germany
PFA (paraformaldehyde), powder	: Merck Millipore, Germany
PLL (poly-L-lysine hydrobromide), powder	: Sigma-Aldrich, Germany
Renlam M-1	: Serva Electrophoresis, Germany
Schiff's reagent	: Sigma-Aldrich, Germany
SDS (sodium dodecyl sulfate), 10% solution	: Sigma-Aldrich, Germany
Sodium thiosulfate pentahydrate	: Merck Millipore, Germany
Tris	: Carl Roth, Germany
Triton X-100	: MP Biomedicals, Germany
Trypsin-EDTA (0.05% and 0.25% solution)	: Gibco, Germany
Trizma base	: Sigma-Aldrich, Germany
Xylazine (Xylarium®)	: Riemser Arzneimittel AG, Germany
Xylol	: Merck Millipore, Germany

2.1.2 Enzymes/proteins

Enzymes/proteins	Provider
DNase I	: Roche, Germany
ExtrAvidin peroxidase, 0.1% solution	: Sigma-Aldrich, Germany
Go-Taq DNA polymerase	: Promega, Germany
IFN γ , recombinant	: R&D Systems, USA
IL-1 β , recombinant	: R&D Systems, USA
Proteinase K	: Sigma-Aldrich, Germany
TNF α , recombinant	: R&D Systems, USA

2.1.3 Kits

Kits	Provider
CellTiter 96® Proliferation Assay	: Promega, Germany
CytoTox-One™ Assay	: Promega, Germany

2.1.4 Consumables

Consumables	Provider
BD Falcon™ cell culture flask, 75 cm ²	: BD Biosciences, Germany
BD Falcon™ tube, 50 ml	: BD Biosciences, Germany
Corning® syringe filters, sterile	: Sigma-Aldrich, Germany
Glass capillary, micropipettes 1-5 µl	: B. Braun Melsungen AG, Germany
Glass microscope slides, 76x26 mm/3x1 inch	: Knittel Glasbearbeitungs GmbH, Germany
Neubauer counting chamber (surface 0.0025 mm ²):	Brand GmbH, Germany
Ocular counting grid, WHSZ 10X-H	: Olympus, Germany
Petri dish	: Greiner Bio-One GmbH, Germany
12-well tissue culture plates 665180, sterile	: Greiner Bio-One GmbH, Germany
96-well cell culture plates 655180, sterile	: Greiner Bio-One GmbH, Germany

2.1.5 Technical devices

Technical devices	Provider
Camera for light microscope DP71	: Olympus, Germany
Camera for fluorescence microscope XM10	: Olympus, Germany
Cell incubator CWJ300DABA	: Cellstar, Nunc GmbH, Germany
Centrifuge 5810 R	: Eppendorf, Germany
Dental drill control tool K44974	: Kavo, Dental Excellence, Germany
Dental drill 4912	: Kavo, Dental Excellence, Germany
Fluorescence microscope BX51	: Olympus, Germany
Inertsil ODS-4 chromatographic column (3 µm, 75 x 2.1 mm equipped with guard column Inertsil ODS-4, 3 µm, 10 x 1.5 mm)	: GL Sciences, USA
Light microscope BX41	: Olympus, Germany
Mass spectrometer TSQ Quantum Ultra AM	: Thermo Finnigan, Germany
Microtome SM2000R	: Leica, Germany
Microwave NN-E201W	: Panasonic, Germany
T3 Thermocycler	: Biometra, Germany

Technical devices	Provider
Speed vacuum Concentrator 5301	: Eppendorf, Germany
Stereotactic device STO-51730	: FMI GmbH-Stoelting, Germany
Safire plate reader	: Tecan, Germany
Tissue processor TP 1020	: Leica, Germany
Thermo mixer comfort	: Eppendorf, Germany

2.1.6 Solutions

Chloral hydrate, 14% solution	: 14 g chloral hydrate 100 ml bidistilled water
DAPI	: 1 μ l DAPI 10,000 μ l PBS
Ketamine/xylazine mixture	: 1.2 ml ketamine 1 ml xylazine 7.8 ml NaCl
Lysolecithin, 1% solution (Hall, 1972)	: 10 mg lysolecithin 1 ml sterile PBS
Metapyrin	: 3 ml Metapyrin® 1 l water
Monastral blue, 3% solution	: 0.3 g Monastral blue 10 ml sterile PBS Filtration
PFA, 4% solution	: 40 g PFA 1,000 ml 1-fold PBS 50 μ l NaOH, adjust to pH 7.4 Filtration

Tail lysis buffer	:	6.057 g Tris 400 ml bidistilled water HCl, adjust to pH 8.5 5 ml 5 mM EDTA 20 ml 200 mM NaCl 10 ml 0.2% SDS
TBE buffer	:	10.8 g Tris 5.5 g boric acid 4 ml 0.5 M EDTA 1,000 ml water

Electron microscopy (EM)

Glutaraldehyde, 3% solution	:	12 ml 25% glutaraldehyde 88 ml PBS
Richardson`s Stain (Richardson <i>et al.</i> , 1960)	:	2 ml 1% Azure II 1 ml 2% Methylene blue 1 ml 1% Borax
Synthetic resin	:	27 ml Renlam M-1 23 ml DDSA 0.75-1 ml DMP-30

(Immuno-) histochemistry

AgNO ₃ , 20% solution	:	10 g AgNO ₃ 50 ml distilled water
Citric acid buffer, 10 mM	:	2.1 g citric acid 1,000 ml distilled water NaOH, adjust to pH 6

CuSO ₄ working solution	:	1 ml 2% CuSO ₄ 50 ml NaCl
DAB working solution	:	49 ml PBS 1 ml DAB 20 µl hydrogen peroxide
Developer stock solution	:	20 ml formalin 0.5 g citric acid 100 µl nitric acid 500 ml distilled water
Eosin, 1% solution	:	2 ml eosin 198 ml 70% isopropyl alcohol, Filtration
LFB working solution	:	1 g LFB 1 l ethanol 5 ml acetic acid (add after complete solution of LFB) Filtration
Sodium thiosulfate, 2% solution	:	10 g sodium thiosulfate pentahydrate 500 ml distilled water
Tris-EDTA, 1 mM	:	1.21 g Trizma base 1 ml 0.1 M EDTA 1,000 ml distilled water Adjust to pH 8
Triton, 1% solution	:	100 µl Triton X-100 10 ml PBS

Cell culture

DMEM+ working solution	:	500 ml DMEM
		50 ml inactivated FCS
		5 ml pen/strep
		Sterile filtration

2.1.7 Software

Software		Provider
Analysis TM	:	Olympus, Germany
GraphPad Prism	:	GraphPad, California, USA
SPSS 12	:	IBM, Germany

2.2 Animal experiments**2.2.1 Mice**

8- to 10-weeks-old Tg(GFAP)10Mes, Rag1^{tm1Mom}, and male C57BL/6J mice were used in these experiments. Tg(GFAP)10Mes animals overexpressing human GFAP and were from now on referred to as Tg(hGFAP). They were obtained on FVB/N genetic background and backcrossed to C57BL/6N. Their wild type littermates served as controls. Rag1^{tm1Mom} mice lacking T and B cells and were from now on referred to as Rag1^{-/-} animals. They were developed and first described by Mombaerts (Mombaerts *et al.*, 1992).

Mice	Provider
C57BL/6J	Charles River, Germany
Tg(hGFAP) (C57BL/6N background)	Animal facility of the University of Göttingen
Rag1 ^{-/-} (C57BL/6J background)	Animal facility of the University of Göttingen Jackson Laboratories, USA

All mice were kept in groups up to 5 animals on a 12/12 hour (h) light/dark cycle with food and water *ad libitum*. Mice were acclimated to the new environment for at least 7 days before experiments were started. Animal experiments were conducted in accordance with the European Communities Council Directive of 24 November 1986 (86/EEC) and were approved by the Government of Lower Saxony, Germany. Each experiment contained 6-8 mice per treatment group and was performed at least twice. The analyses of naïve Tg(hGFAP) and wild type mice were performed using 3-8 animals per group.

2.2.2 Genotyping of transgenic mice

2.2.2.1 DNA extraction

For genotyping, DNA was extracted from tail or ear tissue of Tg(hGFAP) and Rag1^{-/-} mice. Therefore, 350 µl tail lysis buffer containing 20 µl proteinase K was added to the tissue and digested over night in a thermo mixer at 350 rounds per minute (rpm) and 56°C. Digested tissue was centrifugated for 5 minutes (min) at 13,200 rpm at room temperature. Supernatant was transferred to a new tube and 350 µl isopropyl alcohol was added. Supernatant mixture was centrifugated again for 5 min at 13200 rpm at room temperature. Supernatant was rejected and pellet was washed with 350 µl 70% ethanol. After removing the supernatant by centrifugation, pellet was dried for 10 min by speed vac and then resuspended in 100 µl bidistilled water.

2.2.2.2 Genotyping of Tg(hGFAP) mice

Amplification of DNA *in vitro* was carried out by polymerase chain reaction (PCR). This reaction included 2 µl of the extracted DNA from mice as template, 1 µl 10 mM dNTP Mix, 2 µl oligonucleotide primer (MB-114, Pr. 35, each 1 µl), 0.2 µl Go-Taq polymerase, 5 µl of the supplied buffer (5x PCR buffer) and 14.8 µl bidistilled water.

Primer for Tg(hGFAP)	Sequence	Provider
MB-114	5'-CTC ATA CTC ATG ATG GGG AG-3'	Promega, Germany
Pr. 35	5'-AAC AGC CTA TGG AGG GAC TG-3'	Promega, Germany

All PCR reactions were run on a T3 thermocycler with cycle parameters listed below.

95°C	180 seconds (s)		Pre-denaturation
95°C	40 s	} 35 cycles	Denaturation
62°C	30 s		Annealing
72°C	60 s		Elongation
72°C	600 s		Final elongation
4°C	∞		Storage

For visualization of PCR products, 10 µl of the probes were loaded on a 1.8% agarose gel (1.8 g agarose diluted in 100 ml TBE buffer) containing 3 µl ethidium bromide. Electrophoresis was performed at 100 Volt (V) for 60 min. One single PCR product of 381 bp labeled heterozygous Tg(hGFAP) mice (mice that are homozygous for the transgene are not viable). 5 µl of a 100 bp DNA ladder was used to estimate PCR product length.

2.2.2.3 Genotyping of Rag1-deficient mice

This reaction included 2 µl of the extracted DNA from mice as template, 1 µl 10 mM dNTP Mix, 3 µl oligonucleotide primer (oIMR1746, oIMR3104, oIMR8162, 1 µl each), 0.2 µl Go-Taq polymerase, 5 µl of the supplied buffer and 13.8 µl bidistilled water.

Primer for Rag1 ^{-/-} mice	Sequence	Provider
oIMR1746	5'- GAG GTT CCG CTA CGA CTC TG-3'	Promega, Germany
oIMR3104	5'- CCG GAC AAG TTT TTC ATC GT-3'	Promega, Germany
oIMR8162	5'- TGG ATG TGG AAT GTG TGC GAG-3'	Promega, Germany

All PCR reactions were run on a T3 thermocycler with cycle parameters listed below.

94°C	120 s		Pre-denaturation
94°C	30 s	} 35 cycles	Denaturation
58°C	45 s		Annealing
72°C	45 s		Elongation
72°C	120 s		Final elongation
4°C	∞		Storage

Probes were then loaded on an agarose gel and electrophoresis was performed as described above. One single PCR product at 530 bp labeled mice that are homozygous for the Rag1 mutation. Two PCR products of 530 bp and 474 bp (PCR product of wild type mice) labeled heterozygous Rag1 mice. A 100 bp DNA ladder was used to estimate PCR product length.

2.2.3 Cuprizone treatment

Cuprizone is a copper chelator and is known to induce toxic demyelination. At 8 to 10 weeks of age, wild type C57BL/6J, Tg(hGFAP) and Rag1^{-/-} mice received a 0.25% cuprizone diet *ad libitum*. Therefore, 2.5 g cuprizone was mixed into 1,000 g ground mouse chow. To investigate apoptosis, animals received cuprizone diet for 1 week. For studying effects on demyelination of the corpus callosum, mice were fed with cuprizone for 6 weeks. Body weights of animals were controlled once per week. Body weights of Tg(hGFAP) mice were converted in percent since transgenic animals were much smaller than their wild type littermates. The mean of the initial body weights of Tg(hGFAP) mice was set to hundred percent and the subsequent body weights of transgenic animals during cuprizone challenge were then converted in relation to the original weight at the beginning of the experiment. The same process was then applied for the body weights of wild type littermates. Graphs of body weights of wild type C57BL/6, Tg(hGFAP) and Rag1^{-/-} mice were shown in mean values of body weight with standard errors of the mean (SEM).

For investigating effects on remyelination in wild type C57BL/6, cuprizone diet was first fed for 6 weeks, cuprizone was then removed from the diet and mice were fed for the

following 4 days with ground mouse chow. Remyelination started after withdrawal of cuprizone.

2.2.4 Extraction of mouse sera

8-weeks-old male C57BL/6J mice received 0.25% cuprizone for 1 week. 9-weeks-old naïve male C57BL/6J animals served as controls. For mass spectrometry analyses, mice were sacrificed after 1 week of 0.25% cuprizone by i. p. injection of 200 µl 14% chloral hydrate solution. Blood samples were collected and serum was separated by centrifugation for 15 min at 4°C and 1,000 rpm. The sera for mass spectrometry and *in vivo* and *in vitro* experiments were stored at -80°C.

2.2.5 Laquinimod treatment

LAQ was synthesized at TEVA Pharmaceutical Industries, Ltd. The compound was dissolved in water. The solution was stored at 4°C and used within 1 week of preparation. C57BL/6J mice were treated daily with 5 or 25 mg/kg LAQ. Rag1^{-/-} mice were treated daily with 25 mg/kg. LAQ was administered orally by gavage at a volume of 0.2 ml. Control animals received vehicle (water). For investigating effects on cuprizone-induced demyelination, daily LAQ treatment was administered together with the cuprizone diet for 1 week or 6 weeks. For investigating effects on remyelination, LAQ treatment started after withdrawal of cuprizone after 6 weeks and was carried out for the period of remyelination of 4 days. For examining effects on LPC-induced demyelination, daily treatment with 25 or 40 mg/kg LAQ started 3 days before stereotactic injection and was carried out until 4 days after injection.

2.2.6 Intracerebral stereotactic injection

C57BL/6J mice were first anaesthetized by i. p. injection of ketamine/xylazine mixture (100 µl/10 g body weight of mouse). After loss of consciousness, a rostro-caudal cut on the

top of the head was made to expose the skull. Animals were fixed on a stereotactic device. A fine hole was drilled through the skull 1 mm caudal and 2 mm sagittal to the bregma by a dental drill. To avoid damage to the brain, drilling was stopped until only a thin layer of bone was left. The remaining thin bone layer was then carefully removed by a fine scraper giving access to the brain surface. Monastral blue solution was added to the injection substances (LPC, cuprizone, PBS, serum from naïve or cuprizone-treated mice) to mark the injection site. This mixture was inserted stereotactically into the corpus callosum by a finely calibrated glass capillary. The injection substances were slowly administered to avoid tissue damage. After injection the capillary was carefully removed and the skin was sutured. For pain therapy, animals were treated with Metapyrin. Metapyrin administration started 1-2 days before and was carried out for 2 days after stereotactic injection.

2.2.6.1 Focal demyelination induced by lysolecithin

LPC is a membrane-solubilizing agent which is toxic especially for myelin. At 9 to 10 weeks of age male C57BL/6J mice were intracerebrally, stereotactically injected with 1 µl 1% LPC into the corpus callosum to induce focal demyelination. LPC was diluted in sterile PBS. Controls were injected with PBS (vehicle). Animals were sacrificed 4 days after injection.

Experiments investigating the effect of 25 mg/kg LAQ on LPC-induced demyelination were performed using 7 mice in the control group and 5 animals in the LAQ group. Experiments evaluating the effect of 40 mg/kg LAQ on LPC-induced demyelination were performed using 3 mice in the control group and 4 animals in the LAQ group.

2.2.6.2 Stereotactical injection of cuprizone or serum

To test for potential direct effects of cuprizone or serum after focal cerebral administration, 1 µl of one of the following four agents were injected stereotactically into the corpus callosum of 9- to 10-weeks-old male C57BL/6J mice. Animals received stereotactic injections of either (1) 200 µM cuprizone diluted in sterile PBS, (2) vehicle (PBS), (3) pure serum from cuprizone-treated mice to examine whether a metabolite of cuprizone

leads to cuprizone-induced pathology or (4) pure serum from 9-weeks-old naïve male C57BL/6J animals.

All mice were sacrificed 4 days after stereotactic injection. Experiments with each agent were performed with at least 3 animals for the four different groups.

2.3 Histology

After completion of experiments, mice were injected i. p. with a lethal dose of 14% chloral hydrate solution. After loss of consciousness and protective reflexes, transcardial perfusion was performed through the left heart ventricle with PBS followed by 4% PFA. Brains, livers and spleens were collected and stored in 4% PFA at 4°C for 2 days post-fixation. Then tissue samples were transferred in PBS. For cuprizone experiments, brains were dissected in at least 4 transverse sections. For stereotactical injections, one brain section including the injection site was cut following the Monastral blue trace. For paraffin embedding, tissue was washed in water and then gradually dehydrated over night by performing a graded alcohol/xylene/paraffine series using an automated tissue processor. Histological evaluation was performed on 1 µm thick sections using a sliding microtome.

Prior the staining procedure tissue sections were deparaffinized for at least 30 min at 54°C and rehydrated. Rehydration steps were done as follows:

4x	10 min	xylol
1x	5 min	isoxylol
2x	5 min	100% isopropyl alcohol
1x	5 min	90% isopropyl alcohol
1x	5 min	70% isopropyl alcohol
1x	5 min	50% isopropyl alcohol
Distilled water		

After the staining procedure, stained sections were dehydrated by performing above described series in reversed order with only 2-3 min incubation time to avoid excessive weakening of the staining. Finally, stained sections were mounted in DePex medium.

2.3.1 Histochemical staining

2.3.1.1 Hematoxylin and eosin (HE) staining

For a general overview of the sections, HE staining was performed especially with regard to inflammation and apoptosis. Rehydrated sections were incubated for 8 min in Mayers Hämalaun. Tissue sections were then incubated shortly in 1% HCl and were washed in distilled water for differentiation of the tissue. Bluing was done by rinsing slides in running water for 10 min. Slides were incubated shortly in distilled water and transferred in 1% eosin solution for 6 min.

2.3.1.2 Luxol fast blue-periodic acid Schiff (LFB-PAS) staining

To assess the extent of demyelination, LFB-PAS staining was performed. After the 90% isopropyl alcohol rehydration step, sections were incubated in LFB working solution at 60°C over night. Next day, tissue sections were washed with 90% isopropyl alcohol. For differentiation, the following 3 steps were repeated until only the myelin was stained deep blue: Sections were first incubated shortly in 0.05% lithium carbonate (diluted in water), incubated shortly in 70% isopropyl alcohol and then washed extensively in distilled water to stop differentiation. Stained sections were transferred in 1% periodic acid (diluted in water) for 5 min and then washed thoroughly in distilled water. Sections were stained in Schiff's reagent for 20 min. Slides were washed under running water for 10 min. Counterstaining was performed by transferring tissue sections for 3 min in Mayers Hämalaun. Slides were washed in distilled water and incubated shortly in 1% HCl. After washing shortly in distilled water, bluing was achieved by rinsing slides in running water for 10 min.

2.3.1.3 Bielschowsky silver impregnation

Bielschowsky silver impregnation was performed to investigate axonal integrity. Rehydrated sections were transferred in AgNO₃ solution and incubated for 20 min. Tissue sections were washed with distilled water. Ammonia solution was added drop by drop to the AgNO₃ solution until the formed precipitation cleared up. Sections were transferred in

this cleared mixture and incubated in the dark for 15 min. Slides were then transferred in 50 ml bidistilled water containing 150 µl ammonium chloride. 500 µl developer stock solution was then added to the AgNO₃/ammonium chloride solution which was used previously. Slides were transferred in this solution for about 3 to 5 min until the axons were stained black and the color of the tissue turned to ochery. Tissue slides were washed in bidistilled water and transferred in 2% sodium thiosulfate solution for 2 min.

2.3.2 Immunohistochemistry and fluorescence staining

Immunohistochemistry was performed with antibodies against activated microglia (Mac3), acutely damaged axons (amyloid precursor protein; APP), GFAP (polyclonal), mature oligodendrocytes (NogoA), MBP, CNPase and apoptosis (active caspase3). Immunofluorescence staining involved antibodies against NF-κB and GFAP (monoclonal). Tissue sections were pre-treated by heating 10 mM citric acid buffer or 1 mM Tris-EDTA buffer in a microwave for 5 times (3 min each). Therefore, tissue sections were transferred in glass cuvettes filled with corresponding buffer. Glass cuvettes were then refilled alternately after each microwave step with distilled water or corresponding buffer to dilute buffer. For staining against the polyclonal GFAP antibody, sections were only washed in PBS instead of pre-treatment in a microwave. To block endogenous peroxidase, all sections were first washed in PBS and then incubated for 20 min in 3% hydrogen peroxide solution at 4°C. After 3 washing steps with PBS, sections were blocked for 20 min with 10% FCS in PBS at room temperature to inhibit unspecific antibody binding. Caspase3 staining required treatment with 1% Triton solution for 1 h instead of FCS. Primary antibodies (Tab. 1) were diluted in 10% FCS in PBS and incubated over night at 4°C in a wet chamber. Control sections were incubated in the absence of primary antibody or with isotype control antibodies. Sections were then washed in PBS for 3 times. For fluorescence double-labeling, bound antibody was visualized with Streptavidin cyanine (Cy)3-conjugated goat-anti rabbit IgG and Cy2-conjugated goat-anti-mouse IgG. Additionally, DAPI was used to counterstain the nuclei.

Tab. 1: Primary antibodies for immunohistochemistry and fluorescence staining

Antigen	Marker for	Clonality	Species/ antigen	Dilution	Antigen demasking	Provider
APP	Amyloid precursor protein, early axonal damage	Mono-clonal	Mouse/ 22C11	1:2,000	Microwave, citric acid buffer	Merck Millipore
Caspase3	Activated caspase3, apoptosis	Poly-clonal	Rabbit/ C92-605	1:150	Microwave, Tris-EDTA	BD Biosciences
CNPase	Myelin protein	Mono-clonal	Mouse/ SMI-91R	1:200	Microwave, citric acid buffer	Covance
GFAP	Glial fibrillary acidic protein, astrocytes specific protein	Poly-clonal	Rabbit/ Z0334	1:1,000	None	Dako
GFAP	Glial fibrillary acidic protein, astrocytes specific protein	Mono-clonal	Mouse/ 134B1	1:500	Microwave, citric acid buffer	Synaptic Systems
Mac3	Macrophages/activated microglia in mice	Mono-clonal	Mouse/ M3/84	1:200	Microwave, citric acid buffer	Pharmingen
MBP	Myelin basic protein	Poly-clonal	Rabbit/ 62301	1:1,000	None	Dako
NogoA	Mature oligodendrocytes	Mono-clonal	Mouse/ 11C7	1:15,000	Microwave, citric acid buffer	Gift from M. Schwab, Zürich (Oertle <i>et al.</i> , 2003)
NF- κ B p65	Subunit of NF- κ B transcription complex	Poly-clonal	Rabbit/ C-20	1:1,000	Microwave, Tris-EDTA	Santa Cruz

For immunohistochemistry, antibody binding of biotin-conjugated secondary antibodies was visualized by using peroxidase and DAB. Biotinylated secondary antibodies (Tab. 2) were diluted in 10% FCS in PBS. After 1 h of incubation, remaining unbound antibodies were removed by washing with PBS. Slides were transferred for 1 h in peroxidase

(diluted in 10% FCS in PBS) at room temperature. After washing with PBS for 3 times, the unbound peroxidase was removed. DAB working solution was used to visualize the antibody binding. DAB was oxidized by the bound peroxidase developing a brown staining. Additionally, caspase3 staining was amplified with CuSO_4 working solution. Slides were counterstained with hemalaun.

Tab. 2: Secondary antibodies for immunohistochemistry and fluorescence staining

Antibody	Host	Directed against	Dilution	Provider
Goat anti-rabbit IgG (H+L)-Biotin	Goat	Anti-rabbit	1:500	Dianova
Biotinylated anti-mouse Ig	Sheep	Anti-mouse	1:200	Amersham Biosciences
Streptavidin Cy3	Goat	Anti-rabbit IgG	1:100	Jackson ImmunoResearch
Streptavidin Cy2	Goat	Anti-mouse IgG	1:100	Jackson ImmunoResearch

2.4 Electron microscopy (EM)

In a subset of animals (n = 5 per group), electron microscopic analysis of the corpus callosum was carried out to confirm the extent of demyelination. Mice treated with 0 and 25 mg/kg LAQ were sacrificed after 6 weeks of cuprizone feeding. Therefore, animals were injected i. p. with a lethal dose of 14% chloral hydrate solution. After loss of consciousness and protective reflexes, transcardial perfusion was performed through the left heart ventricle with PBS. The corpora callosa were collected and stored in 3% glutaraldehyde at 4°C for at least 7 days post-fixation. Para-sagittal slices of 1 mm thickness were obtained from the corpus callosum. Sections were processed through osmium tetroxide, dehydrated and embedded in synthetic resin. Ultrathin sections were then cut for electron microscopy. Semi thin sections were stained with Richardson`s Stain and evaluated by light microscopy.

2.5 Morphometry and data acquisition

To evaluate the extent of demyelination in the corpus callosum of each animal, LFB-PAS stained sections after 6 weeks of cuprizone were analyzed using a semi quantitative scoring system: No demyelination (0), minimal demyelination (0.5), < 33% demyelination (1), 33% - 66% demyelination (2), and > 66% demyelination (3). GFAP-stained sections were also investigated semi quantitatively after 6 weeks of cuprizone using the following scoring system: No reactive astrogliosis (0), minimal astrogliosis (1), moderate astrogliosis (2) or severe reactive astrogliosis (3). APP-positive axons and Mac3-positive microglia were also examined after 6 weeks of cuprizone. NogoA-positive oligodendrocytes, HE-stained and caspase3-positive apoptoses were assessed after 1 week of cuprizone. Apoptotic cells were identified by a pyknotic nucleus or apoptotic bodies as well as eosinophilic cytoplasm. NogoA-positive oligodendrocytes were also evaluated after 4 days of remyelination. The density of axons and cells were determined by counting stained axons and cells in the corpus callosum using a light microscope at 400x magnification and an ocular counting grid.

Immunofluorescent pictures were taken of the corpus callosum to assess the proportion of GFAP-positive astrocytes with nuclear NF- κ B p65 translocation after 6 weeks of cuprizone. The total number of GFAP positive astrocytes were determined as well as the number of GFAP positive astrocytes with nuclear p65 signal to calculate the percentage of GFAP-positive cells with nuclear p65 translocation.

For investigating the lesion size of LPC-induced demyelination, images were taken at a 100x original magnification and further processed using the software AnalysisTM.

All histological quantifications were carried out in a blinded manner. For representation of the results graphs were generated by GraphPad Prism software.

2.6 Mass spectrometry analysis

To measure cuprizone concentrations in brain and plasma, brain and plasma samples were frozen on dry ice, stored at -80°C and send to Dr. Marta Patfalusi (Aurigon-Toxicoop Research Center, Department Analytics, Budapest, Hungary).

Cuprizone was then quantified in brain and plasma samples by reverse phase high performance liquid chromatography (HPLC) with mass spectrometer detection. For brain

samples, 40 μ l of 1 μ g/ml freshly prepared internal standard solution (omeprazole) and 2 ml of chloroform:acetonitrile (1:1) v/v (each volume) mixture were added to the frozen mouse brain and homogenized immediately by an ultrasonic homogenizer for 5-10 s. The sample was then mixed followed by centrifugation at 6,000 rpm for 10 min at 5°C. 5 μ l of the organic phase was injected onto the HPLC column.

For plasma samples, 50 μ l of mouse plasma were added to 10 μ l of 1 μ g/ml freshly prepared internal standard solution (omeprazole), 10 μ l of acetonitrile and 200 μ l of chloroform. The solution was thoroughly mixed by vortexing followed by centrifugation at 10,000 rpm for 5 min at 5°C. 200 μ l volume of the lower phase was then transferred into 200 μ l of acetonitrile. 5 μ l of the solution was injected onto the HPLC column.

For both brain and plasma samples, the chromatographic separation was performed by gradient elution on an Inertsil ODS-4 chromatographic column. Mass spectrometer analysis was performed using a TSQ Quantum Ultra AM mass spectrometer in positive ionization mode. The following multiple reaction monitoring (MRM) transitions were monitored: Mass-to-charge ratio (m/z) 279.2 \rightarrow 139.1 for cuprizone and 346.1 \rightarrow 198.0 for omeprazole.

Mass spectrometry analyses of brain and plasma samples of wild type C57BL/6J and Tg(hGFAP) mice were performed at least twice (2 independent experiments) with at least 5 animals per group. Many plasma samples showed cuprizone levels below the limit of quantification and had to be excluded from the statistical analyses. Therefore, the presented data on plasma samples with detectable cuprizone plasma levels included a minimum of only 3 mice per group. Graphs showing spectrometric data show mean values with the corresponding standard deviation.

2.7 Primary cell cultures

2.7.1 Isolation of primary astrocytes from newborn mice

Newborn C57BL/6J mice (p0 or p1) were decapitated. Heads were transferred to a Petri dish with cold HBSS medium to rinse off the blood. The skull was opened and brains were transferred into fresh HBSS. Cerebella were removed and discarded. Meninges of

cerebrums were removed to prevent that meningeal fibroblasts interfere with the glial cell growth. Isolated cerebrums were transferred in a 50 ml Falcon™ tube filled with HBSS and stored on ice. After preparation, HBSS was removed and cells were isolated by incubating the brains in 0.25% Trypsin-EDTA (2 ml per brain) mixed with DNase (33.33 µl per brain) for 10 min and 37°C. After washing with 10 ml HBSS brains were transferred in 5 ml DMEM+. A cell suspension was prepared by mechanical dissociation of brains in DMEM+ with first a 10 ml pipette and second a 1,000 µl pipet tip. The cell suspension was filled in PLL-coated cell culture flasks containing 10 ml DMEM+ (ca. 2 to 3 brains per flask). The primary culture including astrocytes, oligodendrocytes and microglia was cultivated for 7 to 10 days in a tissue culture incubator at 37°C and 5% CO₂. Medium was changed every 3 to 4 days.

After 7 to 10 days of cultivation, mixed glial cell cultures were shaken vigorously to remove most of oligodendrocytes and microglia. The medium containing detached cells was removed and remaining cells in culture flasks were washed with PBS twice. 5 ml 0.05% Trypsin-EDTA was added to remaining astrocytes for 2 to 3 min to detach cells. The reaction was stopped by adding 10 ml DMEM + 10% FCS. Cell suspension was transferred to a 50 ml Falcon™ tube and centrifuged for 10 min at 900 rpm to remove EDTA and isolate astrocytes. Supernatant was discarded and the cell pellet was resuspended in DMEM+. The number of astrocytes was determined in a Neubauer counting chamber. For the cell viability and membrane integrity assay, astrocytes were plated at a density of 10,000 cells per well in a 96-well-plate coated with PLL. For the migration assay, astrocytes were plated at a density of 200,000 cells per well in a PLL-coated 12-well-plate. Before starting experiments astrocytes were incubated in DMEM+ for at least 48 h to ensure differentiation of astrocytes. For cuprizone treatment, 1 µM, 10 µM or 100 µM cuprizone (diluted in DMEM+) were added to the cells. For serum treatment, 10% serum from cuprizone-treated mice or 10% serum from naïve mice (each diluted in DMEM+) was added to astrocytes. Astrocytes were treated for 24 h with cuprizone or serum. Untreated cells served as controls. Each group was measured in triplicates.

2.7.2 Cell viability assay (MTT assay)

To assess mitochondrial respiration after treatment with cuprizone or serum, the CellTiter 96® Non-Radioactive Cell Proliferation Assay was used. Therefore, supernatant was removed after treatment with cuprizone or serum and fresh DMEM+ was added to the cells. 15 µl of the Dye Solution was added to each well. The 96-well plate was incubated at 37°C and 5% CO₂ for 4 h. 100 µl of the Solubilization Solution/Stop Mix was then added to each well and incubated for 1 h. Each well was then mixed slightly. Absorbance was recorded at 570 nm wavelength and a reference wavelength at 650 nm to reduce background using a Tecan Safire plate reader. Mitochondrial respiration was converted to percent since the measured values differed in their baseline levels. Hence, the mean of mitochondrial respiration of control condition was set to hundred percent and the treatment conditions were expressed in relation to the control group. Cell viability assays were performed at least 3 times with at least 2 wells per treatment condition.

2.7.3 Membrane integrity assay

The amount of astrocytic cell damage was examined after treatment with cuprizone or serum by using the CytoTox-One™ Homogenous Membrane Integrity Assay. 100 µl of CytoTox-One™ Reagent was added to each well and incubated for 10 min at 22°C. 50 µl of the Stop Solution was then added to each well. The 96-well-plate was shaken slightly for 10 s. Fluorescence was recorded with an excitation wavelength of 560 nm and an emission wavelength of 590 nm using a Tecan Safire plate reader. The membrane integrity assay was performed 3 times with at least 2 wells per treatment condition.

2.7.4 Migration assay

To test for the ability of astrocytes to migrate into a cell-free area, a migration assay was performed. After grown to a confluent cell monolayer, the cell monolayer was scraped in a straight line with a 200 µl pipet tip to create a scratch as a cell-free area (Liang *et al.*, 2007). The cellular debris was removed by washing twice with culture medium. A reference

point was created by etching the outer bottom of the dish slightly with a razor blade. After treatment with cuprizone or serum, the dish was placed in a tissue culture incubator at 37°C and 5% CO₂. Representative images were taken after 0, 24 and 42 h. Migration assays were performed 3 times with at least 2 wells per treatment condition.

2.8 Statistical analysis

Statistical analyses were carried out using the software package SPSS. Histological differences between vehicle and LAQ-treated or wild type and transgenic mice were analyzed by Mann-Whitney-U tests for nonparametric data. Statistical significance was defined as $p < 0.05$.

Parametric data were analyzed by independent t tests as follows: For the subsequent analyses of astrocytic NF- κ B activation in both LAQ and Tg(hGFAP) experiments, effect of cuprizone or serum on mitochondrial respiration and cell damage in primary astrocytes. Statistical significance was defined as $p < 0.05$.

3 Results

3.1 Evaluating the effect of LAQ on toxic de- and remyelination in mice

3.1.1 Reduced cuprizone-induced weight loss and oligodendroglial apoptosis under LAQ in wild type mice

The effect of preventive treatment with 25 mg/kg LAQ was examined after cuprizone treatment. Clinical and histological analyses were performed to assess vehicle- and LAQ-treated mice. Body weights of both groups were evaluated after each week of cuprizone treatment. After one week of 0.25% cuprizone, vehicle-treated controls showed substantial weight loss, whereas LAQ-treated animals showed no weight loss (Fig. 2). During the following five weeks of cuprizone challenge, LAQ-treated mice always displayed significantly higher body weights than vehicle-treated animals at all time points ($p < 0.001$ each).

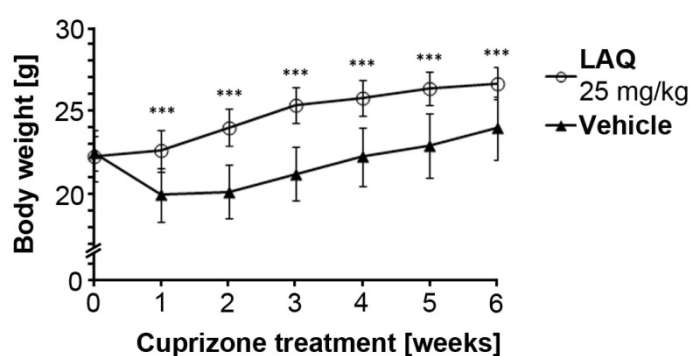


Fig. 2: No weight loss under LAQ treatment during 6 weeks cuprizone challenge. Vehicle-treated controls and mice treated with 25 mg/kg LAQ at weeks 0-6 during 0.25% cuprizone challenge. During the 6 weeks of cuprizone treatment, animals treated with LAQ show significantly higher body weights than vehicle-treated mice (** $p < 0.001$).

The effects of LAQ treatment on cuprizone-induced pathology were first determined after one week of cuprizone challenge to investigate whether LAQ affects oligodendrocyte survival. At this time point, oligodendroglial apoptosis is typically observed (Hesse *et al.*, 2010). Apoptotic cells were first visualized morphologically on HE-stained sections and then stained for active caspase3, a marker for cells undergoing apoptosis. Vehicle-treated mice

showed numerous apoptosis in the corpus callosum (Fig. 3A) whereas LAQ-treated animals displayed only scattered apoptotic cells (Fig. 3B).

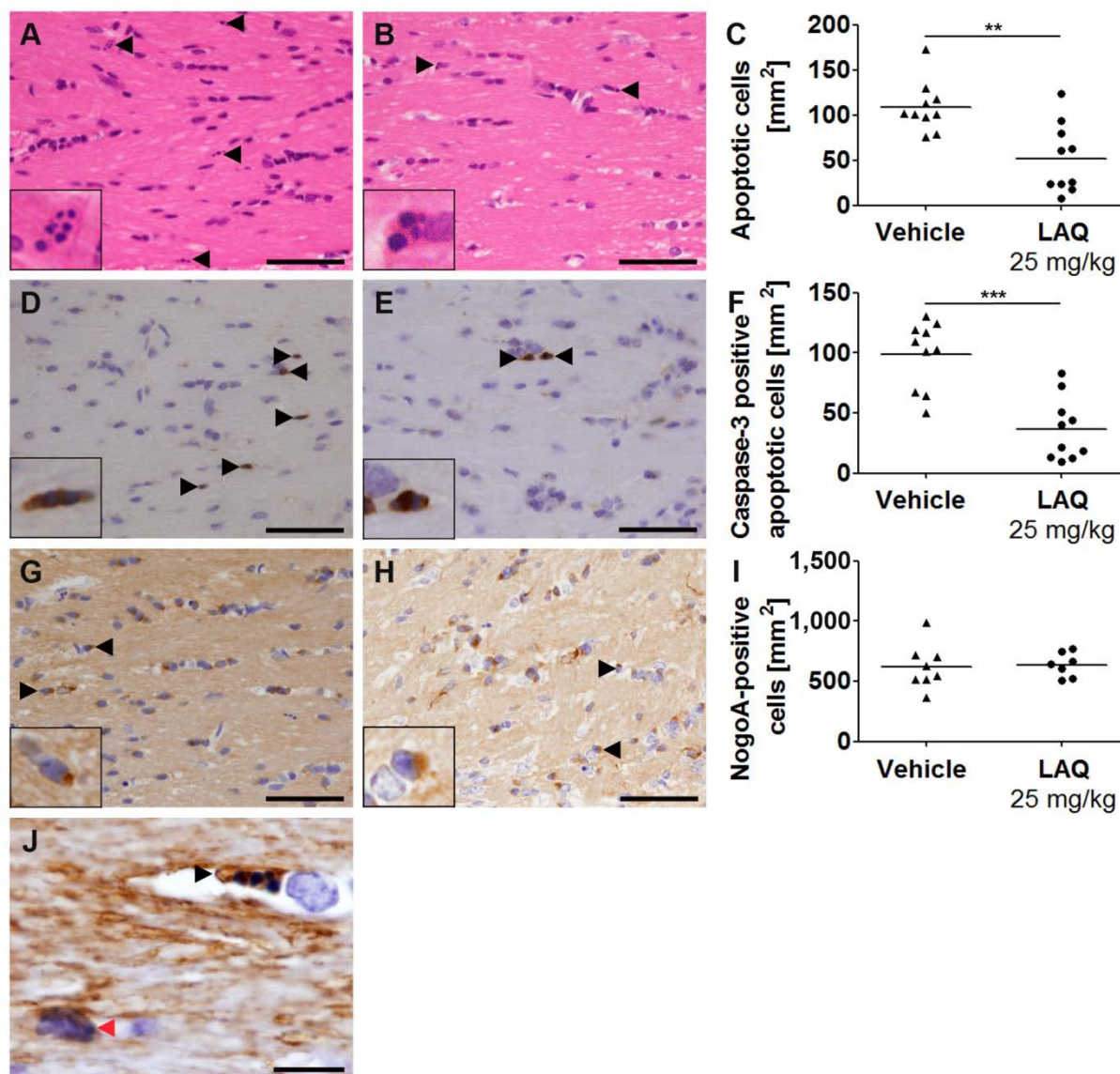


Fig. 3: Decreased cuprizone-induced oligodendroglial apoptosis under LAQ treatment. Evaluation of apoptotic cells and oligodendrocytes after 1 week of 0.25% cuprizone in vehicle- (A, D, G) and LAQ-treated mice (B, E, H). Vehicle group (A) shows significantly more HE-stained apoptotic cells (arrowheads) in the corpus callosum than LAQ group (B, C) (** $p < 0.01$). Density of apoptotic cells stained positively for active caspase3 (arrowheads) are significantly higher in vehicle-treated (D) compared to LAQ-treated animals (E, F) (** $p < 0.001$). NogoA-positive oligodendrocytes (arrowheads) are detected in both groups (G, H). The density of mature oligodendrocytes is similar in LAQ- and vehicle-treated mice (I) ($p > 0.05$). Oligodendrocytes are positive for CNPase (red arrowhead) (J). Only scattered apoptotic cells are CNPase-positive (black arrowhead) indicating that these apoptotic cells are oligodendrocytes. Representative images of the medial part of the corpus callosum were taken at 400x original magnification (scale bars: 50 μ m) (A-H) or at 1,000x original magnification (scale bar: 10 μ m) (J). Inserts show magnified representative cells.

The quantitative analysis revealed that the density of apoptotic cells was significantly lower in mice treated with LAQ (52 ± 38 apoptoses per mm^2) in comparison to controls treated with vehicle (109 ± 28 apoptoses per mm^2 ; $p < 0.01$) (Fig. 3C).

Compared to vehicle-treated animals (Fig. 3D) the number of caspase3-positive apoptotic cells was significantly reduced in the corpus callosum of LAQ-treated mice (98 ± 28 vs. 37 ± 26 caspase3-positive apoptosis per mm^2 ; $p < 0.001$) (Fig. 3E, F).

To investigate mature oligodendrocytes, immunohistological stainings for the oligodendroglial marker NogoA were performed. NogoA-positive mature oligodendrocytes were detected in the callosal white matter of both groups. Quantitative evaluation revealed that numbers of mature oligodendrocytes were slightly, but not significantly higher in LAQ- (598 ± 25 NogoA-positive cells per mm^2) (Fig. 3H) compared to vehicle-treated mice (570 ± 25 NogoA-positive cells per mm^2 ; $p > 0.05$) (Fig. 3G, I). Scattered apoptotic cells were immunopositive for CNPase identifying these apoptotic cells as oligodendrocytes (Fig. 3J).

3.1.2 Dose-dependent inhibition of cuprizone-induced demyelination by LAQ

To assess whether preventive treatment with 5 and 25 mg/kg LAQ exerts effects on cuprizone-induced demyelination, mice were treated for six weeks with cuprizone. Demyelination was investigated in the corpus callosum of both groups. Vehicle-treated mice displayed extensive demyelination in the corpus callosum (Fig. 4A, D) whereas animals treated with 25 mg/kg LAQ showed reduced demyelination (Fig. 4C, F). Mice given the lower dose of 5 mg/kg LAQ showed moderate demyelination of the corpus callosum (Fig. 4B, E). Furthermore, vehicle-treated controls showed a moderate increase of cell density in the callosal white matter in comparison to LAQ-treated animals (Fig. 4D, F). More PAS-positive microglia were observed in vehicle-treated controls (Fig. 4D). The semi quantitative assessment of demyelination in the corpus callosum revealed significantly higher demyelination in vehicle-treated mice (score 2.4 ± 0.5) than in animals treated with the lower (score 1.8 ± 0.8) and higher dose of LAQ (score 0.6 ± 0.3 ; $p < 0.001$) (Fig. 4G). Mice treated with 5 mg/kg LAQ displayed significantly more demyelination than animals treated with 25 mg/kg ($p < 0.01$) (Fig. 4G). LAQ-treated mice also displayed less demyelination in other brain areas such as the cortex and cerebellum (data not shown).

Electron microscopic evaluation demonstrated numerous demyelinated axons in the corpus callosum of vehicle-treated controls and only little signs of remyelination (Fig. 4H). In contrast, animals treated with 25 mg/kg LAQ showed only scattered demyelinated axons and many intact myelin sheaths (Fig. 4I).

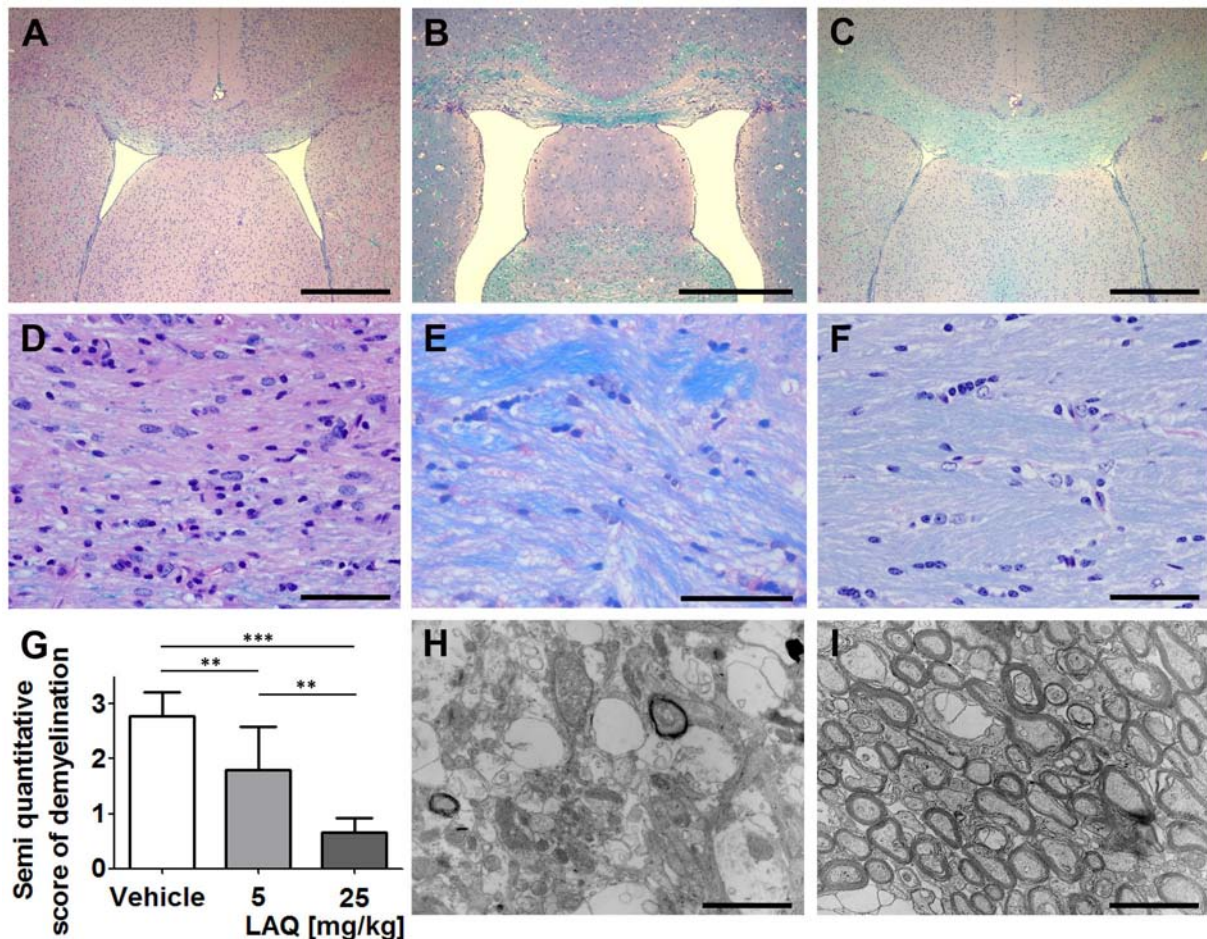


Fig. 4: Callosal demyelination is reduced in a dose-dependent manner under LAQ after 6 weeks of cuprizone. Vehicle-treated controls show extensive demyelination (A, D), while mice treated with 5 mg/kg LAQ show moderate (B, E) and animals treated with 25 mg/kg LAQ show minimal demyelination (C, F). The semi quantitative evaluation of demyelination (G) reveals significantly more demyelination in vehicle-treated controls than in both LAQ groups. Mice treated with 25 mg/kg LAQ demonstrate significantly less demyelination than animals treated with 5 mg/kg LAQ (**p < 0.01; ***p < 0.001). Representative electron microscopic images show many demyelinated axons and single remyelinated axons in vehicle-treated mice (H). In contrast, animals treated with 25 mg/kg LAQ show many intact myelin sheaths with almost no signs of demyelination (I). Scale bars: A-C 500 μ m, D-F 50 μ m, H-I 2 μ m.

3.1.3 Decreased cuprizone-induced microglial activation, axonal damage and astrogliosis by LAQ

The effect of LAQ on activated microglia was determined by evaluating Mac3-positive cells in the corpus callosum after six weeks of cuprizone. Mac3 staining revealed more activated microglia cells in vehicle-treated animals (Fig. 5A) than in mice treated with 25 mg/kg LAQ (Fig. 5B). Quantitative analysis of the microglia density within the corpus callosum demonstrated significantly reduced numbers of microglia under LAQ (185 ± 84 Mac3-positive cells per mm^2) compared to vehicle treatment (1000 ± 298 Mac3-positive cells per mm^2 ; $p < 0.001$) (Fig. 5C).

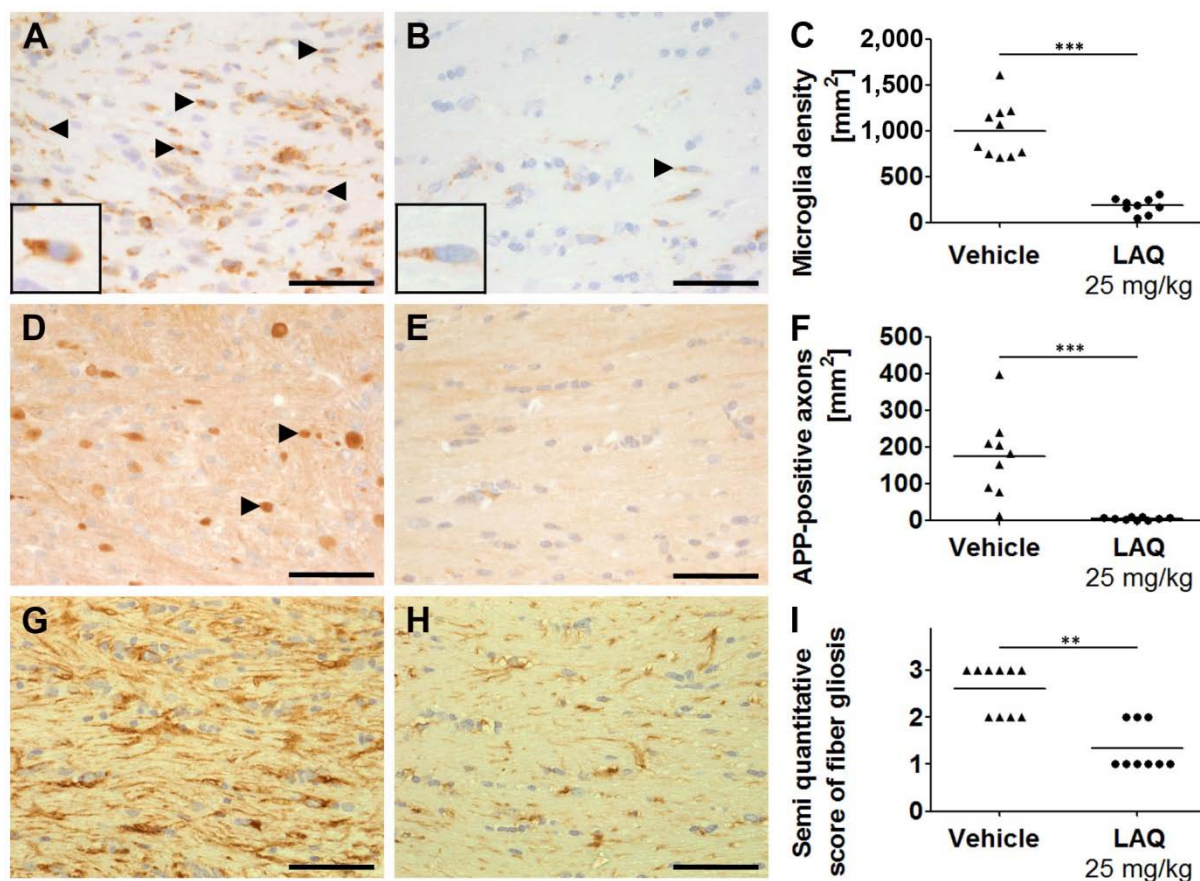


Fig. 5: LAQ treatment reduces cuprizone-induced microglial activation, axonal damage and gliosis. LAQ-treated mice display less microglial activation (A-C), axonal damage (D-F) and fibrillary gliosis (G-I) after 6 weeks of 0.25% cuprizone. The density of Mac3-positive activated microglia (arrowheads) is significantly higher in vehicle-treated animals (A) compared to LAQ-treated mice (B, C) (**p < 0.001). Inserts show magnified representative cells. APP-positive axonal spheroids (arrowheads) are significantly higher in vehicle-treated (D) compared to LAQ-treated animals (E, F) (**p < 0.001). The density of GFAP-positive glial fibers is significantly higher in the vehicle (G) than in the LAQ group (H, I) (**p < 0.01). Representative images of the medial part of the corpus callosum were taken at 400x original magnification (scale bars: 50 μm).

To examine the effect of LAQ on axonal integrity, acutely damaged axons characterized by accumulation of APP were analyzed. Vehicle-treated animals showed numerous damaged axons (Fig. 5D) whereas APP-positive axons were nearly absent in mice treated with 25 mg/kg LAQ (Fig. 5E). The quantitative analysis revealed a significant reduction of acute axonal damage under LAQ treatment (5 ± 3 APP-positive axons per mm^2) in comparison to vehicle-treated controls (173 ± 111 APP-positive axons per mm^2 , $p < 0.001$) (Fig. 5F).

To investigate whether LAQ treatment affects astrocytes, reactive astrogliosis was assessed semi quantitatively by staining with an antibody against GFAP. Reactive astrogliosis was prominent in the corpus callosum of vehicle-treated animals (score 2.6 ± 0.5) (Fig. 5G) whereas GFAP stained astrogliosis was reduced in mice treated with 25 mg/kg LAQ (score 1.3 ± 0.5) (Fig. 5H). The semi quantitative analysis confirmed a significant reduced fiber gliosis in the LAQ group compared to the vehicle group ($p = 0.001$) (Fig. 5I).

3.1.4 Similar cerebral cuprizone concentrations in mice treated with LAQ and vehicle

To investigate whether cuprizone levels were comparable in both groups, cuprizone concentrations were measured in brains after one week (Fig. 6A) and six weeks (Fig. 6B) of cuprizone feeding.

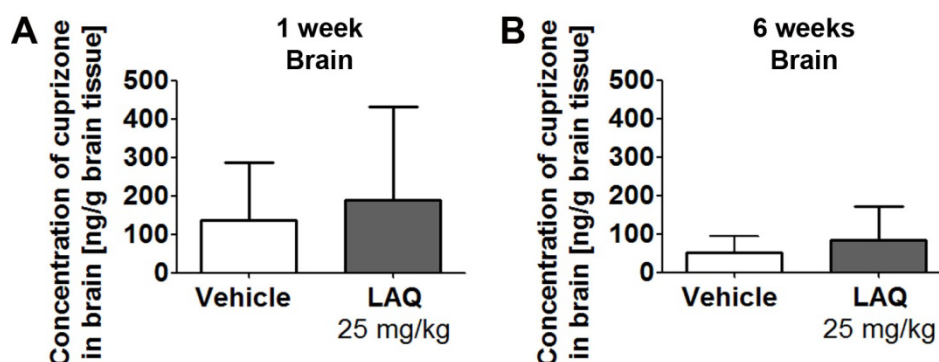


Fig. 6: Similar cuprizone concentration in brains of LAQ- and vehicle-treated mice after 1 week and 6 weeks of cuprizone. After 1 week (A) and 6 weeks (B) of 0.25% cuprizone treatment, cuprizone was quantified in brain samples of 25 mg/kg LAQ- and vehicle-treated mice by RP-HPLC mass spectrometry analysis. Cuprizone concentrations are similar for both treatment regimes at both time points ($p > 0.05$).

Mass spectrometry analyses revealed that the cerebral cuprizone concentrations did not differ significantly between vehicle- and LAQ-treated mice after one week (136 ± 150 ng/g brain tissue for the vehicle group and 190 ± 242 ng/g brain tissue for the LAQ group) and after six weeks of cuprizone (51 ± 43 ng/g brain tissue for the vehicle group, 84 ± 89 ng/g brain tissue for the LAQ group).

To determine whether cuprizone levels in serum were also comparable in both groups, mass spectrometry analyses were performed after one week cuprizone challenge (Fig. 7). Cuprizone concentrations in plasma were very low in both groups and did not show any significant differences between both groups after one week (2 ± 1 ng/ml plasma for the vehicle group and 1 ± 0 ng/ml plasma for the LAQ group).

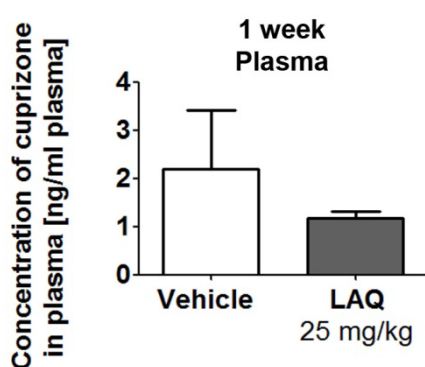


Fig. 7: Low cuprizone concentration in plasma of LAQ- and vehicle-treated mice after 1 week of cuprizone. After 1 week of 0.25% cuprizone treatment, cuprizone was quantified in plasma samples of 25 mg/kg LAQ- and vehicle-treated mice by RP-HPLC mass spectrometry analysis. Cuprizone concentrations are similar for both treatment regimes in plasma ($p > 0.05$).

3.1.5 Reduced cuprizone-induced pathology under LAQ also in Rag1-deficient mice

To determine whether the effects of LAQ treatment are independent of T and B cells, Rag1^{-/-} mice lacking T and B cells were treated with vehicle or 25 mg/kg LAQ during cuprizone feeding for six weeks. The results were similar to findings in wild type mice: LAQ-treated Rag1^{-/-} mice displayed significantly higher body weights compared to corresponding vehicle-treated Rag1^{-/-} animals (Fig. 8).

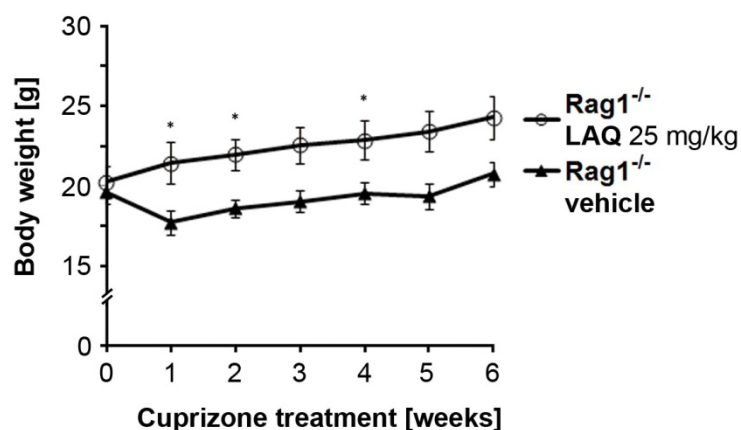


Fig. 8: No cuprizone-induced weight loss in LAQ-treated Rag1^{-/-} mice. Body weights of vehicle- and LAQ-treated Rag1^{-/-} animals after 6 weeks of 0.25% cuprizone. LAQ-treated Rag1^{-/-} mice show significantly higher body weights after cuprizone compared to vehicle-treated animals (* $p < 0.05$).

After six weeks of cuprizone, vehicle-treated mice showed extensive demyelination (Fig. 9A) whereas LAQ-treated Rag1^{-/-} animals displayed reduced demyelination in the corpus callosum (Fig. 9B). Semi quantitative analysis revealed significantly lower demyelination scores in LAQ-treated Rag1^{-/-} mice (score 0.5 ± 0) compared to vehicle-treated Rag1^{-/-} animals (score 2.4 ± 0.5 ; $p < 0.001$) (Fig. 9C).

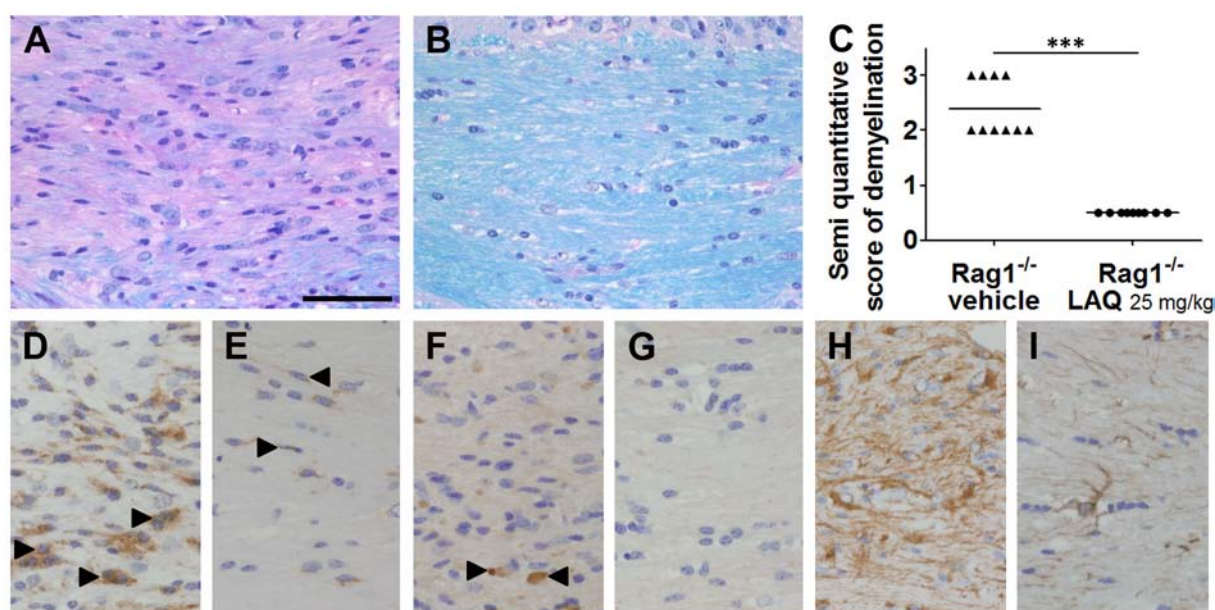


Fig. 9: Reduced demyelination, activated microglia, acute axonal damage and astrogliosis in LAQ-treated Rag1^{-/-} mice compared to vehicle-treated controls after 6 weeks of cuprizone. Compared to vehicle-treated Rag1^{-/-} mice (A) LAQ-treated Rag1^{-/-} mice (B) show significantly less demyelination on LFB-PAS-stained sections (** $p < 0.001$). The density of callosal microglia (arrowheads) is higher in vehicle-treated Rag1^{-/-} mice (D) than in the LAQ group (E). Vehicle treated Rag1^{-/-} mice show higher APP-positive axonal spheroids (arrowhead) in the corpus callosum (F) than the LAQ-treated group (G). Vehicle group displays more extensive fiber gliosis in the corpus callosum (H) than LAQ-treated mice (I). Representative images of the medial part of the corpus callosum were taken at 400x original magnification (scale bars: 50 μ m).

Many activated microglia were detected in the corpus callosum of vehicle-treated *Rag1*^{-/-} mice (Fig. 9D) whereas only scattered microglia were observed under LAQ treatment (Fig. 9E). Numerous APP-positive axonal spheroids were detected in the vehicle group (Fig. 9F), but LAQ-treated *Rag1*^{-/-} animals showed fewer axonal damage in the corpus callosum (Fig. 9G). In addition, GFAP staining revealed that *Rag1*^{-/-} mice treated with vehicle displayed more extensive fiber gliosis in the corpus callosum (Fig. 9H) than LAQ-treated *Rag1*^{-/-} animals (Fig. 9I).

3.1.6 Decreased astrocytic NF-κB activation under LAQ treatment after cuprizone

The data presented above provide evidence that LAQ protects from cuprizone-induced pathology through CNS-intrinsic mechanisms. Similar protective effects as observed in the present cuprizone experiments have been observed in mice in which the NF-κB pathway was selectively inhibited in astrocytes (Raasch *et al.*, 2011). Hence, the effects of LAQ on NF-κB activation in astrocytes were analyzed in detail. Therefore, astrocytic p65 translocation was examined after six weeks of cuprizone.

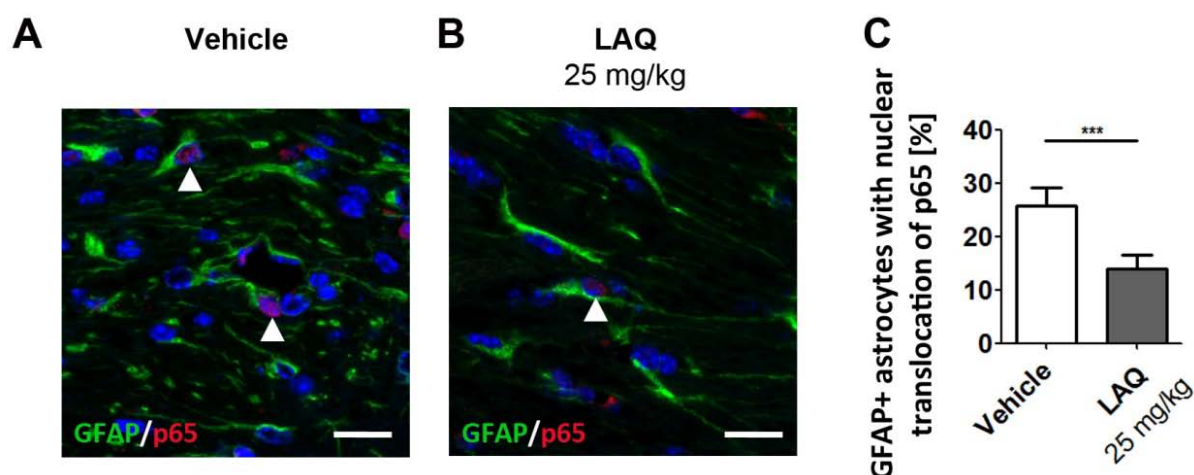


Fig. 10: LAQ reduces astrocytic NF-κB activation after 6 weeks of cuprizone challenge. Double immunohistochemistry with antibodies against p65 (red) and GFAP (green) shows significantly fewer GFAP-positive astrocytes with nuclear p65 immunoreactivity in the corpus callosum in LAQ-treated (14% ± 1%) (B) in comparison to vehicle-treated mice (26% ± 1%, ****p* < 0.001) (A, C). Representative images of the corpus callosum were taken at 400x original magnification (scale bars: 20 μm).

Double immunofluorescence staining against antibodies of p65 and GFAP were performed to detect nuclear translocation of p65/RelA, the main transactivating NF- κ B subunit, in astrocytes. Compared to vehicle-treated mice (Fig. 10A) fewer p65-positive astrocytes were detected in the corpus callosum of LAQ-treated animals (Fig. 10B). Quantitative analysis revealed that the proportion of astrocytes with nuclear p65 immunoreactivity was significantly lower in the LAQ group ($14\% \pm 1\%$ GFAP-positive astrocytes with nuclear translocation of p65) compared to the vehicle group ($26\% \pm 1\%$; $p < 0.001$) (Fig. 10C).

3.1.7 No LAQ effect on LPC-induced demyelination

To assess the effect of preventive treatment with 25 mg/kg LAQ in a model with focal rapid demyelination, 1 μ l 1% LPC was injected stereotactically in the corpus callosum. Vehicle-treated controls and LAQ-treated animals were evaluated histologically. Four days after LPC injection, demyelination was examined in the corpus callosum of both groups.

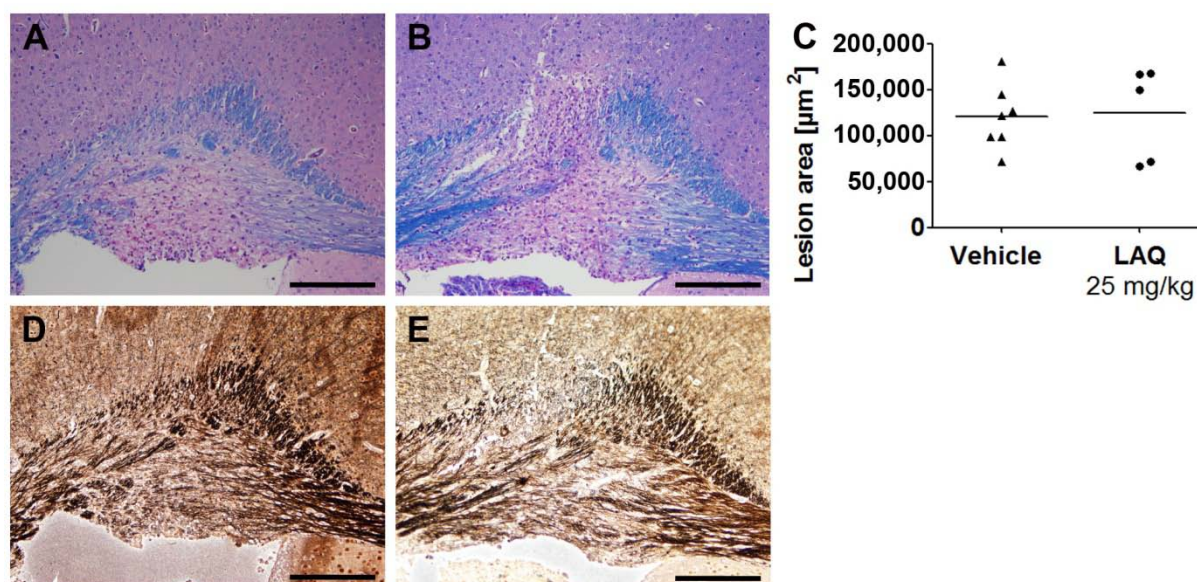


Fig. 11: No effect of 25 mg/kg LAQ on LPC-induced demyelination. Similar extent of demyelination in vehicle-treated mice (A) and animals treated with 25 mg/kg LAQ (B) on LFB-PAS-stained sections of the corpus callosum 4 days after focal injection. Evaluation of the lesion area revealed no significant difference between both treatment groups ($p > 0.05$) (C). The Bielschowsky staining of the LPC-induced lesion displayed intact axons in vehicle- (D) and LAQ-treated (E) mice. Representative images of the lesion site were taken at 100x original magnification (scale bars: 200 μm).

Vehicle- and LAQ-treated mice displayed focal demyelination in the corpus callosum (Fig. 11A, B). Evaluation of the lesion area revealed a similar extent of demyelination in both groups (vehicle: $120,539 \pm 35,482 \mu\text{m}^2$; LAQ: $124,400 \pm 50,648 \mu\text{m}^2$; $p > 0.05$) (Fig. 11C). There was only little axonal damage in both groups after LPC injection (Fig. 11D, E).

Further experiments were performed with a higher LAQ concentration of 40 mg/kg. In these experiments, vehicle- (Fig. 12A) and LAQ-treated animals (Fig. 12B) displayed focal demyelination of the corpus callosum. However, evaluation of the lesion area demonstrated a similar extent of demyelination after four days of LAQ treatment (vehicle: $107,821 \pm 38,802 \mu\text{m}^2$; LAQ: $94,561 \pm 42,071 \mu\text{m}^2$; $p > 0.05$) (Fig. 12C). Only minimal axonal damage was observed in vehicle-treated mice (Fig. 12D) and animals treated with the higher LAQ concentration (Fig. 12E).

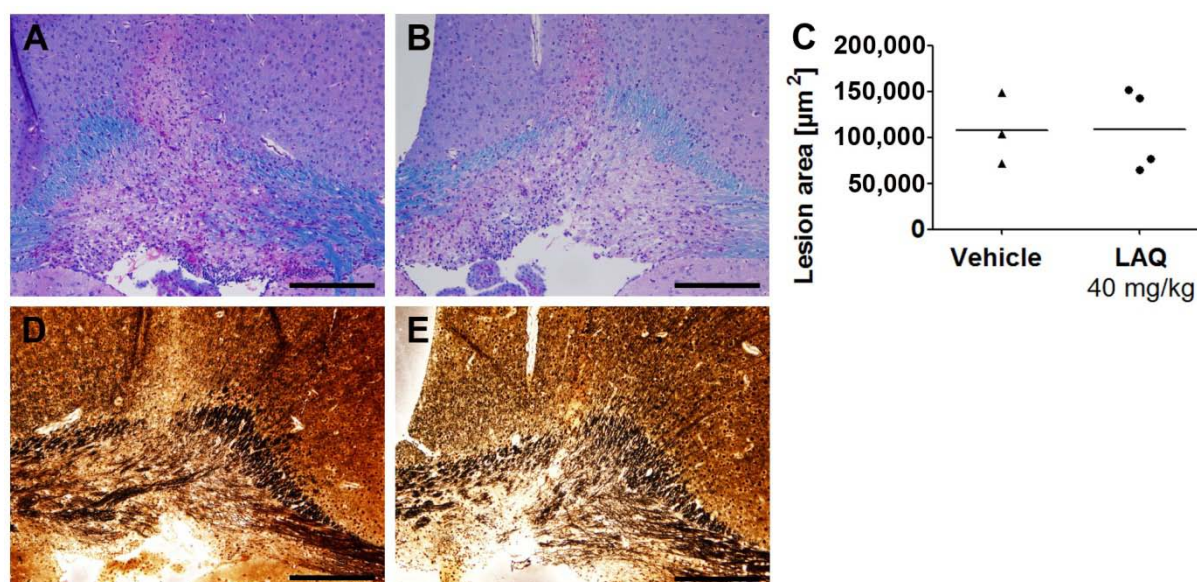


Fig. 12: No effect of 40 mg/kg LAQ on LPC-induced demyelination. Similar callosal demyelination in vehicle-treated animals (A) and mice treated with 40 mg/kg LAQ (B) on LFB-PAS stained sections 4 days after stereotactical injection. Evaluation of the lesion area of the corpus callosum demonstrates no significant difference between vehicle and LAQ group ($p > 0.05$) (C). The Bielschowsky staining of the LPC-induced lesion area displays intact axons in vehicle (D) and LAQ-treated (E) mice. Representative images of the lesion site were taken at 100x original magnification (scale bars: 200 μm).

3.1.8 Similar remyelination under LAQ after cuprizone withdrawal

To investigate the effect of LAQ on remyelination and oligodendrocyte repopulation, mice received a 0.25% cuprizone diet for six weeks without LAQ treatment to induce demyelination. After cuprizone withdrawal, mice were treated with vehicle or 25 mg/kg LAQ during the remyelinating period of four days. Both groups were evaluated histologically. After four days of remyelination, vehicle- (Fig. 13A) and LAQ-treated mice (Fig. 13B) displayed extensive remyelination which was evidenced by immunohistological staining using an antibody against MBP. The myelin density was similar in LAQ- and vehicle-treated animals.

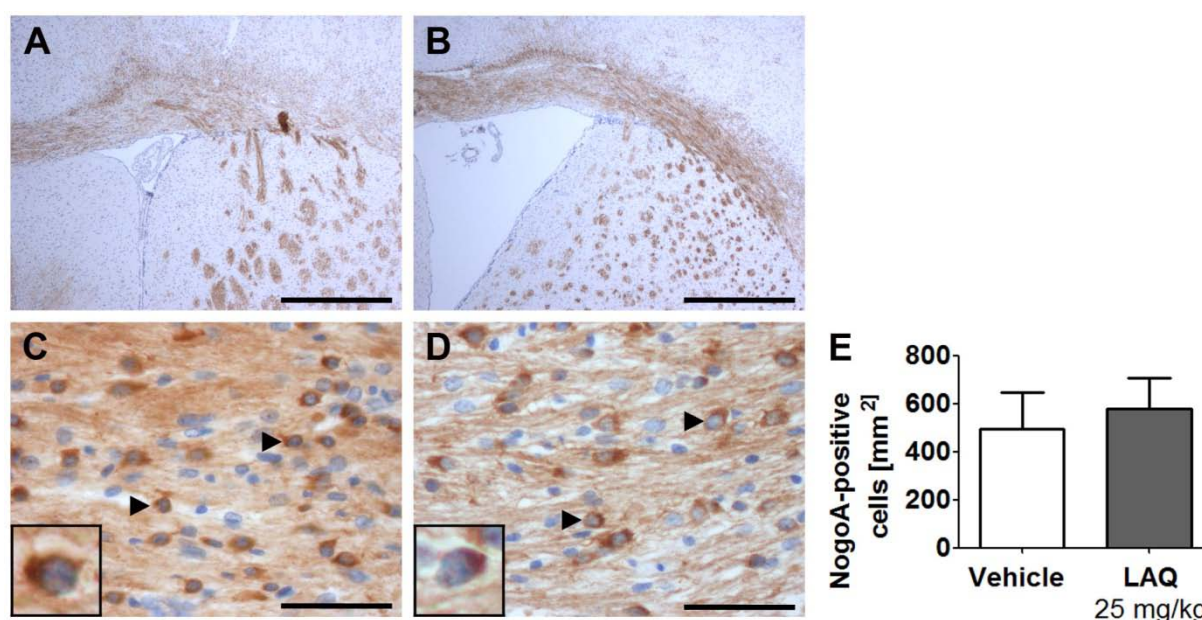


Fig. 13: No effect of LAQ on remyelination after cuprizone-induced demyelination. Vehicle-treated animals (A) and mice treated with 25 mg/kg LAQ (B) show extensive remyelination 4 days after withdrawal from 6 weeks 0.25% cuprizone challenge. Density of NogoA-positive oligodendrocytes (arrowheads) is similar in both treatment groups (C, D). Quantification of mature oligodendrocytes reveals no significant difference between vehicle- and LAQ-treated animals (E) ($p > 0.05$). Representative images of the corpus callosum were taken at 100x (A, B) or 400x (C, D) original magnification (scale bars: 200 μm (A, B) and 50 μm (C, D)). Inserts show magnified representative cells.

To determine oligodendroglial repopulation, the density of callosal NogoA-positive oligodendroglial cells was quantified. Vehicle- (Fig. 13C) and LAQ-treated mice (Fig. 13D) showed numerous oligodendrocytes in the corpus callosum after four days of remyelination.

The densities of mature oligodendrocytes were similar in both groups (vehicle: 496 ± 152 NogoA-positive cells per mm^2 ; LAQ: 580 ± 125 NogoA-positive cells per mm^2 ; $p > 0.05$) (Fig. 13E). In conclusion, LAQ did not affect remyelination and oligodendroglial repopulation after cuprizone challenge.

3.2 Investigating the impact of human GFAP overexpression on toxic demyelination in mice

3.2.1 Increased astrogliosis, but regular myelin and oligodendroglial density in naïve Tg(hGFAP) mice

Before evaluation of potential cuprizone-induced effects on Tg(hGFAP) mice, naïve animals of this transgenic line were characterized. Previous studies indicate that these animals overexpressing human GFAP show an increased astrogliosis without external stimuli (Messing *et al.*, 1998). In eight-weeks-old naïve wild type mice, the cortex showed nearly no GFAP-positive astrocytes (Fig. 14A) whereas age-matched naïve Tg(hGFAP) animals showed many islets of GFAP-positive astrocytes (Fig. 14B). At the age of 14 weeks, a time point comparable with six weeks of cuprizone feeding, naïve transgenic mice showed extensive GFAP-positive astrocytes in the cortex (Fig. 14C). At the age of eight weeks, the subpial cortex of naïve wild type animals showed only scattered GFAP-positive astrocytes (Fig. 14D) whereas the subpial cortex of age-matched transgenic mice showed increased GFAP-positive astrocytes with thickened astrocytic branches and magnified nuclei (Fig. 14E). Even more GFAP-positive astrocytes with magnified nuclei and astrogliosis were observed at 14 weeks of age (Fig. 14F). Compared to eight-weeks-old wild type animals (Fig. 14G) the corpus callosum of Tg(hGFAP) mice showed increased GFAP-positive astrocytes with abnormal appearing branches (Fig. 14H). At the age of 14 weeks, the corpus callosum of transgenic animals showed even more GFAP-positive astrocytes and thickened astrocytic branches (Fig. 14I).

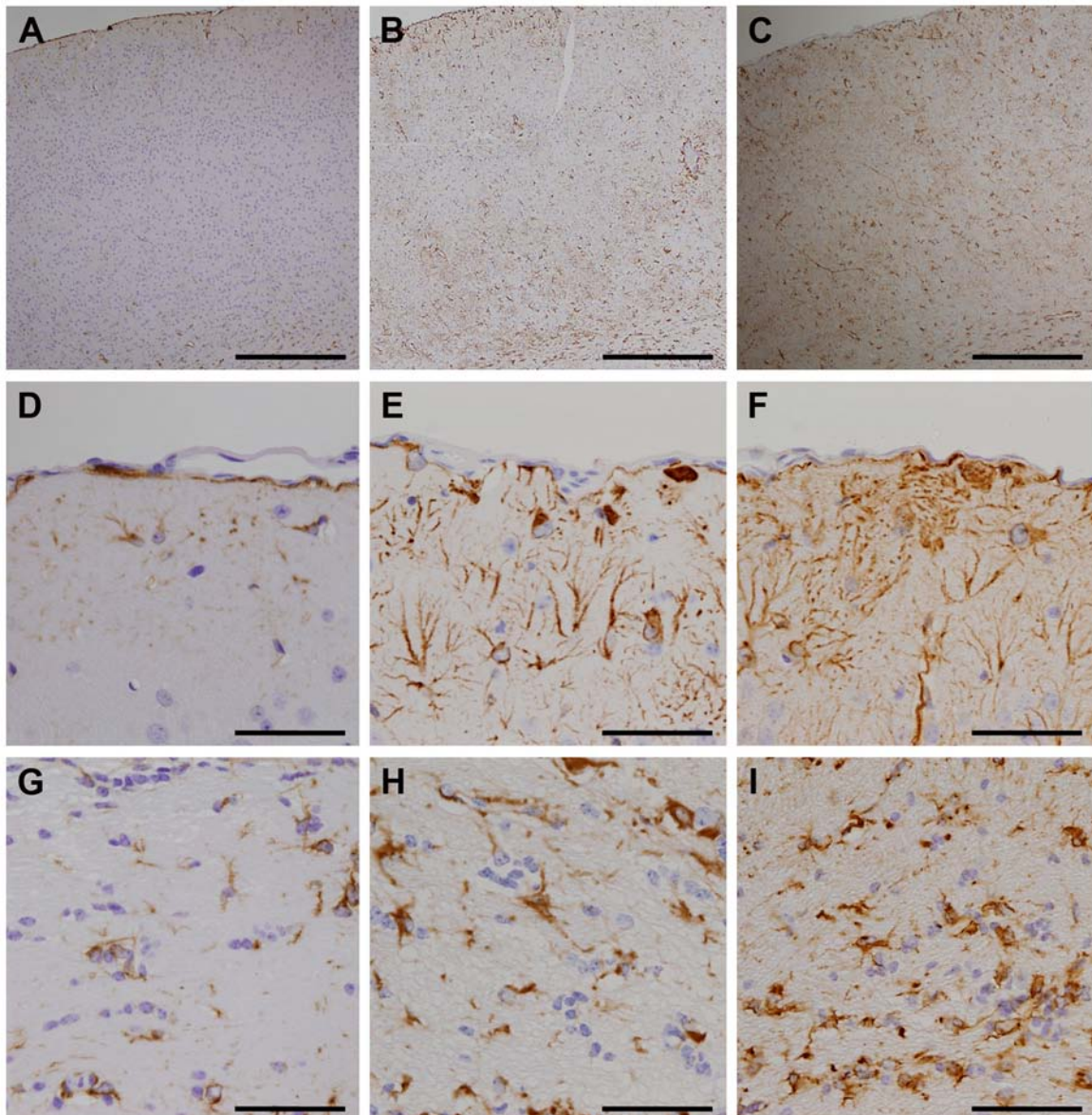


Fig. 14: Increased astrogliosis in naïve Tg(hGFAP) mice. Compared to wild type animals (A, D, G) mice overexpressing human GFAP (B-C, E-F, H-I) show increased GFAP-positive astrocytes in the cortex (A-C), subpial cortex (D-F) and corpus callosum (G-I) at the age of 8 weeks (A-B, D-E, G-H) and 14 weeks (C, F, I). Representative images were taken at 40x (A-C) and 400x original magnification (D-I) (scale bars: 500 μ m and 50 μ m).

The myelin content, the presence of activated microglia and number of mature oligodendrocytes were investigated in naïve animals. Eight-weeks-old naïve wild type mice showed a regular myelin content of the corpus callosum (Fig. 15A) which appeared similar in age-matched Tg(hGFAP) animals (Fig. 15B). Only few activated microglia were detected in the corpus callosum of naïve wild type mice (Fig. 15C). Animals overexpressing human GFAP demonstrate scattered activated microglia (Fig. 15D) and their density appeared similar to wild type mice.

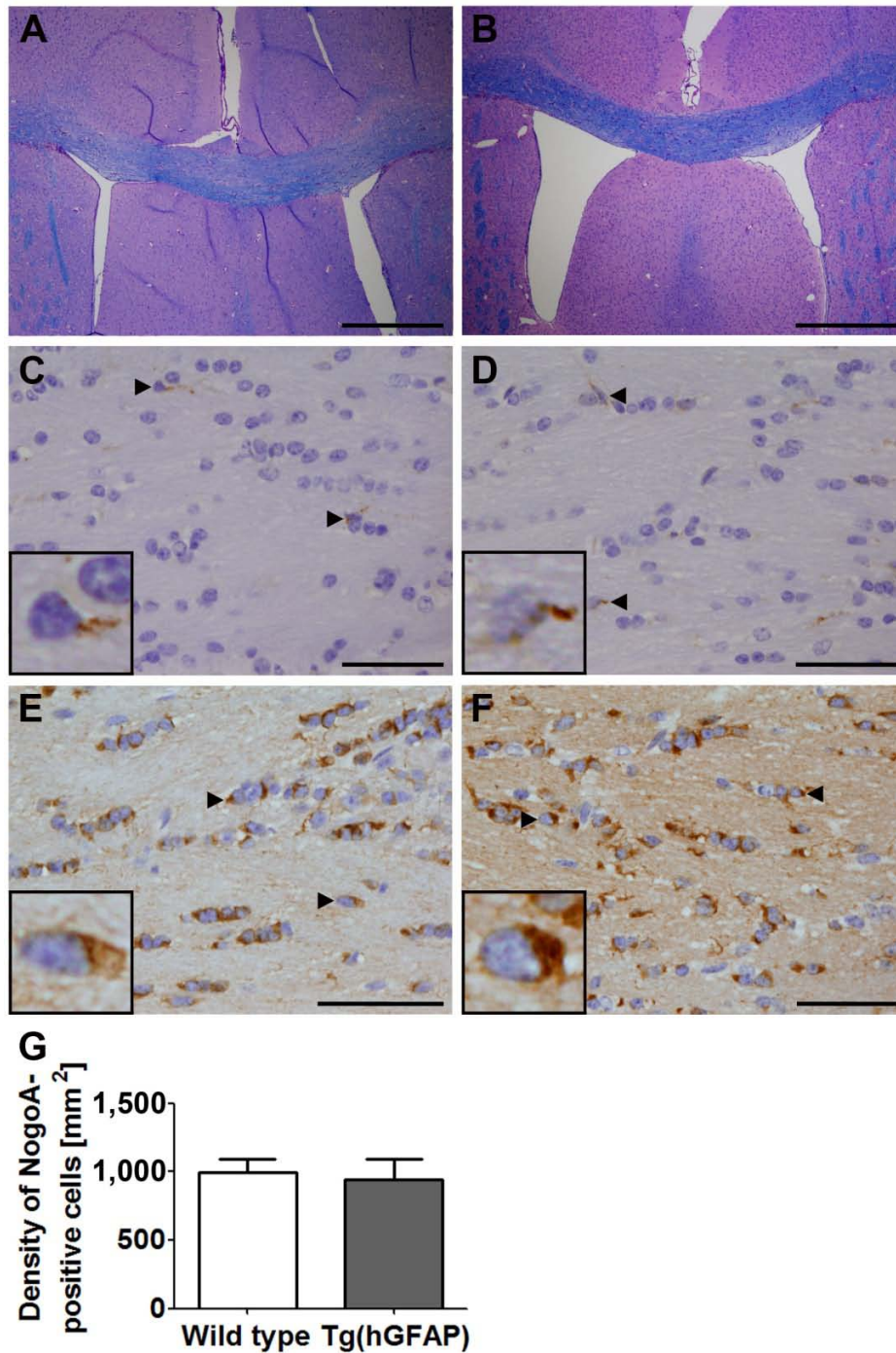


Fig. 15: Regular myelin content, activated microglia and number of mature oligodendrocytes in Tg(hGFAP) mice at the age of 8 weeks. Compared to naïve wild type mice (A, C, E) age-matched naïve Tg(hGFAP) mice (B, D, F) show similar myelin content of the corpus callosum on LFB-PAS-stained sections (A-B). Mac3-staining reveals similar densities of activated microglia (arrowheads) in the corpus callosum of wild type (C) and transgenic animals (D). Similar densities for NogoA-positive oligodendrocytes (arrowheads) are detected in the corpus callosum of wild type (E) and transgenic mice (F). Quantification of mature oligodendrocytes confirmed no significant difference in the number of oligodendrocytes between both groups (G) ($p > 0.05$). Representative images were taken at 40x (A-B) and 400x original magnification (C-F) (scale bars: 500 μm and 50 μm). Inserts show magnified representative cells.

Many mature oligodendrocytes were obvious in the corpus callosum of eight-week-old wild type (Fig. 15E) and transgenic mice (Fig. 15F). Quantification of NogoA-positive oligodendrocytes revealed similar numbers of mature oligodendrocytes in both groups (wild type: 996 ± 95 NogoA-positive cells per mm^2 ; Tg(hGFAP): 943 ± 149 NogoA-positive cells per mm^2 ; $p > 0.05$) (Fig. 15G).

3.2.2 Reduced cuprizone-induced oligodendroglial apoptosis in Tg(hGFAP) mice

The effect of an increased astrogliosis on cuprizone-induced demyelination was evaluated clinically and histologically in wild type and Tg(hGFAP) mice. Both groups showed an initial weight loss during the first week of cuprizone challenge. During six weeks of cuprizone treatment, transgenic mice showed significantly relative less weight loss than wild type mice after four, five and six weeks of cuprizone (Fig. 16).

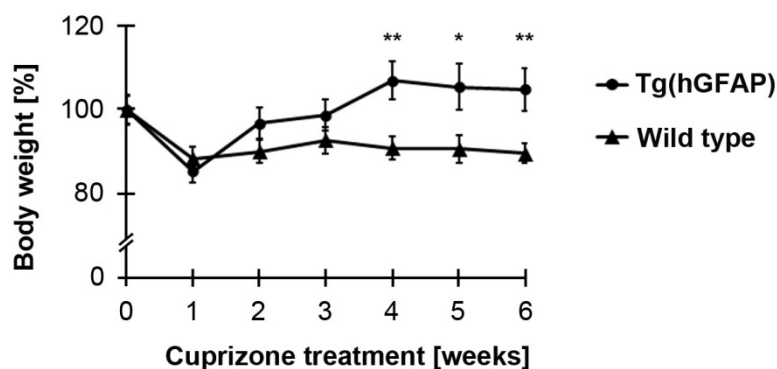


Fig. 16: Reduced weight loss in Tg(hGFAP) mice after cuprizone. Body weights of wild type and transgenic mice at weeks 0-6 during 0.25% cuprizone challenge. Transgenic mice show significantly higher body weights than wild type animals after 4, 5 and 6 weeks of cuprizone (** $p < 0.01$; * $p < 0.05$).

After one week of cuprizone, wild type animals showed numerous HE-stained apoptotic cells in the corpus callosum (Fig. 17A) whereas Tg(hGFAP) mice displayed only scattered apoptotic cells (Fig. 17B). Quantitative analysis revealed that the density of apoptotic cells was significantly reduced in transgenic animals after one week of cuprizone

(28 ± 19 apoptoses per mm^2) in comparison to wild type mice (102 ± 35 apoptoses per mm^2 ; $p < 0.001$) (Fig. 17C).

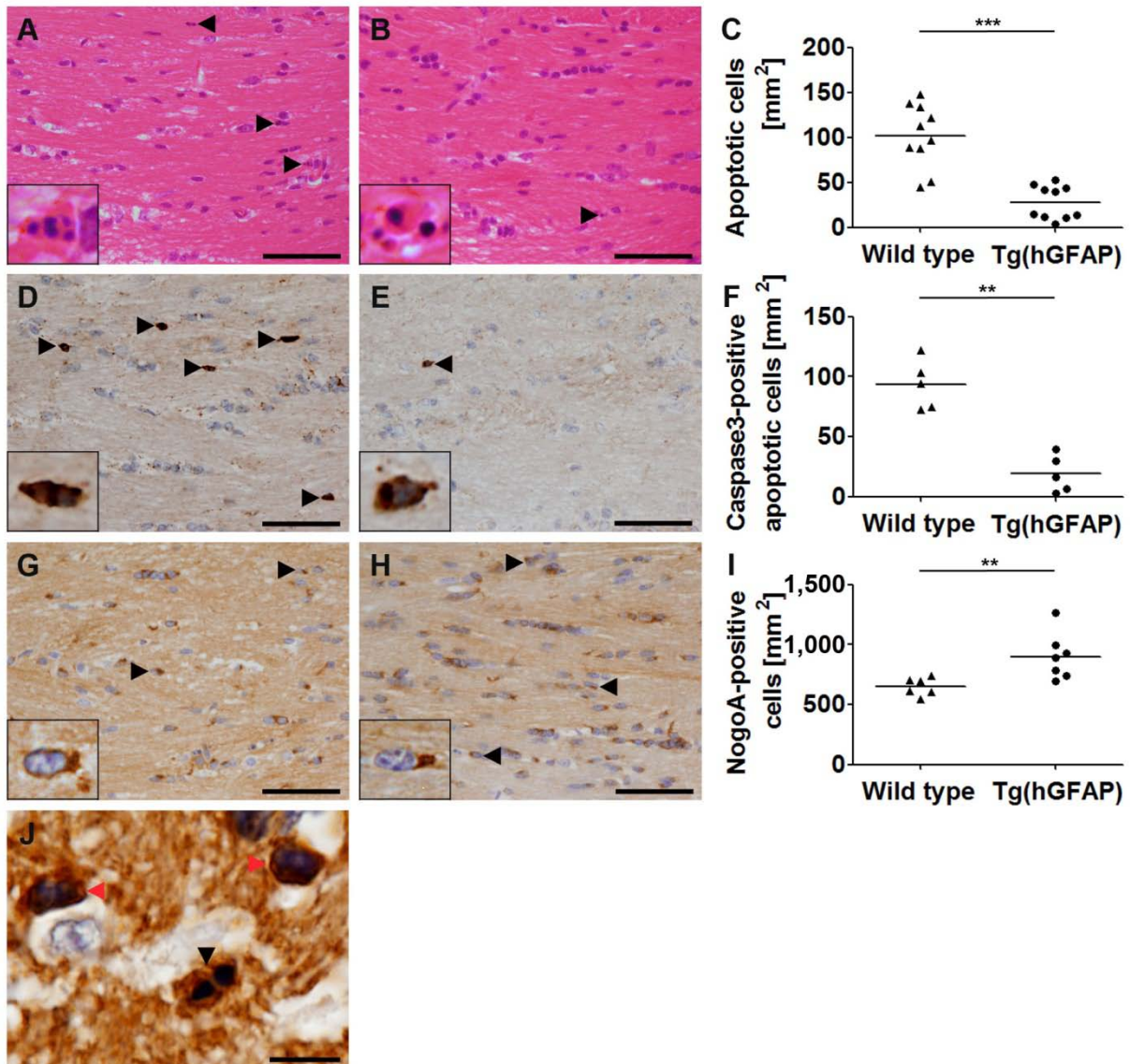


Fig. 17: Decreased oligodendroglial apoptosis in Tg(hGFAP) mice. Wild type animals (A) show significantly more apoptotic cells (arrowheads) in the corpus callosum than mice overexpressing human GFAP (B, C) after 1 week of 0.25% cuprizone (***) ($p < 0.001$). Compared to wild type mice (D) caspase3-positive apoptotic cells (arrowheads) are significantly decreased in transgenic animals (E, F). NogoA-positive oligodendrocytes (arrowheads) are significantly lower in wild type (G) compared to transgenic animals (** $p < 0.01$) (H, I). Oligodendrocytes are positive for CNPase (red arrowhead) (J). Some of the apoptotic cells are CNPase-positive (black arrowhead) indicating that these apoptotic cells are oligodendrocytes. Representative images of the medial part of the corpus callosum were taken at 400x original magnification (scale bars: 50 μm) (B-I) or at 1,000x original magnification (scale bar: 10 μm) (K). Inserts show magnified representative cells.

Wild type animals displayed widespread callosal demyelination (Fig. 18A, C) whereas the myelin appeared mainly intact in the corpus callosum of transgenic mice (Fig. 18B, D). Demyelination scores were significantly higher in wild type mice (score 2.9 ± 0.3) compared to transgenic animals (score 0.4 ± 0.5 ; $p < 0.001$) (Fig. 18E).

3.2.4 Less microglial activation and axonal damage in Tg(hGFAP) mice after cuprizone challenge

To detect further effects of an increased astrogliosis on cuprizone-induced pathology, microglial activation and axonal damage were evaluated in wild type and human GFAP transgenic animals. Mac3 staining revealed fewer activated microglial cells in the corpus callosum of transgenic animals (Fig. 19B) in comparison to wild type mice (Fig. 19A). The microglia density within the corpus callosum was significantly reduced in Tg(hGFAP) (171 ± 106 Mac3-positive cells per mm^2) compared to wild type animals (684 ± 330 Mac3-positive cells per mm^2 ; $p < 0.001$) (Fig. 19C).

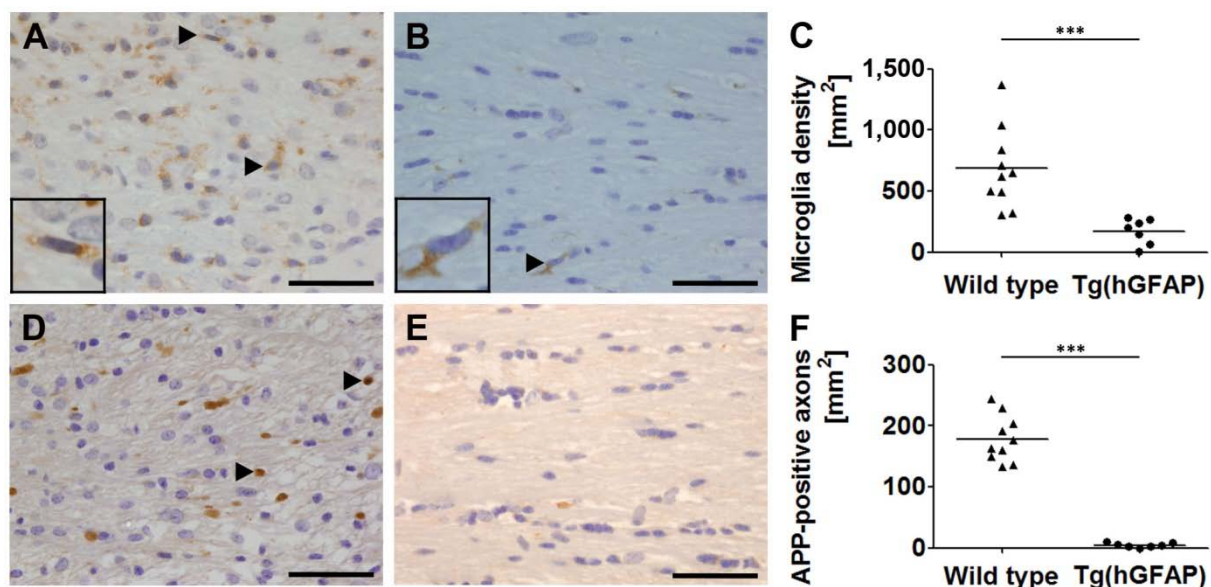


Fig. 19: Reduced cuprizone-induced microglial activation and axonal damage in human GFAP transgenic mice. Transgenic animals display less microglial activation (A-C) and axonal damage (D-F) compared to wild type mice after 6 weeks of 0.25% cuprizone. The density of Mac3-positive microglia (arrowheads) is significantly higher in wild type (A) compared to human GFAP transgenic mice (B, C) ($***p < 0.001$). Inserts show magnified representative cells. Compared to wild type mice (D) APP-positive axonal spheroids (arrowheads) are significantly reduced in Tg(hGFAP) animals (E, F) ($***p < 0.001$). Representative images of the medial part of the corpus callosum were taken at 400x original magnification (scale bars: 50 μm).

Wild type animals showed numerous damaged axons (Fig. 19D) whereas nearly no APP-positive axons were detected in transgenic mice (Fig. 19E). The quantitative analysis revealed a significant reduction of acute axonal damage in human GFAP transgenic compared to wild type mice (5 ± 4 vs. 179 ± 38 APP-positive axons per mm^2 , $p < 0.001$) (Fig. 19F).

3.2.5 Similar cerebral cuprizone concentrations in Tg(hGFAP) and wild type mice

To assess whether cuprizone levels were comparable in human GFAP overexpressing and wild type animals, cuprizone concentrations were measured in brain tissue of both groups after one week (Fig. 20A) and six weeks (Fig. 20B) of cuprizone feeding. The cerebral cuprizone concentrations did not differ significantly between wild type and transgenic mice after one week (wild type: 108 ± 74 ng/g brain tissue, Tg(hGFAP): 230 ± 175 ng/g brain tissue) (Fig. 20A) and after six weeks of cuprizone (wild type: 143 ± 69 ng/g brain tissue, Tg(hGFAP): 228 ± 128 ng/g brain tissue) (Fig. 20B).

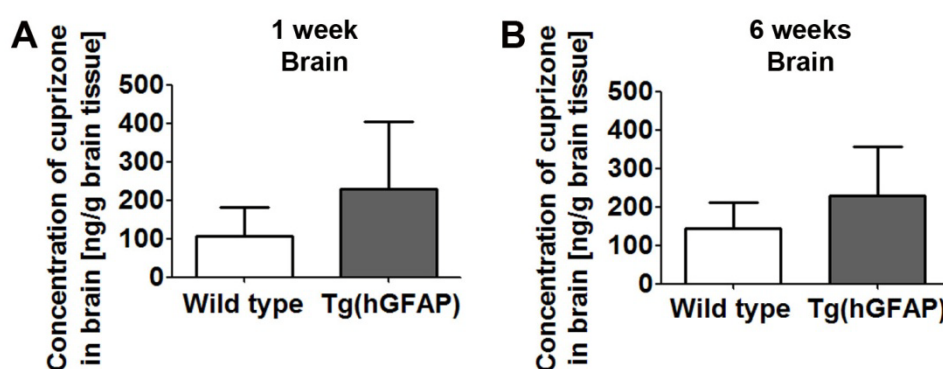


Fig. 20: Similar cuprizone concentration in brains of human GFAP transgenic and wild type mice. After 1 week (A) and 6 weeks (B) of 0.25% cuprizone treatment, cuprizone was quantified in brain samples of Tg(hGFAP) and wild type animals by RP-HPLC mass spectrometry analysis. Cuprizone concentrations are similar for both treatment regimes after both time spans ($p > 0.05$).

To determine whether cuprizone levels in plasma were comparable in both groups, mass spectrometry analyses were performed after one week (Fig. 21). Cuprizone

concentrations in plasma were very low and similar in both groups. They did not show any significant differences between wild type and human GFAP overexpressing animals (wild type: 3 ± 2 ng/ml plasma, Tg(hGFAP): 3 ± 2 ng/ml plasma).

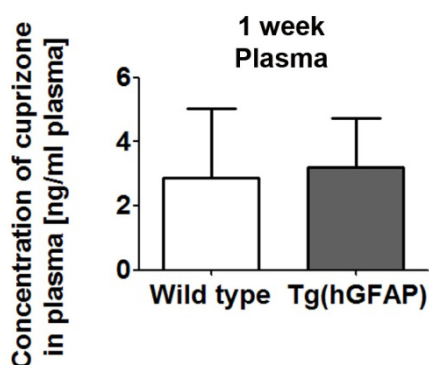


Fig. 21: Low cuprizone concentration in plasma of human GFAP transgenic and wild type mice. After 1 week of 0.25% cuprizone treatment, cuprizone was quantified in plasma samples of Tg(hGFAP) and wild type animals by RP-HPLC mass spectrometry analysis. Cuprizone concentrations are similar for both treatment regimes ($p > 0.05$).

3.2.6 Reduced astrocytic NF- κ B activation in Tg(hGFAP) mice after cuprizone

To investigate whether the overexpression of human GFAP exerts effects on NF- κ B activation in astrocytes, nuclear translocation of p65/RelA in astrocytes was detected by double immunofluorescence staining against antibodies of p65 and GFAP after six weeks of cuprizone. The proportion of astrocytes with nuclear p65 immunoreactivity was significantly reduced in Tg(hGFAP) ($5\% \pm 1\%$) compared to wild type mice ($25\% \pm 3\%$; $p < 0.01$) (Fig. 22).

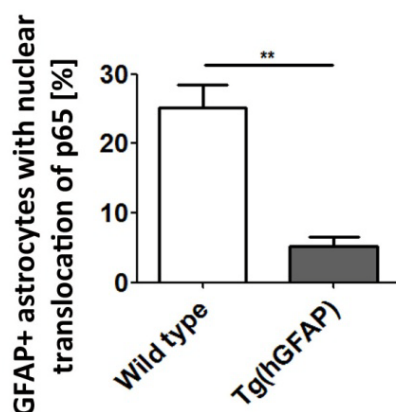


Fig. 22: Reduction of astrocytic NF- κ B activation in Tg(hGFAP) mice. Proportion of callosal astrocytes with nuclear p65 immunoreactivity is significantly reduced in Tg(hGFAP) animals ($5\% \pm 1\%$) in comparison to vehicle-treated mice ($25\% \pm 3\%$, $**p < 0.01$) after 6 weeks of 0.25% cuprizone which was indicated by double immunohistochemistry with antibodies against p65 and GFAP.

3.3 Examining the short-term effects of cuprizone *in vitro* and *in vivo*

3.3.1 No effect of cuprizone on astrocytic viability, but on astrocytic migration *in vitro*

To examine whether cuprizone directly affects astrocytic viability *in vitro*, primary mouse astrocytes were treated with 1 μ M, 10 μ M or 100 μ M cuprizone for 24 h. Untreated astrocytes served as controls. Mitochondrial respiration assessed by MTT assays was not affected by the treatment with 1 μ M (102% \pm 4% respiration capacity), 10 μ M (100% \pm 7% respiration capacity) or 100 μ M cuprizone (92% \pm 11% respiration capacity) compared to untreated control astrocytes (100% \pm 3% respiration capacity; $p > 0.05$) (Fig. 23A). The amount of astrocytic cell damage measured by lactate dehydrogenase assays (CytoTox One-Assay) was not significantly increased after treatment with 1 μ M (11,637 RFU \pm 1,620 RFU), 10 μ M (11,541 RFU \pm 3,970 RFU) or 100 μ M cuprizone (11,624 RFU \pm 3,213 RFU) compared to controls (9,168 RFU \pm 1,759 RFU; $p > 0.05$) (Fig. 23B).

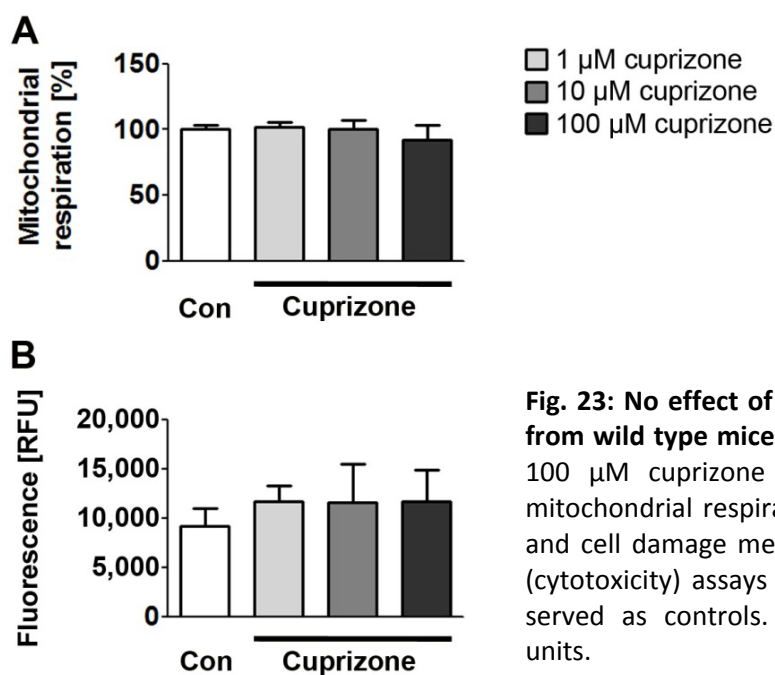


Fig. 23: No effect of cuprizone on primary astrocytes from wild type mice. Treatment with 1 μ M, 10 μ M or 100 μ M cuprizone for 24 h shows no effect on mitochondrial respiration assessed by MTT assays (A) and cell damage measured by lactate dehydrogenase (cytotoxicity) assays (B) in astrocytes. Untreated cells served as controls. B: RFU = relative fluorescence units.

To test whether cuprizone treatment affects the ability of astrocytes to migrate in a cell-free area, a scratch was made in a cell monolayer and astrocytes were treated with different cuprizone concentrations for up to 42 h. Primary astrocytes were treated with 1 μM cuprizone (Fig. 24B, F, J), 10 μM (Fig. 24C, G, K) or 100 μM cuprizone (Fig. 24D, H, L). Untreated astrocytes served as controls (Fig. 24A, E, I). At the beginning of the experiment, the size of the cell-free area was similar in all treatment conditions (Fig. 24A-D). After 24 h, astrocytes migrated into the cell-free area which has become smaller (Fig. 24E-H). After 42 h, the scratch was almost completely closed after treatment with 0 and 1 μM cuprizone (Fig. 24I, J), but the gap was still visible after treatment with the higher cuprizone doses of 10 and 100 μM (Fig. 24 K, L). Hence, treatment with high cuprizone doses showed no effect on astrocytic survival, but led to mild inhibition of astrocytic migration.

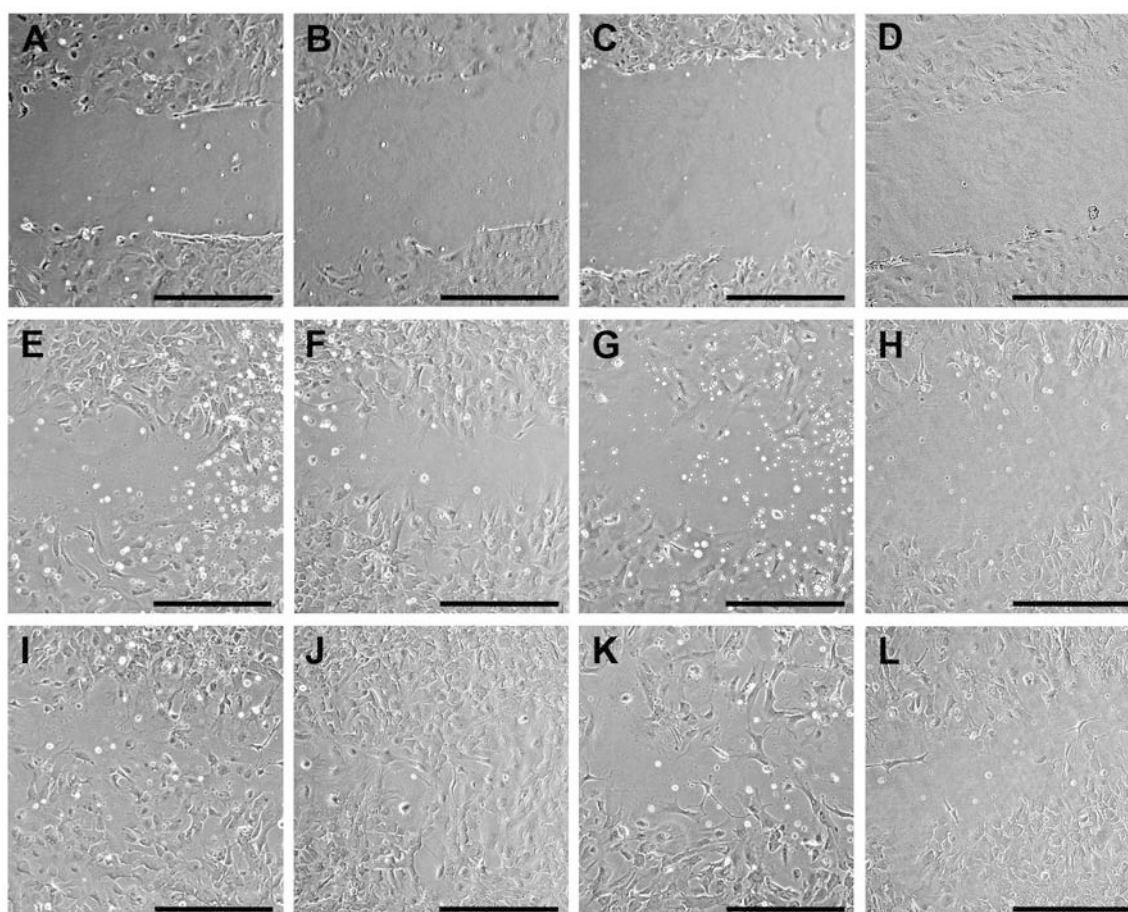


Fig. 24: Mildly reduced astrocytic migration under high cuprizone doses. A scratch is made in a cell monolayer at the beginning (0 h, A-D) and the ability to migrate is compared after 24 h (E-H) and 42 h (I-L). Treatment with the higher cuprizone doses of 10 μM (C, G, K) and 100 μM cuprizone (D, H, L) show a mild inhibition of astrocytic migration in comparison to astrocytes treated with 0 (A, E, I) or 1 μM cuprizone (B, F, J) (scale bars: 5 μm).

3.3.2 No effect of serum from cuprizone-treated mice on astrocytic viability and migration *in vitro*

To assess whether a metabolite of cuprizone might exert direct effects on astrocytes *in vitro*, primary mouse astrocytes were treated with medium containing 10% serum from cuprizone-treated mice or 10% serum from naïve mice as control for 24 h. Untreated astrocytes served as controls. Astrocytes treated with medium containing 10% serum from cuprizone-treated mice showed similar mitochondrial respiration ($113\% \pm 19\%$ respiration capacity) as control astrocytes ($100\% \pm 0\%$ respiration capacity) which was assessed by MTT assays (Fig. 25). Furthermore, astrocytes treated with 10% serum from cuprizone-treated animals demonstrated similar mitochondrial respiration as astrocytes treated with medium containing 10% serum from naïve animals ($109\% \pm 4\%$; $p > 0.05$) (Fig. 25). The effect of serum on astrocytic cell damage was not evaluated by lactate dehydrogenase assays (CytoTox One Assay) since serum itself interfered with fluorescence measurements.

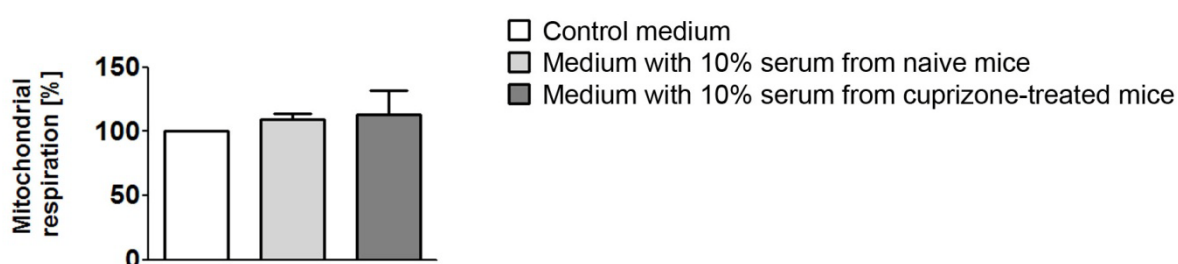


Fig. 25: No effect of serum from cuprizone-treated mice on mitochondrial respiration in primary astrocytes from wild type animals. No effect of serum from cuprizone-treated mice on astrocytes assessed by MTT assays ($p > 0.05$). Primary astrocytes were treated with medium containing 10% serum from naïve mice or 10% serum from cuprizone-treated animals for 24 h. Untreated cells served as controls.

To determine whether the serum from cuprizone-treated mice affects astrocytic migration, a scratch was made in a cell monolayer and astrocytes were treated with medium containing 10% serum from cuprizone-treated mice (Fig. 26C, F, I) or 10% serum from naïve animals (Fig. 26B, E, H) for 42 h. Untreated astrocytes only incubated with medium without any serum served as controls (Fig. 26A, D, G). At the beginning of the experiment the cell-free area was made by scratching the cells (Fig. 26A-C). After 24 h the cell-free area became smaller due to astrocytic migration (Fig. 26D-F). After 42 h the scratch was almost

completely closed by astrocytes. Compared to untreated astrocytes (Fig. 26G) no marked difference between astrocytes treated with serum from naïve mice (Fig. 26H) or serum from cuprizone-treated animals (Fig. 26I) was observed after 42 h. Hence, treatment with serum from cuprizone-treated mice showed no effect on mitochondrial respiration of astrocytes or astrocytic migration.

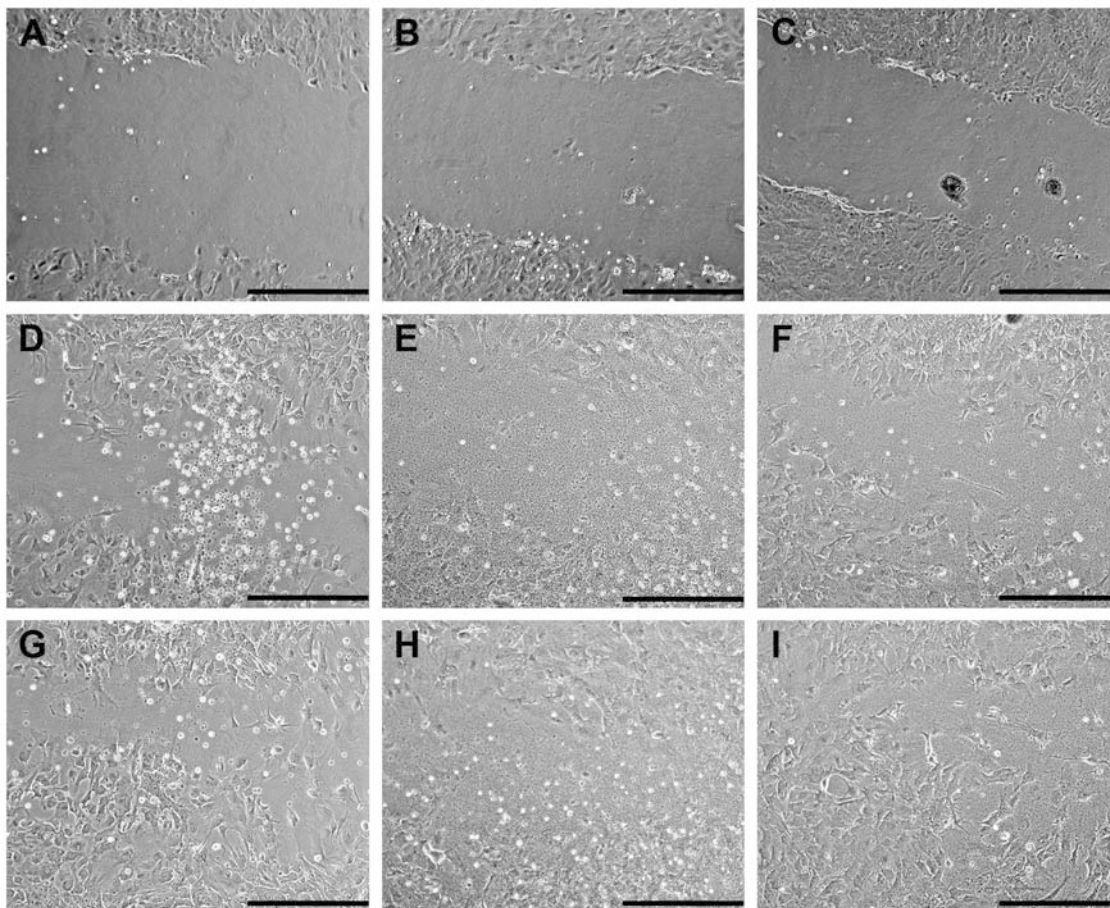


Fig. 26: No effect of serum from cuprizone-treated mice on migration of primary mouse astrocytes. A scratch is made in a cell monolayer at the beginning (0 h, **A-C**) and the ability to migrate is compared after 24 (**D-F**) and 42 h (**G-I**). Treatment with serum from naïve mice (**B, E, H**) or serum from cuprizone-treated mice (**C, F, I**) shows no effect on migration compared to untreated astrocytes (**A, D, G**) (scale bars: 5 μ m).

3.3.3 No direct cuprizone effect on glial cells after intracerebral injection *in vivo*

To examine whether stereotactical injection of cuprizone might cause demyelination or oligodendroglial apoptosis, mice were focally injected with 200 μ M cuprizone or PBS as control. The lesion site was identified by the blue dye included in the injection solution. Four days after injection, no demyelination was observed in mice injected with PBS (Fig. 27A) or cuprizone (Fig. 27B) and the myelin appeared intact. Evaluation of GFAP-stained sections revealed no loss of astrocytes at the lesion site or in adjacent tissue after focal injection of PBS (Fig. 27C) or 200 μ M cuprizone (Fig. 27D). Staining against NogoA demonstrated no loss of mature oligodendrocytes in both groups (Fig. 27E, F). Only few scattered apoptotic cells were observed after stereotactical injection of cuprizone or PBS (data not shown). Hence, focal injection of cuprizone did not affect myelin content or the presence of astrocytes and oligodendrocytes.

3.3.4 No direct effect of serum from cuprizone-treated mice after intracerebral injection *in vivo*

Focal injection of cuprizone did not cause demyelination or loss of oligodendrocytes and astrocytes raising the question whether a metabolite of cuprizone leads to cuprizone-induced pathology *in vivo*. Therefore, serum from cuprizone-treated mice was injected in the corpus callosum of wild type animals. Control mice were injected with serum from naïve animals. Four days after injection, similar myelin content was observed in mice injected with naïve serum (Fig. 28A) or serum from cuprizone-treated animals (Fig. 28B). Around the injection site GFAP-positive astrocytes were present in both groups (Fig. 28C, D). Mature oligodendrocytes appeared to be unaffected by focal injection of naïve serum (Fig. 28E) or serum from cuprizone-treated mice (Fig. 28F). Only few apoptosis were observed after stereotactical injection of cuprizone or control serum and the density of apoptotic cells were similar in both groups (data not shown). Hence, focal injection of serum from cuprizone-treated mice did not cause demyelination or loss of oligodendrocytes and astrocytes.

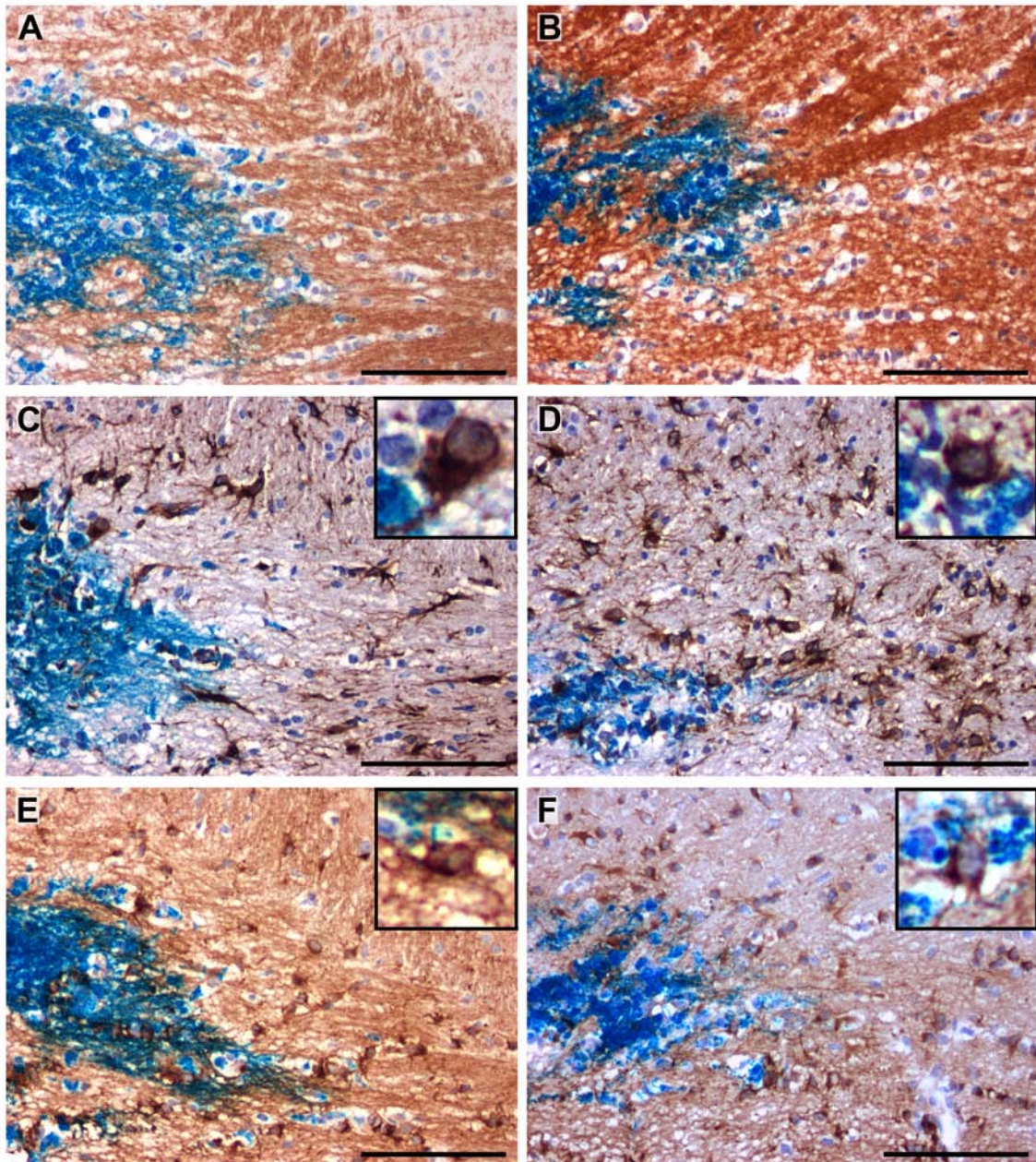


Fig. 27: No effect of cuprizone after focal injection in wild type mice. The lesion site was identified by the blue dye. Similar myelin content (A-B), presence of astrocytes (C-D) and mature oligodendrocytes (E-F) 4 days after stereotactical injection of PBS (A, C, E) and 200 μ M cuprizone (B, D, F). MBP-stained sections show no demyelination after focal injection of PBS (A) or cuprizone (B). GFAP-positive astrocytes are present after focal injection of PBS (C) and cuprizone (D). NogoA-positive oligodendrocytes are present in the injection site and in adjacent tissue in PBS- (E) and cuprizone-injected mice (F). Representative images of the lesion site were taken at 100x original magnification (scale bars: 200 μ m). Inserts show magnified representative cells.

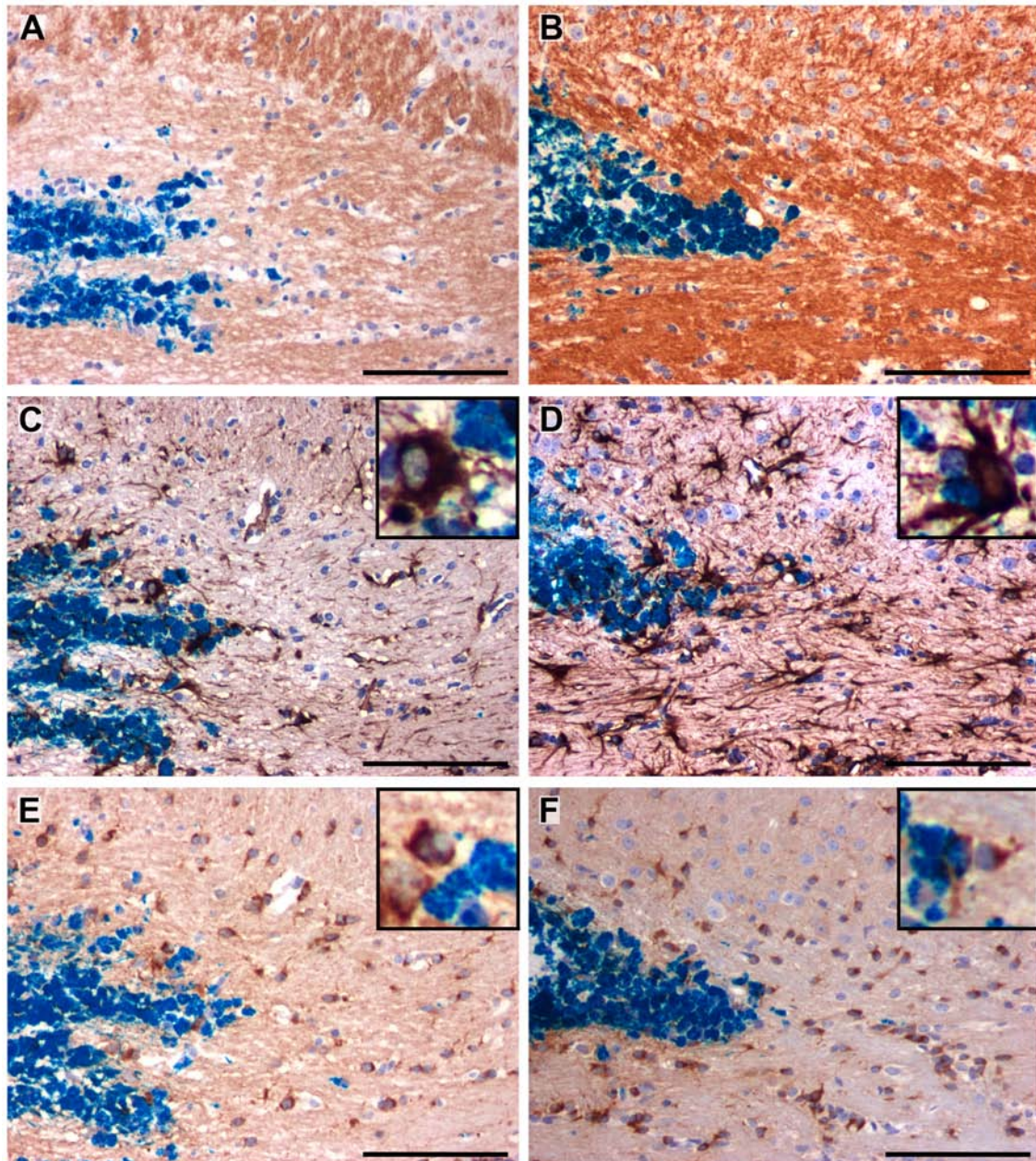


Fig. 28: No effect of serum from cuprizone-treated mice after focal injection in wild type animals. The lesion site was identified by the blue dye. Similar myelin content (**A-B**), presence of astrocytes (**C-D**) and mature oligodendrocytes (**E-F**) in mice 4 days after focal injection of serum from cuprizone-treated animals (**B, D, F**) and naïve serum (**A, C, E**). No demyelination was detected on MBP-stained sections after stereotactical injection of control serum (**A**) or cuprizone serum (**B**). GFAP-stained astrocytes are present in the injection site and in adjacent tissue after focal injection of cuprizone serum (**D**) compared to naïve serum (**C**). NogoA staining reveals no loss of oligodendrocytes after injection of naïve serum (**E**) and serum from cuprizone-treated mice (**F**). Representative images of the lesion site were taken at 100x original magnification (scale bars: 200 μ m). Inserts show magnified representative cells.

4 Discussion

The present study investigated intrinsic and therapy-induced astrocytic effects on cuprizone-induced pathology in mice.

The first aim of this work was to study the effects of LAQ on toxin-induced changes. In the cuprizone model, LAQ prevented demyelination, microglial activation, axonal damage, reactive astrogliosis and oligodendroglial apoptosis. Astrocytic NF- κ B activation was significantly decreased by 46% under 25 mg/kg LAQ compared to the vehicle group after six weeks of cuprizone. These data indicate that LAQ might protect from cuprizone-induced pathology through CNS-intrinsic mechanisms by reducing NF- κ B activation in astrocytes. This effect of LAQ was independent of T and B cells as evidenced by similar findings in Rag1-deficient mice. However, LAQ did not affect remyelination after cuprizone challenge or LPC-induced demyelination.

The second aim of this work was to study the impact of increased astrocytic GFAP expression on cuprizone-induced changes. Transgenic mice overexpressing human GFAP showed less demyelination, microglial activation and axonal damage. Oligodendroglial apoptosis and loss of oligodendrocytes were reduced after short cuprizone challenge. After six weeks of cuprizone transgenic mice displayed an 80% reduction of astrocytic NF- κ B activation compared to wild type mice.

A third minor aim of the present work was to examine direct effects of cuprizone on astrocytes *in vitro* and *in vivo*. *In vitro*, neither cuprizone nor serum from cuprizone-treated mice did affect mitochondrial respiration, astrocytic cell damage or migration capacity in primary mouse astrocytes. *In vivo*, myelin content and glial cells were not affected by focal stereotactic injection of cuprizone or serum from cuprizone-treated mice into the corpus callosum.

4.1 Reduced cuprizone-induced pathology under LAQ by down-regulation of astrocytic NF- κ B activation

4.1.1 Reduced cuprizone-induced weight loss and oligodendroglial apoptosis under LAQ

After one week of cuprizone challenge, there was no cuprizone-induced weight loss under LAQ treatment. At this time point, body weights in the vehicle group were reduced by 11% compared to initial weights whereas body weights in the LAQ group were not affected. During the further course of cuprizone challenge LAQ-treated mice displayed significantly higher body weights compared to vehicle-treated animals. Oligodendroglial apoptosis was reduced by 62% in LAQ-treated mice compared to vehicle-treated controls after one week of cuprizone.

To date, the exact mechanisms leading to cuprizone-induced weight loss as well as oligodendroglial apoptosis are not known. Both weight loss and oligodendroglial cell death under cuprizone are early changes that can be observed within the first week of cuprizone exposure (Hesse *et al.*, 2010). It is possible that cuprizone-induced oligodendroglial dysfunction and apoptosis might lead to slight cerebral dysfunction resulting in reduced general condition paralleled by a loss of appetite during the first and perhaps the following week(s) of cuprizone exposure.

4.1.2 Dose-dependent inhibition of demyelination under LAQ

After six weeks of cuprizone, LAQ-treated animals showed preservation of myelin in a dose-dependent manner. Vehicle-treated controls showed almost complete demyelination whereas mice treated with 5 mg/kg LAQ showed moderate demyelination compared to mainly intact myelin in animals treated with 25 mg/kg LAQ as shown by histological examination. These data demonstrate significantly reduced cuprizone-induced demyelination in the LAQ-treated group.

The concentration of 25 mg/kg LAQ was chosen for experiments since this concentration was well-tolerated and showed good efficacy in previous EAE studies

(Runström *et al.*, 2006). The lower concentration of 5 mg/kg LAQ was also shown to attenuate EAE severity in SJL/N animals (Brunmark *et al.*, 2002).

In clinical trials the administered LAQ concentration in humans is 0.6 mg per day since this dose was well-tolerated and showed clinical effects on relapses and disability (Comi *et al.*, 2012). The different dosages between mice and man are partly explained by a longer half-life in humans (approximately 70 hours) compared to mice (approximately three to seven hours) (Brück and Wegner, 2011).

4.1.3 Less microglial activation, axonal damage and astrogliosis under LAQ

After six weeks of cuprizone, LAQ-treated mice demonstrated significantly less microglial activation, axonal damage and astrogliosis within the CNS. Density of activated microglia was reduced by 82% in LAQ-treated compared to vehicle-treated animals. Acute axonal damage, measured as APP-positive axonal spheroids, was reduced by 97% under LAQ treatment compared to the vehicle group. Reactive astrogliosis was also inhibited in LAQ-treated compared to vehicle-treated mice after six weeks of cuprizone.

Activation of CNS-resident microglia appeared to be the most important component for cuprizone-induced demyelination whereas macrophages and T cells only have a minor contribution to cuprizone-induced pathology (Remington *et al.*, 2007). T cells recruited to the demyelinated tissue did not appear activated and infiltration of macrophages was negligible (Remington *et al.*, 2007).

Demyelination is associated with axonal damage and astrogliosis in the CNS. This acute axonal damage leads to irreversible axonal loss. This axonal damage was almost absent in LAQ-treated compared to vehicle-treated mice. This reduced tissue damage in the LAQ group is probably due to reduced cuprizone-induced demyelination under LAQ. Previously, LAQ was shown to exert similar beneficial effects on inflammation and axonal pathology in mice with EAE (Wegner *et al.*, 2010).

In demyelinated tissue GFAP protein expression in astrocytes is elevated as response to tissue damage. This increase of GFAP is a major feature of complex astrocytic changes referred to as reactive astrogliosis (Roessmann and Gambetti, 1986).

4.1.4 Similar cerebral cuprizone concentrations in LAQ- and vehicle-treated mice

Mass spectrometry analyses demonstrated no significant difference between cerebral cuprizone concentrations of LAQ- and vehicle-treated mice neither after one week nor after six weeks of cuprizone challenge. Cuprizone concentrations in plasma did not show any significant difference between both groups after one week of cuprizone either. These data suggest that the observed differences in demyelination, microglial activation, axonal damage and astrogliosis between both groups cannot be explained by different cuprizone concentrations in brain and plasma.

Previous studies also demonstrated the presence of cuprizone in brain and plasma samples after six months of cuprizone challenge which was assessed by mass spectrometry analyses (Zatta *et al.*, 2005). Further explanations for the observed differences in demyelination, microglial activation, axonal damage and astrogliosis between LAQ and vehicle groups might be the existence of cuprizone-related metabolites which could also be responsible for cuprizone-induced effects. However, the existence of potential cuprizone metabolites is not known (Zatta *et al.*, 2005) and hence could not be measured in the present thesis.

4.1.5 LAQ-related changes independent of T and B cells

Similar to wild type mice, LAQ-treated Rag1^{-/-} animals lacking T and B cells demonstrated reduced cuprizone-induced pathology after six weeks of cuprizone. Treated mice displayed reduced cuprizone-induced weight loss, demyelination, microglial activation, axonal damage and astrogliosis. These results indicate that the effect of LAQ in the cuprizone model is independent of T and B cells. Indeed, cuprizone-induced demyelination takes place in the near absence of T cells with an intact BBB as evidenced by previous studies indicating similar findings in Rag1^{-/-} and wild type mice after cuprizone challenge (Matsushima and Morell, 2001; Hiremath *et al.*, 2008). In healthy mice, studies using whole-body autoradiography demonstrate that 7 to 8% of LAQ penetrates through the intact BBB and reaches the brain in relation to the blood concentration (Brück and Wegner, 2011). Taken

together, these findings in Rag1^{-/-} and wild type mice suggest that LAQ has direct protective effects on the CNS.

4.1.6 Reduced astrocytic NF-κB activation by LAQ

The significant inhibition of reactive astrogliosis in the present study, as well as the observation that astrocytic NF-κB activation is necessary for cuprizone-induced demyelination (Raasch *et al.*, 2011), led to more detailed examinations of the role of astrocytic NF-κB activation. The reduced reactive astrogliosis seen in LAQ-treated animals was paralleled by a 46% reduction of astrocytic NF-κB activation in LAQ-treated mice *in vivo* after six weeks of cuprizone. In addition, microglial NF-κB activation did not differ between LAQ- and vehicle-treated animals after six weeks of cuprizone (oral communication by Dr. N. Kramann, Dept. of Neuropathology, University Medical Center Göttingen, Germany).

Further evidence comes from *in vitro* studies demonstrating that astrocytic, but not microglial, NF-κB activation was also reduced by LAQ by 46% in primary mouse cells assessed by NF-κB reporter assays (Brück *et al.*, 2012). The inhibition of astrocytic NF-κB activation *in vitro* was already observed after one hour. In addition, this publication also showed that LAQ-treated primary astrocytes displayed a down-regulation of various astrocytic pro-inflammatory markers (Brück *et al.*, 2012). *In vivo* and *in vitro* data demonstrating reduced astrocytic, but similar microglial, NF-κB activation under LAQ suggesting that LAQ affects upstream pathways causing NF-κB activation differentially in astrocytes and microglia.

In the CNS, astroglial NF-κB activation has a dual role and can cause both deleterious and beneficial effects. Beneficial effects include ischemia-related changes of glutamate transport in mice constitutively deficient for GFAP and Vimentin (Li L. *et al.*, 2008) and increased neurotrophic factors in primary rat astrocytic cultures (Zaheer *et al.*, 2001). Deleterious effects of astrocytic NF-κB activation include an increased excitotoxicity in postnatal rats (Acarin *et al.*, 2001) and an impaired neurite outgrowth demonstrated in cultured rat astrocytes (de Freitas *et al.*, 2002). Further studies showed that inhibition of astroglial NF-κB activation improved functional recovery after mouse spinal cord injury (Brambilla *et al.*, 2005) and EAE (Brambilla *et al.*, 2009). Collectively, these findings indicate a

potential role for the astrocytic NF- κ B pathway for the therapeutic treatment of CNS diseases.

4.1.7 No impact of LAQ on remyelination after cuprizone withdrawal

Therapeutic treatment with 25 mg/kg LAQ during the remyelination phase after six weeks of cuprizone challenge displayed similar extensive remyelination in LAQ- and vehicle-treated mice. Extensive remyelination was already detected four days after cuprizone withdrawal. The myelin content appeared similar in the corpus callosum of both treatment groups. This was further strengthened by the similar numbers of mature oligodendrocytes in LAQ- and vehicle-treated animals.

These results are further supported by recently published findings that LAQ did not directly affect primary mouse oligodendroglial cells (Brück *et al.*, 2012). In this study LAQ did not exert effects on oligodendroglial viability and staurosporin-induced cell death *in vitro* (Brück *et al.*, 2012). Taken together, these data indicate that LAQ does not show any marked effects on oligodendroglial cells or remyelination.

4.1.8 No effect of LAQ on LPC-induced demyelination

In contrast to the findings in the cuprizone model, LAQ demonstrated no significant effect on LPC-induced demyelination, a model with focal rapid demyelination. The amount of LPC-induced demyelination was similar in vehicle-treated mice and in animals treated with 25 mg/kg LAQ. Even higher doses of LAQ (40 mg/kg) did not show any effect on the amount of LPC-induced demyelination compared to vehicle-treated mice.

This lacking effect on LPC-induced demyelination might be due to differences in the underlying pathological mechanism of the two different models of toxic (focal versus global) cerebral demyelination. Potential reasons for the lack of effect of LAQ on LPC-induced demyelination could be the different targets of the toxins: LPC is directly toxic for myelin and glial cells whereas the toxic effects of cuprizone appear to be mediated by astrocytes (Woodruff and Franklin, 1999b; Raasch *et al.*, 2011). A second possible explanation for the

observed difference could be the time course of demyelination in both models: LPC-induced demyelination is very quick, it can be observed already four days after injection, whereas the cuprizone-induced demyelination takes place over several weeks (over five to six weeks) (Ludwin, 1978; Hiremath *et al.*, 1998). A third factor could be the tissue damage: LPC-induced demyelination is slightly destructive and leads at least partially to BBB damage. Hence, infiltration of peripheral inflammatory cells cannot be excluded. Finally, the lacking effect of LAQ on LPC-induced demyelination might also be related to the fact that astrocytic NF- κ B activation does not play a crucial role in LPC-mediated demyelination. This is further supported by the finding that mice lacking constitutive astrocyte-specific NF- κ B activation also showed similar LPC-induced demyelination as wild type mice (Raasch *et al.*, 2011).

4.1.9 Pronounced effects of LAQ on cuprizone-induced pathology compared to other immunomodulatory drugs

In the present study, nearly complete preservation of myelin and axons were observed under preventive therapy with LAQ in the cuprizone model. So far, LAQ is the only substance with marked effects in the murine cuprizone model. Only fingolimod, a sphingosine 1-phosphatate receptor agonist, attenuated cuprizone-induced demyelination, whereby moderate callosal demyelination was still observed in fingolimod-treated mice compared to marked demyelination in controls (Kim *et al.*, 2011). Treatment with fumaric acids (trans-butenedioic acids) did not affect demyelination or glial reactions in this model (Moharreggh-Khiabani *et al.*, 2010). The present thesis showed that LAQ did not affect remyelination after cuprizone withdrawal. Similar negative effects on remyelination were reported for fingolimod in this model (Kim *et al.*, 2011). Corticosteroids impaired remyelination after cuprizone-induced demyelination (Clarner *et al.*, 2011). However, statins showed inhibitory effects on remyelination after cuprizone challenge (Miron *et al.*, 2009). Up to now, there are no reports on the effects of glatiramer acetate on cuprizone-induced pathology. However, glatiramer acetate was shown to enhance oligodendrogenesis and remyelination after LPC-induced demyelination in mice (Skihar *et al.*, 2009). Furthermore, *in vitro* studies demonstrated that supernatants from human glatiramer acetate-reactive T

lymphocytes potentiated oligodendrocyte numbers in rodent and human OPC cultures (Zhang *et al.*, 2010).

4.1.10 Further potential factors contributing to central LAQ effects

Previous studies reported that LAQ exerted neuroprotective effects by modulation of BDNF. Studies in the EAE model revealed a more severe EAE course in mice constitutively lacking BDNF and treated with LAQ compared to wild type animals (Thöne *et al.*, 2012). Furthermore, studies in MS patients demonstrated that LAQ-treated MS patients showed higher serum levels of BDNF (Thöne *et al.*, 2012).

BDNF is expressed by multiple cell types including neurons and glia in the adult CNS (Riley *et al.*, 2004). Especially astroglial BDNF seems to play a role in neuroprotection since astroglial BDNF was up-regulated after treatment with several neuroprotective compounds in cultured mouse and rat astrocytes (Labie *et al.*, 1999; Mizuta *et al.*, 2001; Ohta *et al.*, 2002; Cardile *et al.*, 2003). Further studies reported an up-regulation of BDNF in primary rat astrocytes by NF- κ B after stimulation with TNF α (Saha *et al.*, 2006). Additionally, BDNF also activated NF- κ B in cultured rat hippocampal neurons (Kairisalo *et al.*, 2009) further supporting the view that LAQ might exert its beneficial effects via modulating astrocytic NF- κ B activity.

BDNF seems also play a role in the cuprizone model since BDNF protein levels were reduced in the corpus callosum of mice after cuprizone treatment (VonDran *et al.*, 2011). Furthermore, mice with constitutively reduced levels of BDNF exhibited increased numbers of oligodendrocyte progenitors and reduced levels of myelin proteins during de- and remyelination processes after cuprizone (VonDran *et al.*, 2011).

Phase III studies indicate that LAQ treatment leads to reduced brain atrophy and disability (Comi *et al.*, 2012). The present experimental data and these clinical findings suggest that the effects of LAQ are not limited to inflammatory focal lesions in MS.

4.1.11 Conclusion

In conclusion, preventive LAQ treatment led to reduced cuprizone-induced demyelination, microglial activation, axonal damage, astrogliosis and apoptosis. Furthermore, LAQ treatment decreased astrocytic NF- κ B activation despite similar cuprizone concentrations in the brains of LAQ- and vehicle-treated mice. These effects were independent of T and B cells. However, LAQ did not affect remyelination after cuprizone withdrawal or LPC-induced focal demyelination. Taken together, these data together with the clinical findings suggest a CNS-protective effect of LAQ by modulation of the astrocytic inflammatory response via NF- κ B down-modulation. These findings indicate that LAQ might be a promising future treatment of MS and potentially also other neurological diseases.

4.2 Less cuprizone-induced demyelination and astrocytic NF- κ B activation in transgenic mice overexpressing human GFAP

4.2.1 Regular cerebral myelin and oligodendrocyte density in naïve Tg(hGFAP) transgenic mice

Naïve mice overexpressing human GFAP showed regular cerebral myelin content and regular densities of mature oligodendrocytes at the age of eight weeks compared to their wild type littermates. Density of activated microglia was also similar in transgenic and wild type animals. Compared to wild type mice, animals overexpressing human GFAP showed increased astrogliosis and reactive astrocytes at the age of eight weeks.

The finding of regular myelin in these mice is in accordance with previous studies demonstrating regular myelin content in 13-day-old Tg(hGFAP) animals by electron microscopy (Messing *et al.*, 1998). Previous studies reported an increase of activated microglia at four month of age in these naïve transgenic mice which was assessed by quantitative PCR of brain samples (Hagemann *et al.*, 2005). This increased microglial activation appeared to be due to an initiated stress response of astrocytes leading to an activation of microglia (Hagemann *et al.*, 2005). In the present work, density of activated microglia did not seem to be increased in naïve animals, but microglial density was only

assessed histologically. The data on age-related increased astrogliosis in these transgenic mice are in line with previous publications (Messing *et al.*, 1998). Another transgenic mouse line (Tg 73.4) overexpressing similar hGFAP levels as the Tg(hGFAP) mice used in this thesis (line Tg 73.7) displayed also GFAP levels that were three- to five-fold higher than in wild type animals at the age of 14 days. This elevation even increased to over 10-fold in Tg 73.4 mice that were aged one year or older (Messing *et al.*, 1998).

4.2.2 Reduced oligodendroglial apoptosis in Tg(hGFAP) mice

After one week of cuprizone, both wild type and transgenic mice displayed reduced body weights in relation to their original weights. However, significantly higher relative weight gain was observed in Tg(hGFAP) animals after four, five and six weeks of cuprizone challenge. After one week of cuprizone, oligodendroglial apoptosis was reduced by 80% in Tg(hGFAP) mice compared to their wild type littermates. Mature oligodendrocytes were reduced by 28% in wild type animals whereas transgenic mice still showed similar densities of detectable oligodendrocytes comparable to oligodendroglial levels in naïve transgenic and wild type animals. These data suggest that astrocytic dysfunction in these transgenic mice led to reduced astrocyte-mediated oligodendroglial cell death compared to wild type animals.

4.2.3 Less cuprizone-induced demyelination in Tg(hGFAP) mice

After six weeks of cuprizone, the callosal myelin appeared present in animals overexpressing human GFAP compared to almost complete demyelination in wild type littermates as shown by histological examination. These findings indicate that the astrocytic changes related to the overexpression of human GFAP are responsible for the seemingly still present myelin in Tg(hGFAP) mice after cuprizone challenge. Future examinations are under way to determine which astrocytic factors and upstream pathways are responsible for the differential effects of cuprizone in Tg(hGFAP) animals compared to wild type animals.

4.2.4 Reduction of cuprizone-induced microglial activation and axonal damage in Tg(hGFAP) mice

After six weeks of cuprizone, acute axonal damage was almost absent in transgenic mice. The density of axonal spheroids was 97% higher in wild type animals compared to Tg(hGFAP) mice. At this time point, the density of activated microglia within the corpus callosum was 75% higher in the wild type group compared to the transgenic group. Differences in cerebral astrogliosis were already obvious in naïve transgenic mice at eight weeks of age. Hence, it was not possible to quantify and compare fiber gliosis between transgenic and wild type animals after six weeks of cuprizone challenge since the level of astrogliosis was already different in naïve mice.

4.2.5 Similar cerebral cuprizone concentrations in Tg(hGFAP) and wild type mice

Mass spectrometry analyses revealed no significant differences between cerebral cuprizone concentrations of wild type and Tg(hGFAP) mice after one and six weeks of cuprizone. However, absolute values of cuprizone concentrations in the brain were higher in transgenic compared to wild type animals. These data indicate that the reduced cuprizone-induced changes in Tg(hGFAP) mice cannot be related to lower cerebral cuprizone concentrations in these animals.

The findings mentioned above argue against a peripheral effect caused by GFAP-expressing cells outside the CNS. However, these peripheral cells exist. Previous studies showed that enteric glial cells were also rich in GFAP (Jessen and Mirsky, 1980). These cells extend throughout the different neural plexus, surround neuronal cell bodies and axons and contact blood vessels and epithelial cells. Further GFAP-expressing cells outside the CNS include satellite cells that envelope neurons, non-myelinating Schwann cells that surround non-myelinating axons as well as mesenchymal stellate cells in organs including liver, kidney, pancreas, lungs and testes. Although the functional role of these astrocytes-related cells are widely unknown, they appear to share astrocytic functions in tissue repair and scar formation as well as regulation of local immune and inflammatory responses (Sofroniew and

Vinters, 2010). However, the present data with similar cerebral cuprizone concentrations in both groups argue against an interference of GFAP-expressing cells outside the CNS.

4.2.6 Reduction of astrocytic NF- κ B activation in Tg(hGFAP) mice

After six weeks of cuprizone, transgenic mice overexpressing human GFAP showed a reduced astrocytic NF- κ B activation *in vivo*. The number of astrocytes with nuclear translocation of p65 was reduced by 80% in transgenic compared to wild type animals. These results were further strengthened by unpublished *in vitro* data showing a reduction of NF- κ B activation by approximately 56% in transgenic mice as evidenced by NF- κ B reporter assays (oral communication by Dr. N. Kramann, Dept. of Neuropathology, University Medical Center Göttingen, Germany). The observed findings of reduced astrocytic NF- κ B activation in Tg(hGFAP) animals suggest that the NF- κ B pathway is affected in these transgenic mice. Together with data of LAQ experiments these results indicate that astrocytic NF- κ B activation plays a crucial role for cuprizone-induced pathology.

Further evidence for an involvement of astrocytic NF- κ B pathway in human GFAP transgenic animals comes from previous publications. In three-weeks-old Tg(hGFAP) mice, numerous stress response genes showed increased transcript levels. The nuclear factor (erythroid-derived 2)-like 2 (Nrf2) expression was up-regulated and also the genes regulated by Nrf2 through the antioxidant response element (ARE) were activated (Hagemann *et al.*, 2005). Lacking Nrf2 in constitutive Nrf2-deficient mice seemed to accelerate NF- κ B-mediated pro-inflammatory reaction (Li W. *et al.*, 2008). This result was further strengthened by the observation that diverse Nrf2 activators attenuated LPS-induced NF- κ B activation in human cancer cells (Jeong *et al.*, 2004). Previous studies in human hepatoma cells showed that NF- κ B directly suppressed Nrf2 signaling at the transcription level since NF- κ B/p65 competed against Nrf2 for the transcription co-activator cyclic adenosine monophosphate (cAMP) response element-binding protein (CREB) (Liu *et al.*, 2008). Further studies are needed to shed light on the interplay between Nrf2 and NF- κ B.

4.2.7 Evidence for altered astrocytic function in Tg(hGFAP) mice

Recent publications suggest an altered astrocytic function in Tg(hGFAP) mice. *In vitro*, astrocytes from these animals showed a disrupted cytoskeletal network and suppressed astrocytic growth (Cho and Messing, 2009). Furthermore, the authors demonstrated decreased astrocytic proliferation, increased astrocytic cell death and higher vulnerability to H₂O₂ compared to cells from wild type mice. These findings provide evidence for dysfunctional astrocytes in these transgenic animals.

Factors contributing to astrocytic dysfunction in these transgenic mice might be related to differences in the GFAP amino acid sequence between man and mice. The positions of the two mutation hotspots in AxD are Arg79 and Arg239. The position of Arg79 is equivalent in human and mouse, but the position of amino acid 239 differs in both species (Brenner *et al.*, 1990), since the mouse sequence is offset from the human sequence by the absence of three residues in the head domain. However, further studies are necessary to clarify which factors contribute to astrocytic dysfunction in Tg(hGFAP) mice.

4.2.8 Conclusion

In conclusion, transgenic mice overexpressing human GFAP showed reduced cuprizone-induced demyelination, microglial activation and acute axonal damage after six weeks of cuprizone. These transgenic mice demonstrated reduced oligodendroglial apoptosis and loss after short cuprizone challenge. Furthermore, transgenic mice showed decreased astrocytic NF- κ B activation *in vivo* and *in vitro*. Taken together, these findings and the data from recent publications provide evidence for dysfunctional astrocytes with reduced NF- κ B activation, and recently reported increased Nrf2 expression in these transgenic mice. The reduced astrocytic NF- κ B activation might partly explain the reduced cuprizone-induced changes observed in these transgenic mice.

4.3 No marked direct effects of short-term cuprizone challenge on astrocytic survival *in vitro* and on glial cells *in vivo*

4.3.1 No effect of cuprizone on astrocytic survival, but on astrocytic migration *in vitro*

In the present study, treatment with 1 μM up to 100 μM cuprizone showed no effects on mitochondrial respiration and cell damage in primary astrocytes. However, high cuprizone concentrations (10 μM and 100 μM) seemed to mildly inhibit astrocytic migration *in vitro*. These high cuprizone concentrations, especially the highest concentration of 100 μM cuprizone, are far above the relevant intracerebral cuprizone concentrations *in vivo*. This is supported by the *in vivo* mass spectrometry data of the present thesis which revealed concentrations of < 1 μM cuprizone per gram brain tissue. Mice treated with cuprizone for one or six weeks showed cerebral cuprizone concentrations ranging between ≤ 180 nM and ≤ 510 nM cuprizone per gram brain tissue. The highest concentration of 100 μM cuprizone used in these assays is in line with other *in vitro* studies in rat oligodendrocytes using 100 μM cuprizone or even higher concentrations (Pasquini *et al.*, 2007). Importantly, only astrocytic survival and migration were evaluated in the present study. More detailed cuprizone effects such as the astrocytic secretion of cytokines or chemokines which may potentially influence oligodendrocyte survival have not been investigated. Further examinations are necessary to clarify cuprizone-induced indirect effects mediated by astrocytes on oligodendrocytes.

However, previous studies did not find clear evidence for cuprizone-induced astrocyte-mediated effects on oligodendrocytes. Treatment of primary oligodendrocyte cultures with conditioned medium from cuprizone-treated astrocytes did not lead to changes in oligodendroglial cell viability (Pasquini *et al.*, 2007). Additionally, cuprizone did not affect astrocytic NF- κB activation *in vitro* which was assessed by NF- κB reporter assays (oral communication by Dr. N. Kramann, Dept. of Neuropathology, University Medical Center Göttingen, Germany). Taken together, these data indicate no conclusive effect of cuprizone *in vitro*. Potential explanations for the observed differences *in vivo* and *in vitro* could be the different time courses: *In vivo*, early effects of cuprizone were observed one or six weeks after cuprizone challenge whereas *in vitro*, astrocytes were treated only for 24 h with cuprizone. However, oligodendrocyte death *in vivo* already starts early after initiation of

cuprizone challenge and apoptotic cells are already seen after two days of cuprizone diet in the corpus callosum and cortex (Buschmann *et al.*, 2012) indicating that potential direct *in vitro* effects of cuprizone on glial cells might already be detectable after short incubation times.

A second explanation could be that metabolic processes *in vivo* are necessary for cuprizone-induced pathology involving potential metabolite(s). To control for potential metabolites, primary astrocytes were also treated with serum from cuprizone-treated mice in this thesis, but there were no effects on astrocytic mitochondrial respiration and migration capacity either. Plasma levels of cuprizone itself are low as evidenced by the spectrometric data provided in this thesis. However, the levels and existence of potential cuprizone metabolites are not known. The effect of serum on astrocytic cell damage was not evaluated since the presence of serum interfered with the corresponding assay. To date, there is no evidence for a metabolic transformation of cuprizone (Kipp *et al.*, 2009).

4.3.2 Presence of oligodendrocytes and astrocytes after focal intracerebral injection of cuprizone

Intracerebral injections of different agents - such as cuprizone or serum from cuprizone-treated mice - did not affect local astrocytes, oligodendrocytes or myelin content.

Potential reasons for the lack of effect of cuprizone after focal injection could be the short time course or low exposure to the corresponding agents: After focal injection of cuprizone, mice were already sacrificed after four days. Alternatively a single injection might not have been sufficient for direct effects on glial cells. Potential confounds caused by peripheral effects such as a locally damaged BBB after focal injection could also contribute to these lacking effects under the different conditions.

4.3.3 Conclusion

In conclusion, *in vitro* treatment with cuprizone or serum from cuprizone-treated mice did not affect mitochondrial respiration and astrocytic cell damage, but high cuprizone concentrations mildly inhibited the migration capacity in primary astrocytes. Focal intracerebral injection of these agents did not affect myelin content or detectable astro- and oligodendroglial cells. Taken together, published data and data from the present work indicate no clear *in vitro* effect of cuprizone on astrocytes. In addition, the previously published *in vitro* effects of cuprizone on oligodendroglial cells also remain inconclusive. This *in vivo* part of this thesis indicates no direct effect of cuprizone or serum from cuprizone-treated mice on myelin content and detectable astro- and oligodendroglial cells after intracerebral injection. These results indicate that the mechanism of action of cuprizone differs *in vivo* from *in vitro* and is not well understood. Further studies are required to clarify its mechanism of action.

4.4 Concluding remarks on astrocytic involvement in demyelinating diseases

The current findings emphasize the important contribution of astrocytes during toxic demyelination. However, astrocytes also play a crucial role in human demyelinating diseases as clearly indicated by the finding of autoantibodies against AQP4 in the MS-related disease NMO (Lennon *et al.*, 2005).

Astrocytes contribute to pathological processes including the production of neurotrophic factors, the expression of ion channels and neurotransmitters, as well as the secretion of chemokines and cytokines (Sofroniew, 2009). Astrocytes have a dual role for demyelinating diseases such as MS and can mediate both deleterious and beneficial effects. On the one hand astrocytes can prevent widespread tissue damage by formation of a glial scar around demyelinated lesions. Further beneficial effects of reactive astrocytes include the mediation of anti-inflammatory responses, suppression of T cell activation and repair of the BBB (Nair *et al.*, 2008). On the other hand reactive astrocytes produce hyaluron which accumulates in chronic demyelinated MS lesions and inhibits OPC maturation (Back *et al.*,

2005). Deleterious effects also include the production of proinflammatory cytokines driving inflammation, BBB leakage, and invasion of immune cells into lesions (Nair *et al.*, 2008).

Up to now, the role of astrocytes for MS is not fully understood, but some studies strengthen that astrocytes might be important for MS. The voltage-sensitive sodium channel Nav1.5 is up-regulated in astrocytes in active and chronic MS lesions (Black *et al.*, 2010). GFAP is increased in CSF in patients with progressive MS (Malmeström *et al.*, 2003). Furthermore, serum levels of antibodies to the astrocytic inwardly rectifying potassium channel (KIR) 4.1 are elevated in MS patients compared to healthy persons or those with other neurological diseases (Srivastava *et al.*, 2012).

The data of the present thesis suggest that reduction of the NF- κ B activation in astrocytes might be a potential future therapy for demyelinating diseases such as MS. The effects of LAQ on astrocytic activation are CNS-intrinsic and might explain that LAQ has more pronounced effects on sustained disability progression and brain atrophy than on relapses. The findings from the present work emphasize the role of modulation of astrocytic activation as promising therapeutic target for patients with demyelinating diseases such as MS.

5 Summary and Conclusions

Astrocytes play a crucial role in demyelinating diseases which has been highlighted by pathogenetic autoantibodies against the astrocytic water channel aquaporin-4 in the MS-related disease neuromyelitis optica. Cuprizone-induced demyelination takes place with an intact BBB whereby activation of nuclear factor kappa of activated B cells (NF- κ B) plays a key role for cuprizone-induced pathology. Recent clinical studies in MS suggest that laquinimod (LAQ) might have direct CNS-protective effects in addition to its known peripheral anti-inflammatory properties. The present thesis evaluated intrinsic and therapy-induced astrocytic effects on toxic demyelination in mice.

The first part of this thesis evaluated the impact of LAQ on toxin-induced changes *in vivo*. After one week of cuprizone the density of oligodendrocyte apoptosis was significantly reduced in mice treated with 25 mg/kg LAQ compared to vehicle-treated animals. After six weeks of cuprizone the following findings were observed: Demyelination was decreased in a dose-dependent manner in mice treated with 0, 5 and 25 mg/kg LAQ. Microglial activation, axonal damage and reactive astrogliosis were also reduced under 25 mg/kg LAQ compared to the vehicle group. Astrocytic NF- κ B activation assessed by nuclear translocation of p65 in GFAP-positive astrocytes was significantly decreased by 46% after LAQ treatment. Similar findings were demonstrated in recombination activating gene 1-deficient mice treated with 25 mg/kg LAQ indicating that LAQ exerted effects on cuprizone-induced pathology independent of T and B cells. Mass spectrometry revealed similar cerebral cuprizone concentrations in wild type mice treated with and without LAQ after one and six weeks of cuprizone. Therefore, the observed differences in cuprizone-induced pathology cannot be explained by different cuprizone concentrations. However, LAQ showed no impact on remyelination after previous cuprizone challenge or on lysolecithin-induced demyelination. These findings indicate that LAQ might protect from cuprizone-induced pathology through CNS-intrinsic mechanisms by reducing the astrocytic NF- κ B activation. Recently published *in vitro* data support these findings by demonstrating that LAQ directly inhibited the astrocytic, but not microglial, NF- κ B activation and thereby down-regulated the astrocytic pro-inflammatory response.

The second part of this work investigated the impact of increased astrocytic GFAP expression on cuprizone-induced pathology *in vivo*. Naïve transgenic mice overexpressing human wild type GFAP referred to as Tg(hGFAP) displayed increased astrogliosis, but regular myelin content as well as oligo- and microglial densities, compared to wild type animals. After one week of cuprizone, transgenic mice revealed reduced oligodendroglial apoptosis and increased densities of mature oligodendrocytes compared to wild type animals. After six weeks of cuprizone less demyelination, microglial activation and axonal damage was observed in Tg(hGFAP) compared to wild type mice. Astrocytic NF- κ B activation evidenced by nuclear translocation of p65 was reduced by 80% in Tg(hGFAP) compared to wild type mice. Spectrometric cuprizone concentrations in the brain were similar in both groups after one and six weeks of cuprizone. Therefore, the observed changes in cuprizone-induced pathology cannot be explained by different cuprizone concentrations. The reduced cuprizone-related pathology in Tg(hGFAP) is likely to be related to at least two factors: (1) reduced astrocytic NF- κ B activation as well as (2) widespread astrocytic dysfunction such as compromised proliferation, reduced proteosomal activity and decreased resistance to stress demonstrated previously *in vitro* in these transgenic mice.

The third part of the thesis assessed direct effects of cuprizone on astrocytes *in vitro* and *in vivo*. *In vitro*, neither cuprizone nor serum from cuprizone-treated mice affected mitochondrial respiration and astrocytic cell damage, but high cuprizone concentrations mildly inhibited the migration capacity in primary mouse astrocytes. *In vivo*, focal stereotactic intracerebral injection of cuprizone or serum from cuprizone-treated mice did not affect the myelin content or the presence of astrocytes and oligodendrocytes. However, this thesis did not assess more detailed cuprizone effects such as astrocytic cytokines which may potentially influence oligodendrocyte survival *in vitro*. The current results suggest that the mechanism of action of cuprizone differs *in vivo* from *in vitro* and is still not well understood.

The findings from the present work and recently published data demonstrate that cuprizone-induced pathology is mediated by astrocytic NF- κ B activation. These data emphasize the potential role of modulating astrocytic activation for future treatment of demyelinating diseases such as MS.

References

- Acarin L, Gonzalez B, Castellano B (2001) Triflusal posttreatment inhibits glial nuclear factor-kappaB, downregulates the glial response, and is neuroprotective in an excitotoxic injury model in postnatal brain. *Stroke* 32:2394-2402.
- Acheson ED, Bachrach CA, Wright FM (1960) Some comments on the relationship of the distribution of multiple sclerosis to latitude, solar radiation, and other variables. *Acta Psychiatr Scand Suppl* 35:132-47.
- Alexander WS (1949) Progressive fibrinoid degeneration of fibrillary astrocytes associated with mental retardation in a hydrocephalic infant. *Brain* 72:373-81.
- Alotaibi S, Kennedy J, Tellier R, Stephens D, Banwell B (2004) Epstein-Barr virus in pediatric multiple sclerosis. *JAMA* 291:1875-9.
- Back SA, Tuohy TM, Chen H, Wallingford N, Craig A, Struve J, Luo NL, Banine F, Liu Y, Chang A, Trapp BD, Bebo BF Jr, Rao MS, Sherman LS (2005) Hyaluronan accumulates in demyelinated lesions and inhibits oligodendrocyte progenitor maturation. *Nat Med* 11:966-72.
- Bacon CM, Petricoin EF 3rd, Ortaldo JR, Rees RC, Lerner AC, Johnston JA, O'Shea JJ (1995) Interleukin 12 induces tyrosine phosphorylation and activation of STAT4 in human lymphocytes. *Proc Natl Acad Sci U S A* 92:7307-11.
- Banwell B, Bar-Or A, Arnold DL, Sadovnick D, Narayanan S, McGowan M, O'Mahony J, Magalhaes S, Hanwell H, Vieth R, Tellier R, Vincent T, Disanto G, Ebers G, Wambara K, Connolly MB, Yager J, Mah JK, Booth F, Sebire G, Callen D, Meaney B, Dilenge ME, Lortie A, Pohl D, Doja A, Venketaswaran S, Levin S, Macdonald EA, Meek D, Wood E, Lowry N, Buckley D, Yim C, Awuku M, Cooper P, Grand'maison F, Baird JB, Bhan V, Marrie RA (2011) Clinical, environmental, and genetic determinants of multiple sclerosis in children with acute demyelination: a prospective national cohort study. *Lancet Neurol* 10:436-45.
- Barkhof F, Bruck W, De Groot CJ, Bergers E, Hulshof S, Geurts J, Polman CH, van der Valk P (2003) Remyelinated lesions in multiple sclerosis: magnetic resonance image appearance. *Arch Neurol* 60:1073-81.
- Bettelli E, Das MP, Howard ED, Weiner HL, Sobel RA, Kuchroo VK (1998) IL-10 is critical in the regulation of autoimmune encephalomyelitis as demonstrated by studies of IL-10- and IL-4-deficient and transgenic mice. *J Immunol* 161:3299-306.
- Bieber AJ, Kerr S, Rodriguez M (2003) Efficient central nervous system remyelination requires T cells. *Ann Neurol* 53:680-4.

- Bjartmar C, Trapp BD (2001) Axonal and neuronal degeneration in multiple sclerosis: mechanisms and functional consequences. *Curr Opin Neurol* 14:271-278.
- Black JA, Newcombe J, Waxman SG (2010) Astrocytes within multiple sclerosis lesions upregulate sodium channel Nav1.5. *Brain* 133:835-46.
- Blakemore WF (1973) Remyelination of the superior cerebellar peduncle in the mouse following demyelination induced by feeding cuprizone. *J Neurol Sci* 20:73-83.
- Blakemore WF (1976) Invasion of Schwann cells into the spinal cord of the rat following local injections of lysolecithin. *J Neuropathol Appl Neurobiol* 2:21-39.
- Blakemore WF, Franklin RJ (2008) Remyelination in experimental models of toxin-induced demyelination. *Curr Top Microbiol Immunol* 318:193-212.
- Bø L, Vedeler CA, Nyland HI, Trapp BD, Mørk SJ (2003) Subpial demyelination in the cerebral cortex of multiple sclerosis patients. *J Neuropathol Exp Neurol* 62:723-32.
- Bongcam-Rudloff E, Nistér M, Betsholtz C, Wang JL, Stenman G, Huebner K, Croce CM, Westermark B (1991) Human glial fibrillary acidic protein: complementary DNA cloning, chromosome localization, and messenger RNA expression in human glioma cell lines of various phenotypes. *Cancer Res* 51:1553-60.
- Borrett D, Becker LE (1985) Alexander's disease. A disease of astrocytes. *Brain* 108:367-85.
- Brambilla R, Bracchi-Ricard V, Hu WH, Frydel B, Bramwell A, Karmally S, Green EJ, Bethea JR (2005) Inhibition of astroglial nuclear factor kappaB reduces inflammation and improves functional recovery after spinal cord injury. *J Exp Med* 202:145-156.
- Brambilla R, Persaud T, Hu X, Karmally S, Shestopalov VI, Dvorianchikova G, Ivanov D, Nathanson L, Barnum SR, Bethea JR (2009) Transgenic inhibition of astroglial NF-kappa B improves functional outcome in experimental autoimmune encephalomyelitis by suppressing chronic central nervous system inflammation. *J Immunol* 182:2628-40.
- Brand-Schieber E, Werner P, Iacobas DA, Iacobas S, Beelitz M, Lowery SL, Spray DC, Scemes E (2005) Connexin43, the major gap junction protein of astrocytes, is down-regulated in inflamed white matter in an animal model of multiple sclerosis. *J Neurosci Res* 80:798-808.
- Brenner M, Lampel K, Nakatani Y, Mill J, Banner C, Mearow K, Dohadwala M, Lipsky R, Freese E (1990) Characterization of human cDNA and genomic clones for glial fibrillary acidic protein. *Brain Res Mol Brain Res* 7:277-86.
- Brenner M, Johnson AB, Boespflug-Tanguy O, Rodriguez D, Goldman JE, Messing A (2001) Mutations in GFAP, encoding glial fibrillary acidic protein, are associated with Alexander disease. *Nat Genet* 27:117-20.

- Brunmark C, Runstrom A, Ohlsson L, Sparre B, Brodin T, Astrom M, Hedlund G (2002) The new orally active immunoregulator laquinimod (ABR-215062) effectively inhibits development and relapses of experimental autoimmune encephalomyelitis. *J Neuroimmunol* 130:163-172.
- Brück W, Porada P, Poser S, Rieckmann P, Hanefeld F, Kretzschmar HA, Lassmann H (1995) Monocyte/macrophage differentiation in early multiple sclerosis lesions. *Ann Neurol* 38:788-96.
- Brück W, Wegner C (2011) Insight into the mechanism of laquinimod action. *J Neurol Sci* 306:173-179.
- Brück W, Pfortner R, Pham T, Zhang J, Hayardeny L, Piryatinsky V, Hanisch UK, Regen T, van Rossum D, Brakelmann L, Hagemeyer K, Kuhlmann T, Stadelmann C, John GR, Kramann N, Wegner C (2012) Reduced astrocytic NF- κ B activation by laquinimod protects from cuprizone-induced demyelination. *Acta Neuropathol* 124:411-24.
- Buschmann JP, Berger K, Awad H, Clarner T, Beyer C, Kipp M (2012) Inflammatory response and chemokine expression in the white matter corpus callosum and gray matter cortex region during cuprizone-induced demyelination. *J Mol Neurosci* 48:66-76.
- Cammer W (1999) The neurotoxicant, cuprizone, retards the differentiation of oligodendrocytes in vitro. *J Neurol Sci* 168:116-20.
- Cardile V, Pavone A, Gulino R, Renis M, Scifo C, Perciavalle V (2003) Expression of brain-derived neurotrophic factor (BDNF) and inducible nitric oxide synthase (iNOS) in rat astrocyte cultures treated with Levetiracetam. *Brain Res* 976:227-33.
- Carlton WW (1967) Studies on the induction of hydrocephalus and spongy degeneration by cuprizone feeding and attempts to antidote the toxicity. *Life Sci* 6:11-19.
- Carlton WW (1969) Spongiform encephalopathy induced in rats and guinea pigs by cuprizone. *Exper Mol Pathol* 10:274-287.
- Chang A, Tourtellotte WW, Rudick R, Trapp BD (2002) Premyelinating oligodendrocytes in chronic lesions of multiple sclerosis. *N Engl J Med* 346:165-73.
- Chiba K, Yanagawa Y, Masubuchi Y, Kataoka H, Kawaguchi T, Ohtsuki M, Hoshino Y (1998) FTY720, a novel immunosuppressant, induces sequestration of circulating mature lymphocytes by acceleration of lymphocyte homing in rats. I. FTY720 selectively decreases the number of circulating mature lymphocytes by acceleration of lymphocyte homing. *J Immunol* 160:5037-44.
- Cho W, Messing A (2009) Properties of astrocytes cultured from GFAP over-expressing and GFAP mutant mice. *Exp Cell Res* 315:1260-72.
- Clarner T, Parabucki A, Beyer C, Kipp M (2011) Corticosteroids impair remyelination in the corpus callosum of cuprizone-treated mice. *J Neuroendocrinol* 23:601-11.

- Comi G, Pulizzi A, Rovaris M, Abramsky O, Arbizu T, Boiko A, Gold R, Havrdova E, Komoly S, Selmaj K, Sharrack B, Filippi M; LAQ/5062 Study Group (2008) Effect of laquinimod on MRI-monitored disease activity in patients with relapsing-remitting multiple sclerosis: a multicentre, randomised, double-blind, placebo-controlled phase IIb study. *Lancet* 371:2085-92.
- Comi G, Jeffery D, Kappos L, Montalban X, Boyko A, Rocca MA, Filippi M (2012) Placebo-controlled trial of oral laquinimod for multiple sclerosis. *N Engl J Med* 366:1000-1009.
- De Freitas MS, Spohr TC, Benedito AB, Caetano MS, Margulis B, Lopes UG, Moura-Neto V (2002) Neurite outgrowth is impaired on HSP70-positive astrocytes through a mechanism that requires NF-kappaB activation. *Brain Res* 958:359-370.
- Der Perng M, Su M, Wen SF, Li R, Gibbon T, Prescott AR, Brenner M, Quinlan RA (2006) The Alexander disease-causing glial fibrillary acidic protein mutant, R416W, accumulates into Rosenthal fibers by a pathway that involves filament aggregation and the association of alpha B-crystallin and HSP27. *Am J Hum Genet* 79:197-213.
- Ebers GC, Bulman DE, Sadovnick AD, Paty DW, Warren S, Hader W, Murray TJ, Seland TP, Duquette P, Grey T, Nelson R, Nicolle M, Brunet D (1986) A population-based study of multiple sclerosis in twins. *N Engl J Med* 315:1638-42.
- Evangelou N, Esiri MM, Smith S, Palace J, Matthews PM (2000a) Quantitative pathological evidence for axonal loss in normal appearing white matter in multiple sclerosis. *Ann Neurol* 47:391-5.
- Evangelou N, Konz D, Esiri MM, Smith S, Palace J, Matthews PM (2000b) Regional axonal loss in the corpus callosum correlates with cerebral white matter lesion volume and distribution in multiple sclerosis. *Brain* 123:1845-9.
- Falcone M, Rajan AJ, Bloom BR, Brosnan CF (1998) A critical role for IL-4 in regulating disease severity in experimental allergic encephalomyelitis as demonstrated in IL-4-deficient C57BL/6 mice and BALB/c mice. *J Immunol* 160:4822-30.
- Ferguson B, Matyszak MK, Esiri MM, Perry VH (1997) Axonal damage in acute multiple sclerosis lesions. *Brain* 120:393-399.
- Flatmark T, Kryvi H, Tangerås A (1980) Induction of megamitochondria by cuprizone (biscyclohexanone oxaldihydrazone). Evidence for an inhibition of the mitochondrial division process. *Eur J Cell Biol* 23:141-8.
- Folkerts G, Walzl G, Openshaw PJ (2000) Do common childhood infections 'teach' the immune system not to be allergic? *Immunol Today* 21:118-20.
- Frischer JM, Bramow S, Dal-Bianco A, Lucchinetti CF, Rauschka H, Schmidbauer M, Laursen H, Sorensen PS, Lassmann H (2009) The relation between inflammation and neurodegeneration in multiple sclerosis brains. *Brain* 132:1175-89.
- Goldschmidt T, Antel J, König FB, Brück W, Kuhlmann T (2009) Remyelination capacity of the MS brain decreases with disease chronicity. *Neurology* 72:1914-21.

- Gurevich M, Gritzman T, Orbach R, Tuller T, Feldman A, Achiron A (2010) Laquinimod suppress antigen presentation in relapsing-remitting multiple sclerosis: in-vitro high-throughput gene expression study. *J Neuroimmunol* 221:87-94.
- Hagemann TL, Gaeta SA, Smith MA, Johnson DA, Johnson JA, Messing A (2005) Gene expression analysis in mice with elevated glial fibrillary acidic protein and Rosenthal fibers reveals a stress response followed by glial activation and neuronal dysfunction. *Hum Mol Genet* 14:2443-58.
- Hagemann TL, Connor JX, Messing A (2006) Alexander disease-associated glial fibrillary acidic protein mutations in mice induce Rosenthal fiber formation and a white matter stress response. *J Neurosci* 26:11162-73.
- Haines JL, Terwedow HA, Burgess K, Pericak-Vance MA, Rimmler JB, Martin ER, Oksenberg JR, Lincoln R, Zhang DY, Banatao DR, Gatto N, Goodkin DE, Hauser SL (1998) Linkage of the MHC to familial multiple sclerosis suggests genetic heterogeneity. *Hum Mol Genet* 7:1229-34.
- Hall SM (1972) The effect of injections of lysophosphatidyl choline into white matter of the adult mouse spinal cord. *J Cell Sci* 10:535-46.
- Hein T, Hopfenmüller W (2000) [Projection of the number of multiple sclerosis patients in Germany]. *Nervenarzt* 71:288-94.
- Hermans G, Stinissen P, Hauben L, Van den Berg-Loonen E, Raus J, Zhang J (1997) Cytokine profile of myelin basic protein-reactive T cells in multiple sclerosis and healthy individuals. *Ann Neurol* 42:18-27.
- Hesse A, Wagner M, Held J, Brück W, Salinas-Riester G, Hao Z, Waisman A, Kuhlmann T (2010) In toxic demyelination oligodendroglial cell death occurs early and is FAS independent. *Neurobiol Dis* 37:362-9.
- Hickey WF, Hsu BL, Kimura H (1991) T-lymphocyte entry into the central nervous system. *J Neurosci Res* 28:254-60.
- Hiremath MM, Saito Y, Knapp GW, Ting JP, Suzuki K, Matsushima GK (1998) Microglial/macrophage accumulation during cuprizone-induced demyelination in C57BL/6 mice. *J Neuroimmunol* 92:38-49.
- Hiremath MM, Chen VS, Suzuki K, Ting JP, Matsushima GK (2008) MHC class II exacerbates demyelination in vivo independently of T cells. *J Neuroimmunol* 203:23-32.
- Honorat J, Flocard F, Ribot C, Saint-Pierre G, Pineau D, Peysson P, Kopp N (1993) [Alexander's disease in adults and diffuse cerebral gliomatosis in 2 members of the same family]. *Rev Neurol (Paris)* 149:781-7.
- Howard RS, Greenwood R, Gawler J, Scaravilli F, Marsden CD, Harding AE (1993) A familial disorder associated with palatal myoclonus, other brainstem signs, tetraparesis, ataxia and Rosenthal fibre formation. *J Neurol Neurosurg Psychiatry* 56:977-81.

- Huseby ES, Liggitt D, Brabb T, Schnabel B, Ohlén C, Goverman J (2001) A pathogenic role for myelin-specific CD8(+) T cells in a model for multiple sclerosis. *J Exp Med* 194:669-76.
- Iwaki T, Iwaki A, Tateishi J, Sakaki Y, Goldman JE (1993) Alpha B-crystallin and 27-kd heat shock protein are regulated by stress conditions in the central nervous system and accumulate in Rosenthal fibers. *Am J Pathol* 143:487-95.
- Jeffery ND, Blakemore WF (1995) Remyelination of mouse spinal cord axons demyelinated by local injection of lysolecithin. *J Neurocytol* 24:775-81.
- Jeong WS, Kim IW, Hu R, Kong AN (2004) Modulatory properties of various natural chemopreventive agents on the activation of NF-kappaB signaling pathway. *Pharm Res* 21:661-70.
- Jessen KR, Mirsky R (1980) Glial cells in the enteric nervous system contain glial fibrillary acidic protein. *Nature* 286:736-7.
- Jönsson S, Andersson G, Fex T, Fristedt T, Hedlund G, Jansson K, Abramo L, Fritzson I, Pekarski O, Runström A, Sandin H, Thuveesson I, Björk A (2004) Synthesis and biological evaluation of new 1,2-dihydro-4-hydroxy-2-oxo-3-quinolinecarboxamides for treatment of autoimmune disorders: structure-activity relationship. *J Med Chem* 47:2075-88.
- Kairisalo M, Korhonen L, Sepp M, Pruunsild P, Kukkonen JP, Kivinen J, Timmusk T, Blomgren K, Lindholm D (2009) NF-kappaB-dependent regulation of brain-derived neurotrophic factor in hippocampal neurons by X-linked inhibitor of apoptosis protein. *Eur J Neurosci* 30:958-66.
- Kang Z, Liu L, Spangler R, Spear C, Wang C, Gulen MF, Veenstra M, Ouyang W, Ransohoff RM, Li X (2012) IL-17-induced Act1-mediated signaling is critical for cuprizone-induced demyelination. *J Neurosci* 32:8284-92.
- Karussis DM, Lehmann D, Slavin S, Vourka-Karussis U, Mizrachi-Koll R, Ovadia H, Ben-Nun A, Kalland T, Abramsky O (1993a) Inhibition of acute, experimental autoimmune encephalomyelitis by the synthetic immunomodulator linomide. *Ann Neurol* 34:654-660.
- Karussis DM, Lehmann D, Slavin S, Vourka-Karussis U, Mizrachi-Koll R, Ovadia H, Kalland T, Abramsky O (1993b) Treatment of chronic-relapsing experimental autoimmune encephalomyelitis with the synthetic immunomodulator linomide (quinoline-3-carboxamide). *Proc Natl Acad Sci USA* 90:6400-6404.
- Kesterson JW, Carlton WW (1972) Cuprizone toxicosis in mice-attempts to antidote the toxicity. *Toxicol Appl Pharmacol* 22:6-13.
- Kim HJ, Miron VE, Dukala D, Proia RL, Ludwin SK, Traka M, Antel JP, Soliven B (2011) Neurobiological effects of sphingosine 1-phosphate receptor modulation in the cuprizone model. *FASEB J* 25:1509-1518.

- Kipp M, Clarner T, Dang J, Copray S and Beyer C (2009) The cuprizone animal model: new insights into an old story. *Acta Neuropathol* 118:723-736.
- Kirk J, Plumb J, Mirakhur M, McQuaid S (2003) Tight junctional abnormality in multiple sclerosis white matter affects all calibres of vessel and is associated with blood-brain barrier leakage and active demyelination. *J Pathol* 201:319-27.
- Kotter MR, Zhao C, van Rooijen N, Franklin RJ (2005) Macrophage-depletion induced impairment of experimental CNS remyelination is associated with a reduced oligodendrocyte progenitor cell response and altered growth factor expression. *Neurobiol Dis* 18:166-75.
- Kremenutzky M, Rice GP, Baskerville J, Wingerchuk DM, Ebers GC (2006) The natural history of multiple sclerosis: a geographically based study 9: observations on the progressive phase of the disease. *Brain* 129:584-94.
- Kuhlmann T, Lingfeld G, Bitsch A, Schuchardt J, Brück W (2002) Acute axonal damage in multiple sclerosis is most extensive in early disease stages and decreases over time. *Brain* 125:2202-2212.
- Kuhlmann T, Remington L, Maruschak B, Owens T, Brück W (2007) Nogo-A is a reliable oligodendroglial marker in adult human and mouse CNS and in demyelinated lesions. *J Neuropathol Exp Neurol* 66:238-246.
- Kuhlmann T, Miron V, Cui Q, Wegner C, Antel J, Brück W (2008) Differentiation block of oligodendroglial progenitor cells as a cause for remyelination failure in chronic multiple sclerosis. *Brain* 131:1749-58.
- Kurtzke JF, Dean G, Botha DP (1970) A method for estimating the age at immigration of white immigrants to South Africa, with an example of its importance. *S Afr Med J* 44:663-9.
- Kurtzke JF, Beebe GW, Norman JE Jr (1979) Epidemiology of multiple sclerosis in U.S. veterans: 1. Race, sex, and geographic distribution. *Neurology* 29:1228-35.
- Kurtzke JF (2000) Epidemiology of multiple sclerosis. Does this really point toward an etiology? *Lectio Doctoralis. Neurol Sci* 21:383-403.
- Kutzelnigg A, Lucchinetti CF, Stadelmann C, Brück W, Rauschka H, Bergmann M, Schmidbauer M, Parisi JE, Lassmann H (2005) Cortical demyelination and diffuse white matter injury in multiple sclerosis. *Brain* 128:2705-12.
- Labie C, Lafon C, Marmouget C, Saubusse P, Fournier J, Keane PE, Le Fur G, Soubrié P (1999) Effect of the neuroprotective compound SR57746A on nerve growth factor synthesis in cultured astrocytes from neonatal rat cortex. *Br J Pharmacol* 127:139-44.
- Lang HL, Jacobsen H, Ikemizu S, Andersson C, Harlos K, Madsen L, Hjorth P, Sondergaard L, Svejgaard A, Wucherpfennig K, Stuart DI, Bell JI, Jones EY, Fugger L (2002) A functional and structural basis for TCR cross-reactivity in multiple sclerosis. *Nat Immunol* 3:940-3.

- Lennon VA, Kryzer TJ, Pittock SJ, Verkman AS, Hinson SR (2005) IgG marker of optic-spinal multiple sclerosis binds to the aquaporin-4 water channel. *J Exp Med* 202:473-7.
- Levine JM, Reynolds R (1999) Activation and proliferation of endogenous oligodendrocyte precursor cells during ethidium bromide-induced demyelination. *Exp Neurol* 160:333-47.
- Li L, Lundkvist A, Andersson D, Wilhelmsson U, Nagai N, Pardo AC, Nodin C, Stahlberg A, Aprico K, Larsson K, Yabe T, Moons L, Fotheringham A, Davies I, Carmeliet P, Schwartz JP, Pekna M, Kubista M, Blomstrand F, Maragakis N, Nilsson M, Pekny M (2008) Protective role of reactive astrocytes in brain ischemia. *J Cereb Blood Flow Metab* 28:468-481.
- Li R, Johnson AB, Salomons G, Goldman JE, Naidu S, Quinlan R, Cree B, Ruyle SZ, Banwell B, D'Hooghe M, Siebert JR, Rolf CM, Cox H, Reddy A, Gutiérrez-Solana LG, Collins A, Weller RO, Messing A, van der Knaap MS, Brenner M (2005) Glial fibrillary acidic protein mutations in infantile, juvenile, and adult forms of Alexander disease. *Ann Neurol* 57:310-26.
- Li W, Khor TO, Xu C, Shen G, Jeong WS, Yu S, Kong AN (2008) Activation of Nrf2-antioxidant signaling attenuates NF-kappaB-inflammatory response and elicits apoptosis. *Biochem Pharmacol* 76:1485-9.
- Li X, Commane M, Nie H, Hua X, Chatterjee-Kishore M, Wald D, Haag M, Stark GR (2000) Act1, an NF-kappa B-activating protein. *Proc Natl Acad Sci U S A* 97:10489-93.
- Liang CC, Park AY, Guan JL (2007) In vitro scratch assay: a convenient and inexpensive method for analysis of cell migration in vitro. *Nat Protoc* 2:329-33.
- Liedtke W, Edelmann W, Chiu FC, Kucherlapati R, Raine CS (1998) Experimental autoimmune encephalomyelitis in mice lacking glial fibrillary acidic protein is characterized by a more severe clinical course and an infiltrative central nervous system lesion. *Am J Pathol* 152:251-9.
- Liu GH, Qu J, Shen X (2008) NF-kappaB/p65 antagonizes Nrf2-ARE pathway by depriving CBP from Nrf2 and facilitating recruitment of HDAC3 to MafK. *Biochim Biophys Acta* 1783:713-27.
- Lovas G, Szilágyi N, Majtényi K, Palkovits M, Komoly S (2000) Axonal changes in chronic demyelinated cervical spinal cord plaques. *Brain* 123:308-17.
- Lovett-Racke AE, Trotter JL, Lauber J, Perrin PJ, June CH, Racke MK (1998) Decreased dependence of myelin basic protein-reactive T cells on CD28-mediated costimulation in multiple sclerosis patients. A marker of activated/memory T cells. *J Clin Invest* 101:725-30.
- Lublin FD, Reingold SC (1996) Defining the clinical course of multiple sclerosis: results of an international survey. National Multiple Sclerosis Society (USA) Advisory Committee on Clinical Trials of New Agents in Multiple Sclerosis. *Neurology* 46:907-11.

- Lucchinetti C, Brück W, Parisi J, Scheithauer B, Rodriguez M, Lassmann H (2000) Heterogeneity of multiple sclerosis lesions: implications for the pathogenesis of demyelination. *Ann Neurol* 47:707-717.
- Lucchinetti CF, Mandler RN, McGavern D, Bruck W, Gleich G, Ransohoff RM, Trebst C, Weinshenker B, Wingerchuk D, Parisi JE, Lassmann H (2002) A role for humoral mechanisms in the pathogenesis of Devic's neuromyelitis optica. *Brain* 125:1450-61.
- Lucchinetti CF, Popescu BF, Bunyan RF, Moll NM, Roemer SF, Lassmann H, Brück W, Parisi JE, Scheithauer BW, Giannini C, Weigand SD, Mandrekar J, Ransohoff RM (2011) Inflammatory cortical demyelination in early multiple sclerosis. *N Engl J Med* 365: 2188-97.
- Ludwin SK (1978) Central nervous system demyelination and remyelination in the mouse: an ultrastructural study of cuprizone toxicity. *Lab Invest* 39:597-612.
- Malmeström C, Haghighi S, Rosengren L, Andersen O, Lycke J (2003) Neurofilament light protein and glial fibrillary acidic protein as biological markers in MS. *Neurology* 61:1720-5.
- Matsushima GK, Morell P (2001) The neurotoxicant, cuprizone, as a model to study demyelination and remyelination in the central nervous system. *Brain Pathol* 11: 107-116.
- McDonald WI, Compston A, Edan G, Goodkin D, Hartung HP, Lublin FD, McFarland HF, Paty DW, Polman CH, Reingold SC, Sandberg-Wollheim M, Sibley W, Thompson A, van den Noort S, Weinshenker BY, Wolinsky JS (2001) Recommended diagnostic criteria for multiple sclerosis: guidelines from the International Panel on the diagnosis of multiple sclerosis. *Ann Neurol* 50:121-7.
- Meisingset TW, Risa Ø, Brenner M, Messing A, Sonnewald U (2010) Alteration of glial-neuronal metabolic interactions in a mouse model of Alexander disease. *Glia* 58:1228-34.
- Messing A, Head MW, Galles K, Galbreath EJ, Goldman JE, Brenner M (1998) Fatal encephalopathy with astrocyte inclusions in GFAP transgenic mice. *Am J Pathol* 152:391-8.
- Miller DH, Ormerod IE, Rudge P, Kendall BE, Moseley IF, McDonald WI (1989) The early risk of multiple sclerosis following isolated acute syndromes of the brainstem and spinal cord. *Ann Neurol* 26:635-9.
- Miller DH, Khan OA, Sheremata WA, Blumhardt LD, Rice GP, Libonati MA, Willmer-Hulme AJ, Dalton CM, Miszkiel KA, O'Connor PW (2003) A controlled trial of natalizumab for relapsing multiple sclerosis. *N Engl J Med* 348:15-23.
- Miron VE, Zehntner SP, Kuhlmann T, Ludwin SK, Owens T, Kennedy TE, Bedell BJ, Antel JP (2009) Statin therapy inhibits remyelination in the central nervous system. *Am J Pathol* 174:1880-1890.

- Mishra MK, Wang J, Silva C, Mack M, Yong VW (2012) Kinetics of proinflammatory monocytes in a model of multiple sclerosis and its perturbation by laquinimod. *Am J Pathol* 181:642-51.
- Misu T, Fujihara K, Nakamura M, Murakami K, Endo M, Konno H, Itoyama Y (2006) Loss of aquaporin-4 in active perivascular lesions in neuromyelitis optica: a case report. *Tohoku J Exp Med* 209:269-75.
- Mizuta I, Ohta M, Ohta K, Nishimura M, Mizuta E, Kuno S (2001) Riluzole stimulates nerve growth factor, brain-derived neurotrophic factor and glial cell line-derived neurotrophic factor synthesis in cultured mouse astrocytes. *Neurosci Lett* 310:117-20.
- Moharreggh-Khiabani D, Blank A, Skripuletz T, Miller E, Kotsiari A, Gudi V, Stangel M (2010) Effects of fumaric acids on cuprizone induced central nervous system de- and remyelination in the mouse. *PLoS One* 5:e11769.
- Mombaerts P, Iacomini J, Johnson RS, Herrup K, Tonegawa S and Papaioannou VE (1992) RAG-1-deficient mice have no mature B and T lymphocytes. *Cell* 6:869-877.
- Morrissey SP, Miller DH, Kendall BE, Kingsley DP, Kelly MA, Francis DA, MacManus DG, McDonald WI (1993) The significance of brain magnetic resonance imaging abnormalities at presentation with clinically isolated syndromes suggestive of multiple sclerosis. A 5-year follow-up study. *Brain* 116:135-46.
- Nair A, Frederick TJ, Miller SD (2008) Astrocytes in multiple sclerosis: a product of their environment. *Cell Mol Life Sci* 65:2702-20.
- Noseworthy JH, Wolinsky JS, Lublin FD, Whitaker JN, Linde A, Gjorstrup P, Sullivan HC (2000) Linomide in relapsing and secondary progressive MS: part I: trial design and clinical results. North American Linomide Investigators. *Neurology* 54:1726-1733.
- Oertle T, van der Haar ME, Bandtlow CE, Robeva A, Burfeind P, Buss A, Huber AB, Simonen M, Schnell L, Brösamle C, Kaupmann K, Vallon R, Schwab ME (2003) Nogo-A inhibits neurite outgrowth and cell spreading with three discrete regions. *J Neurosci* 23: 5393-406.
- Ohta K, Ohta M, Mizuta I, Fujinami A, Shimazu S, Sato N, Yoneda F, Hayashi K, Kuno S (2002) The novel catecholaminergic and serotonergic activity enhancer R-(-)-1-(benzofuran-2-yl)-2-propylaminopentane up-regulates neurotrophic factor synthesis in mouse astrocytes. *Neurosci Lett* 328:205-8.
- Ousman SS, David S (2000) Lysophosphatidylcholine induces rapid recruitment and activation of macrophages in the adult mouse spinal cord. *Glia* 30:92-104.
- Pasquini LA, Calatayud CA, Bertone Una L, Millet V, Pasquini JM, Soto EF (2007) The neurotoxic effect of cuprizone on oligodendrocytes depends on the presence of pro-inflammatory cytokines secreted by microglia. *Neurochem Res* 32:279–292.
- Pattison IH, Jebbett JN (1971a) Histopathological similarities between scrapie and cuprizone toxicity in mice. *Nature* 230:115-117.

- Pattison IH, Jebbett JN (1971b) Clinical and histological observations on cuprizone toxicity and scrapie in mice. *Res Vet Sci* 12:378-80.
- Polman C, Barkhof F, Sandberg-Wollheim M, Linde A, Nordle O, Nederman T; Laquinimod in Relapsing MS Study Group (2005) Treatment with laquinimod reduces development of active MRI lesions in relapsing MS. *Neurology* 64:987-91.
- Polman CH, Reingold SC, Banwell B, Clanet M, Cohen JA, Filippi M, Fujihara K, Havrdova E, Hutchinson M, Kappos L, Lublin FD, Montalban X, O'Connor P, Sandberg-Wollheim M, Thompson AJ, Waubant E, Weinshenker B, Wolinsky JS (2011) Diagnostic criteria for multiple sclerosis: 2010 revisions to the McDonald criteria. *Ann Neurol* 69:292-302.
- Prineas JW, Kwon EE, Cho ES, Sharer LR, Barnett MH, Oleszak EL, Hoffman B, Morgan BP (2001) Immunopathology of secondary-progressive multiple sclerosis. *Ann Neurol* 50:646-57.
- Prust M, Wang J, Morizono H, Messing A, Brenner M, Gordon E, Hartka T, Sokohl A, Schiffmann R, Gordish-Dressman H, Albin R, Amartino H, Brockman K, Dinopoulos A, Dotti MT, Fain D, Fernandez R, Ferreira J, Fleming J, Gill D, Griebel M, Heilstedt H, Kaplan P, Lewis D, Nakagawa M, Pedersen R, Reddy A, Sawaishi Y, Schneider M, Sherr E, Takiyama Y, Wakabayashi K, Gorospe JR, Vanderver A (2011) GFAP mutations, age at onset, and clinical subtypes in Alexander disease. *Neurology* 77:1287-94.
- Raasch J, Zeller N, van LG, Merkler D, Mildner A, Erny D, Knobloch KP, Bethea JR, Waisman A, Knust M, Del TD, Deller T, Blank T, Priller J, Bruck W, Pasparakis M, Prinz M (2011) I κ B kinase 2 determines oligodendrocyte loss by non-cell-autonomous activation of NF- κ B in the central nervous system. *Brain* 134:1184-1198.
- Ramagopalan SV, Byrnes JK, Orton SM, Dymont DA, Guimond C, Yee IM, Ebers GC, Sadovnick AD (2010) Sex ratio of multiple sclerosis and clinical phenotype. *Eur J Neurol* 17:634-7.
- Remington LT, Babcock AA, Zehntner SP, Owens T (2007) Microglial recruitment, activation, and proliferation in response to primary demyelination. *Am J Pathol* 170:1713-24.
- Rice GP, Hartung HP, Calabresi PA (2005) Anti- α 4 integrin therapy for multiple sclerosis: mechanisms and rationale. *Neurology* 64:1336-42.
- Richardson KC, Jarett L, Finke EH (1960) Embedding in epoxy resins for ultrathin sectioning in electron microscopy. *Stain Technol* 35:313-325.
- Riise T, Nortvedt MW, Ascherio A (2003) Smoking is a risk factor for multiple sclerosis. *Neurology* 61:1122-4.
- Riley CP, Cope TC, Buck CR (2004) CNS neurotrophins are biologically active and expressed by multiple cell types. *J Mol Histol* 35:771-83.

- Rodriguez D, Gauthier F, Bertini E, Bugiani M, Brenner M, N'guyen S, Goizet C, Gelot A, Surtees R, Pedespan JM, Hernandorena X, Troncoso M, Uziel G, Messing A, Ponsot G, Pham-Dinh D, Dautigny A, Boespflug-Tanguy O (2001) Infantile Alexander disease: spectrum of GFAP mutations and genotype-phenotype correlation. *Am J Hum Genet* 69:1134-40.
- Roessmann U, Gambetti P (1986) Pathological reaction of astrocytes in perinatal brain injury. Immunohistochemical study. *Acta Neuropathol* 70:302-7.
- Runmarker B, Andersen O (1995) Pregnancy is associated with a lower risk of onset and a better prognosis in multiple sclerosis. *Brain* 118:253-61.
- Runstrom A, Leanderson T, Ohlsson L, Axelsson B (2006) Inhibition of the development of chronic experimental autoimmune encephalomyelitis by laquinimod (ABR-215062) in IFN-beta k.o. and wild type mice. *J Neuroimmunol* 173:69-78.
- Sadovnick AD, Armstrong H, Rice GP, Bulman D, Hashimoto L, Paty DW, Hashimoto SA, Warren S, Hader W, Murray TJ, Seland TP, Metz L, Bell R, Duquette P, Gray T, Nelson R, Weinshenkar B, Brunt D, Ebers GC (1993) A population-based study of multiple sclerosis in twins: update. *Ann Neurol* 33:281-5.
- Saha RN, Liu X, Pahan K (2006) Up-regulation of BDNF in astrocytes by TNF-alpha: a case for the neuroprotective role of cytokine. *J Neuroimmune Pharmacol* 1:212-22.
- Sawcer S, Hellenthal G, Pirinen M, Spencer CC, Patsopoulos NA, Moutsianas L *et al.* (2011) Genetic risk and a primary role for cell-mediated immune mechanisms in multiple sclerosis. *Nature* 476:214-9.
- Schluesener HJ and Wekerle H (1985) Autoaggressive T lymphocyte lines recognizing the encephalitogenic region of myelin basic protein: in vitro selection from unprimed rat T lymphocyte populations. *J Immunol* 135:3128.
- Scholz C, Patton KT, Anderson DE, Freeman GJ, Hafler DA (1998) Expansion of autoreactive T cells in multiple sclerosis is independent of exogenous B7 costimulation. *J Immunol* 160:1532-8.
- Schulze-Topphoff U, Shetty A, Varrin-Doyer M, Molnarfi N, Sagan SA, Sobel RA, Nelson PA, Zamvil SS (2012) Laquinimod, a quinoline-3-carboxamide, induces type II myeloid cells that modulate central nervous system autoimmunity. *PLoS One* 7:e33797.
- Schwankhaus JD, Parisi JE, Gullledge WR, Chin L, Currier RD (1995) Hereditary adult-onset Alexander's disease with palatal myoclonus, spastic paraparesis, and cerebellar ataxia. *Neurology* 45:2266-71.
- Sedgwick JD, Mason DW (1986) The mechanism of inhibition of experimental allergic encephalomyelitis in the rat by monoclonal antibody against CD4. *J Neuroimmunol* 13:217-32.
- Seil FJ, Schochet SS Jr, Earle KM (1968) Alexander's disease in an adult. Report of a case. *Arch Neurol* 19:494-502.

- Shen S, Sandoval J, Swiss VA, Li J, Dupree J, Franklin RJ, Casaccia-Bonnel P (2008) Age-dependent epigenetic control of differentiation inhibitors is critical for remyelination efficiency. *Nat Neurosci* 11:1024-34.
- Sicotte NL, Liva SM, Klutch R, Pfeiffer P, Bouvier S, Odesa S, Wu TC, Voskuhl RR (2002) Treatment of multiple sclerosis with the pregnancy hormone estriol. *Ann Neurol* 52:421-28.
- Skihar V, Silva C, Chojnacki A, Doring A, Stallcup WB, Weiss S, Yong VW (2009) Promoting oligodendrogenesis and myelin repair using the multiple sclerosis medication glatiramer acetate. *Proc Natl Acad Sci U S A* 106:17992-17997.
- Skripuletz T, Lindner M, Kotsiari A, Garde N, Fokuhl J, Linsmeier F, Trebst C and Stangel M (2008) Cortical demyelination is prominent in the murine cuprizone model and is strain-dependent. *Am J Pathol* 172:1053-1061.
- Sofroniew MV (2009) Molecular dissection of reactive astrogliosis and glial scar formation. *Trends Neurosci* 32:638-647.
- Sofroniew MV and Vinters HV (2010) Astrocytes: biology and pathology. *Acta Neuropathol* 119:7-35.
- Srivastava R, Aslam M, Kalluri SR, Schirmer L, Buck D, Tackenberg B, Rothhammer V, Chan A, Gold R, Berthele A, Bennett JL, Korn T, Hemmer B (2012) Potassium channel KIR4.1 as an immune target in multiple sclerosis. *N Engl J Med* 367:115-23.
- Strachan DP (1989) Hay fever, hygiene, and household size. *BMJ* 299:1259-60.
- Suzuki K (1969) Giant hepatic mitochondria: production in mice fed with cuprizone. *Science* 163:81-2.
- Taylor LC, Gilmore W and Matsushima GK (2009) SJL mice exposed to cuprizone intoxication reveal strain and gender pattern differences in demyelination. *Brain Pathol* 19:467-479.
- Teitelbaum D, Fridkis-Hareli M, Arnon R, Sela M (1996) Copolymer 1 inhibits chronic relapsing experimental allergic encephalomyelitis induced by proteolipid protein (PLP) peptides in mice and interferes with PLP-specific T cell responses. *J Neuroimmunol* 64:209-217.
- Thöne J, Ellrichmann G, Seubert S, Peruga I, Lee DH, Conrad R, Hayardeny L, Comi G, Wiese S, Linker RA, Gold R (2012) Modulation of autoimmune demyelination by laquinimod via induction of brain-derived neurotrophic factor. *Am J Pathol* 180:267-74.
- Tian R, Gregor M, Wiche G, Goldman JE (2006) Plectin regulates the organization of glial fibrillary acidic protein in Alexander disease. *Am J Pathol* 168:888-97.
- Toft-Hansen H, Füchtbauer L, Owens T (2011) Inhibition of reactive astrocytosis in established experimental autoimmune encephalomyelitis favors infiltration by myeloid cells over T cells and enhances severity of disease. *Glia* 59:166-76.

- Trapp BD, Peterson J, Ransohoff RM, Rudick R, Mork S, Bo L (1998) Axonal transection in the lesions of multiple sclerosis. *New Engl J Med* 338:278-285.
- Tzartos JS, Friese MA, Craner MJ, Palace J, Newcombe J, Esiri MM, Fugger L (2008) Interleukin-17 production in central nervous system-infiltrating T cells and glial cells is associated with active disease in multiple sclerosis. *Am J Pathol* 172:146-55.
- van der Knaap MS, Naidu S, Breiter SN, Blaser S, Stroink H, Springer S, Begeer JC, van Coster R, Barth PG, Thomas NH, Valk J, Powers JM (2001) Alexander disease: diagnosis with MR imaging. *AJNR Am J Neuroradiol* 22:541-52.
- Vieira PL, Heystek HC, Wormmeester J, Wierenga EA, Kapsenberg ML (2003) Glatiramer acetate (copolymer-1, copaxone) promotes Th2 cell development and increased IL-10 production through modulation of dendritic cells. *J Immunol* 170:4483-8.
- VonDrän MW, Singh H, Honeywell JZ, Dreyfus CF (2011) Levels of BDNF impact oligodendrocyte lineage cells following a cuprizone lesion. *J Neurosci* 31:14182-90.
- Wegner C, Esiri MM, Chance SA, Palace J, Matthews PM (2006) Neocortical neuronal, synaptic, and glial loss in multiple sclerosis. *Neurology* 67:960-7.
- Wegner C, Stadelmann C (2009) Gray matter pathology and multiple sclerosis. *Curr Neurol Neurosci Rep* 9:399-404.
- Wegner C, Stadelmann C, Pförtner R, Raymond E, Feigelson S, Alon R, Timan B, Hayardeny L, Brück W (2010) Laquinimod interferes with migratory capacity of T cells and reduces IL-17 levels, inflammatory demyelination and acute axonal damage in mice with experimental autoimmune encephalomyelitis. *J Neuroimmunol* 227:133-43.
- Westland KW, Pollard JD, Sander S, Bonner JG, Linington C, McLeod JG (1999) Activated non-neural specific T cells open the blood-brain barrier to circulating antibodies. *Brain* 122:1283-91.
- Wohlwill FJ, Bernstein J, Yakovlev PI (1959) Dysmyelinogenic leukodystrophy; report of a case of a new, presumably familial type of leukodystrophy with megalobarencephaly. *J Neuropathol Exp Neurol* 18:359-83.
- Wolinsky JS, Narayana PA, Noseworthy JH, Lublin FD, Whitaker JN, Linde A, Gjørstrup P, Sullivan HC (2000) Linomide in relapsing and secondary progressive MS: part II: MRI results. MRI Analysis Center of the University of Texas-Houston, Health Science Center, and the North American Linomide Investigators. *Neurology* 54:1734-1741.
- Woodruff RH, Franklin RJ (1999a) Demyelination and remyelination of the caudal cerebellar peduncle of adult rats following stereotaxic injections of lysolecithin, ethidium bromide, and complement/anti-galactocerebroside: a comparative study. *Glia* 25:216-28.
- Woodruff RH, Franklin RJ (1999b) The expression of myelin protein mRNAs during remyelination of lysolecithin-induced demyelination. *Neuropathol Appl Neurobiol* 25:226-235.

- Yang JS, Xu LY, Xiao BG, Hedlund G, Link H (2004) Laquinimod (ABR-215062) suppresses the development of experimental autoimmune encephalomyelitis, modulates the Th1/Th2 balance and induces the Th3 cytokine TGF-beta in Lewis rats. *J Neuroimmunol* 156:3-9.
- Yasuda CL, Al-Sabbagh A, Oliveira EC, BM az-Bardales, Garcia AA, Santos LM (1999) Interferon beta modulates experimental autoimmune encephalomyelitis by altering the pattern of cytokine secretion. *Immunol Invest* 28:115-126.
- Zaheer A, Yorek MA, Lim R (2001) Effects of glia maturation factor overexpression in primary astrocytes on MAP kinase activation, transcription factor activation, and neurotrophin secretion. *Neurochem Res* 26:1293-1299.
- Zatta P, Raso M, Zambenedetti P, Wittkowski W, Messori L, Piccioli F, Mauri PL, Beltramini M (2005) Copper and zinc dismetabolism in the mouse brain upon chronic cuprizone treatment. *Cell Mol Life Sci* 62:1502-13.
- Zhang Y, Jalili F, Ouamara N, Zameer A, Cosentino G, Mayne M, Hayardeny L, Antel JP, Bar-Or A, John GR (2010) Glatiramer acetate-reactive T lymphocytes regulate oligodendrocyte progenitor cell number in vitro: role of IGF-2. *J Neuroimmunol* 227:71-9.

Curriculum Vitae

PERSONAL DETAILS

Name, surname: Pförtner, Ramona
Date of Birth: August 7th, 1985
Place of Birth: Osterode am Harz, Germany
Citizenship: German
Contact: rp7@gmx.net

EDUCATION AND RESEARCH EXPERIENCE

11/2009 – 10/2012 **University Medical Center Göttingen, Germany**
 Department of Neuropathology
 PhD thesis

11/2009 – 10/2012 **Georg-August-University Göttingen, Germany**
 International Ph.D. program “Molecular Medicine”

10/2004 – 11/2009 **Georg-August-University Göttingen, Germany**
 Studies in Biology, total grade: Very good

2004 **Robert-Koch-Gymnasium Clausthal-Zellerfeld, Germany**
 Abitur (corresponds to A levels)

TEACHING EXPERIENCE

10/2010 **Georg-August-University Göttingen, Germany:** Teaching assistant for the GGNB method course: “Sensory systems”

03/2010 – 04/2010 **Georg-August-University Göttingen, Germany:** Teaching assistant for the advanced neurophysiology course: “Mechanical and electrical properties of a frog heart”

09/2009 **Georg-August-University Göttingen, Germany:** Student assistant for the GGNB method course: “The neuronal basic of acoustic communication in insects. Part II: Control of sound production”

02/2009 – 03/2009 **Georg-August-University Göttingen, Germany:** Student assistant for the advanced neurophysiology course: “Extracellular recording of a peripheral frog nerve”

PUBLICATIONS

Original Articles

- 2012 Brück W*, **Pförtner R***, Pham T, Zhang J, Hayardeny L, Piryatinsky V, Hanisch U, Regen T, Rossum D, Brakelmann L, Hagemeyer K, Kuhlmann T, Stadelmann C, John GR, Kramann N and Wegner C (2012) Reduced astrocytic NF- κ B activation by laquinimod protects from cuprizone-induced demyelination. *Acta Neuropathol* 124:411-24.
*equal contribution
- 2011 Kunst M, **Pförtner R**, Aschenbrenner K and Heinrich R (2011) Neurochemical architecture of the central complex related to its function in the control of grasshopper acoustic communication. *PLoS One* 6:e25613.
- 2010 Wegner C, Stadelmann C, **Pförtner R**, Raymond E, Feigelson S, Alon R, Timan B, Hayardeny L and Brück W (2010) Laquinimod interferes with migratory capacity of T cells and reduces IL-17 levels, inflammatory demyelination and acute axonal damage in mice with experimental autoimmune encephalomyelitis. *J Neuroimmunol* 227: 133-43.

Poster Presentations

- 2012 **Pförtner R**, Kramann R, Brück W and Wegner C “Preventive laquinimod treatment reduces cuprizone-induced pathology in a dose-dependent manner”, presented at 28th congress of the European and Americas Committees for Treatment and Research in Multiple Sclerosis, October 10-13th 2012, Lyon, France
- 2011 **Pförtner R**, Brück W and Wegner C “Laquinimod reduces demyelination and inflammation in cuprizone-treated mice”, presented at 10th European Meeting on Glial Cells in Health and Disease, September 13-17th 2011, in Prague, Czech Republic
- 2011 **Pförtner R**, Brück W and Wegner C “Effect of laquinimod on cuprizone-induced demyelination in mice”, presented at the 9th Göttingen Meeting of the German Neuroscience Society, March 23-27th 2011, Göttingen, Germany